A Non-Invasive Method for Tracking Retinal Motion During Pars Plana Vitrectomy

BY

TanviShri Jatla
B.S., University of Illinois at Chicago, 2014

THESIS

Submitted as partial fulfillment of the requirements
for the degree of Master of Science in Bioengineering
in the Graduate College of the
University of Illinois at Chicago, 2015

Chicago, Illinois

Defense Committee:

Dr. Yannek Leiderman, Chair and Advisor, Ophthalmology and Visual Sciences
Dr. Miiri Kotche
Dr. John Hetling

I would like to dedicate this thesis to my parents, Veeraraghava Rao and Sivabala Sundari Jatla, and my sister, Rutvishri, for giving me their love, encouragement, and guidance. None of my success would have been possible without their blessing.

I also want to dedicate this thesis to my grandfather, Mallipudi Satyanarayana Murty, for encouraging me my entire life to strive to be the best.

I am grateful to have a great support system from my friends and family, who were there for me during my graduate program, without whom it would never have been accomplished. Thank you all for all the love and the support.

ACKNOWLEDGEMENTS

I would like to especially thank my advisor, Dr. Yannek Leiderman, for his patience, motivation, encouragement, and vast knowledge. I could not imagine having a better advisor and mentor for my Masters study. I would also like to thank him for introducing me to the astonishing topic, unique experience, and the vast opportunity.

In addition, I would also like to thank the rest of my thesis committee – Dr. Miiri Kotche, and Dr. John Hetling – for their support and guidance in assisting me in accomplishing my goals and enjoying the experience in the process.

Next, I would like to thank my friends for being there for me. I would like to express a special thank you to Catherine Santis for reassuring and encouraging me and to Minh Tran, Hemanti Chavada, and Palash Jha for helping me in the process.

Lastly, I would like to thank my family for supporting me throughout my entire life.

TSJ

TABLE OF CONTENTS

CHAPTER PAGE

I. INTRODUCTION 1
- A. Anatomy of the Eye 2
  - 1. The Vitreous Body 3
  - 2. The Retina 3
- B. Pars Plana Vitrectomy 4
- C. Vitreous Cutters Used for Pars Plana Vitrectomy 7
- D. In-Vivo Approach to Quantify Retinal Motion 8

II. METHODS 9
- A. Assumptions and Constraints 10
- B. Image Analysis Using ImageJ for Experimental Sections 11
- C. Image Analysis Using ImageJ for Control 17
- D. Validation – Using Camera Edge as Reference Point 18
- E. Validation – Frame-by-Frame Analysis 20

III. RESULTS 22
- A. Image Analysis Using ImageJ for Experimental Sections 23
- B. Image Analysis Using ImageJ for Control 27
- C. Validation – Using Camera Edge as Reference Point 36
- D. Validation – Frame-by-Frame Analysis 37

IV. DISCUSSION 40
- A. Image Analysis Using ImageJ for Experimental Sections 41
- B. Image Analysis Using ImageJ for Control 43
- C. Validation – Using Camera Edge as Reference Point 44
- D. Validation – Frame-by-Frame 45
- E. Sources of Error 46

V. FUTURE ENHANCEMENTS 50

VI. REFERENCES 52

VII. APPENDIX 55
- A. Image Analysis Using ImageJ for Experimental Sections 55
  - 1. Video 1 55
  - 2. Video 2 59
  - 3. Video 3 67

TABLE OF CONTENTS

CHAPTER PAGE

4. Video 4 72
5. Video 5 82
6. Video 6 88
7. Video 7 93

B. Image Analysis Using ImageJ for Control 97
C. Validation – Using Camera Edge as Reference Point 102
D. Validation – Frame-by-Frame Analysis 107

VIII. VITA 114

TABLE OF TABLES

TABLE PAGE

1. Elementary Information of Video 1 28
2. Net Length and Velocity of Video 1 28
3. Elementary Information for Video 2 29
4. Net Length and Velocity of Video 2 29
5. Elementary Information for Video 3 30
6. Net Length and Velocity of Video 3 30
7. Elementary Information for Video 4 31
8. Net Length and Velocity of Video 4 31
9. Elementary Information for Video 5 32
10. Net Length and Velocity of Video 5 32
11. Elementary Information for Video 6 33
12. Net Length and Velocity of Video 6 33
13. Elementary Information for Video 7 34
14. Net Length and Velocity of Video 7 34
15. Elementary Information for Control 35
16. Net Length and Velocity of Control 35
17. Elementary Information for Edge Detection 38
18. Average Distance Away from Mean of Edge Detection 38

TABLE OF TABLES

TABLE PAGE

19. Elementary Information for Frame-by-Frame Analysis 39

20. Relative Error for Frame-by-Frame Analysis 39

21. Summary of Net Distance Traveled and Velocity 41

TABLE OF FIGURES

FIGURE PAGE

1. Sketch of the Eye – Showing the Vitreous Body and its Relations 2

2. Incision Sites for Pars Plana Vitrectomy 5

3. Image Sequence after importing into ImageJ 12

4. Image Stack based on Maximum Intensity on ImageJ 13

5. Kymograph Produced by the Image Sequence 14

6. Applying Threshold to Image Sequence to Turn it into Binary 15

7. Portion of Kymograph Used to Determine Camera Edge as Reference Point 19

8. Plot Profile of Kymograph for Frame-by-Frame Analysis 20

SUMMARY

Pars plana vitrectomy is performed to access the posterior segment of the eye, specifically when vitreoretinal surgery is required. A major indication for surgery of the retina and vitreous is retinal detachment. Rhegmatogeneous retinal detachment is caused by a tear in the neurosensory retina in association with the passage of liquid vitreous through the break and into the subretinal space, causing separation of the retina from the underlying retinal pigment epithelium. The tear in the retina can be instigated by many causes: structural changes in the vitreous humor, ocular injury, diabetes, inflammatory eye diseases, and many more. The most frequent modality used to treat retinal detachment at present is 3-port pars plana vitrectomy. The vitreoretinal surgeon typically employs a cutting/aspirating instrument (the vitrectomy probe), a fiberoptic endoilluminator, and an infusion port to introduce fluids or gases thereby maintaining suitable intraocular pressure and volume as vitreous is aspirated. Surgeons today have numerous types of vitrectomy probes from which to select when performing vitreoretinal surgery. Controlled excision and aspiration of vitreous and other intraocular tissues is performed by the surgeon via the modulation of several parameters including vacuum and/or flow rate, cut rate, and duty cycle. Commercially-available vitrectomy platforms employ peristaltic and/or Venturi pumps to allow for real-time modulation of flow and/or vacuum by the surgeon. Cut rate refers to the frequency of a guillotine blade within the vitrectomy probe that serves to shear tissue entering the port, an opening in the distal aspect of the vitrectomy probe lumen. Duty cycle refers to the ratio of port open- vs. closed time

during a cutting cycle. The common conclusion among the studies is that the cut rate, the vacuum pressure, cutter gauge, and distance the probe is away from the edge are factors that contribute the amount of traction being observed on the retina. Traction is defined to be the adhesive friction force that is used to generate motion between the body and the tangential surface.

Based on literature search, there is no evidence to prove that a method to quantify the movment of the retina *in vivo* during pars plana vitrectomy is developed. This method will aid in the comparison of different instruments and in the effect of varying machine parameters. Based on these measurements, parameters and specifications can be determined to minimize shear force or traction on the retina during pars plana vitrectomy.

After surgery was performed *in vivo*, surgical video recordings were used to determine retinal motion. The movement of the structure in a two-dimensional image time series was determined using ImageJ and Kymograph plugin. A corresponding line was drawn on the image sequence so that the line was perpendicular to the movement of the retina. Since the brightness level for each position was not consistent, the threshold was adjusted to accommodate for the differences, and the image was converted into Binary. The total displacement of a segment of mobile retina was estimated using the minimum and maximum pixel positions of the margin of a retinal tear within the frame for all the frames. The net position was obtained and was divided by elapsed time in order to determine the velocity of retinal movement. The experimental videos had net distance movement ranging from 152 to

389 pixels, and 93 to 101 pixels for the control. The results obtained for all of the experimental values differed and did not seem to have any correlation, especially since the only information initially measured were the net distance traveled. For this reason, the velocity was determined by taking the quotient of the net distance traveled and the distance in order to compare movements among videos. This analysis was performed for seven experimental videos and a control. In addition, acquisition of a common anatomical reference point was not possible, another reference point was established: edge of the camera frame. Finally, a manual frame-by-frame analysis was performed to validate the approach of using ImageJ and Kymograph as a tracking method.

After taking into considerations constraints and assumptions established in the scope of this project, it is evident that the distance between the probe and the retinal tear made an impact on the movement of the retinal at the margin of the retinal break. Decreased velocity of retinal motion was associated with greater distance of the probe from the retinal tear. Based on this analysis, the use of ImageJ is a valid method to measure the motion of the retina during pars plana vitrectomy surgery. Furthermore, comparing the control to experimental values, it is evident that even the least velocity of the retinal motion during vitrectomy was twice the velocity of the control. Therefore, there is a clear distinction between experimental and the control parameters.

With regard to using the camera edge as a reference, the average distance from the edge of the camera frame to the edge of the retina was significantly less than the net

movement of the retinal tear ($p<0.0001$). Therefore, it is satisfactory to assume that the edge of the camera can be a viable reference point. Furthermore, the results for the frame-by-frame analysis showed that the average of the actual value obtained from the Plot Profile on ImageJ was close to the average of the experimental value obtained from the kymograph. The relative error between them of 0.369% articulates that the kymograph provides results very close to the actual results. However, the standard deviation from the mean was about 7% difference. Nonetheless, this could be due to the sources of error, constraints, and the assumptions that were made.

There was good correlation of measures of retinal movement when adjacent segments along a retinal tear were measured, while increasing variability of retinal motion measures was observed with increasing separation of retinal segments. This supports our algorithm as a valid tool to determine retinal motion.

In summary, a novel method to detect the movement of the retina was introduced. This approach has been established to quantitatively detect the movement of the retina during pars plana vitrectomy *in vivo*.

I. INTRODUCTION

Pars plana vitrectomy is necessary to access the posterior segment of the eye. The surgeons today have numerous types of probes to select from when performing vitreoretinal surgery. The studies previously performed are based on the pressure, traction, cut rate, and distance the probe is from the retina. However, using imaging software, a novel approach has been established to quantitatively detect the movement of the retina during pars plana vitrectomy. This new approach is implemented *in vivo* after the surgery has been performed. To my knowledge, no quantitative method has been reported to determine the movement of the retina *in vivo* using ImageJ.

The goal of the experiment was to determine a method of measuring the motion of the retina during pars plana vitrectomy *in vivo*.

A. Anatomy of the Eye

The eye as shown in Figure 1 is an essential organ that gives us the ability to see; it is one of the five primary senses. The eye allows the interpretation of the shape, color, and dimension of an object; it also helps detect the brightness and adjust the view accordingly. There are many components to the eye; however, for the purposes of this thesis, the concentration will be placed on vitreous body and the retina.

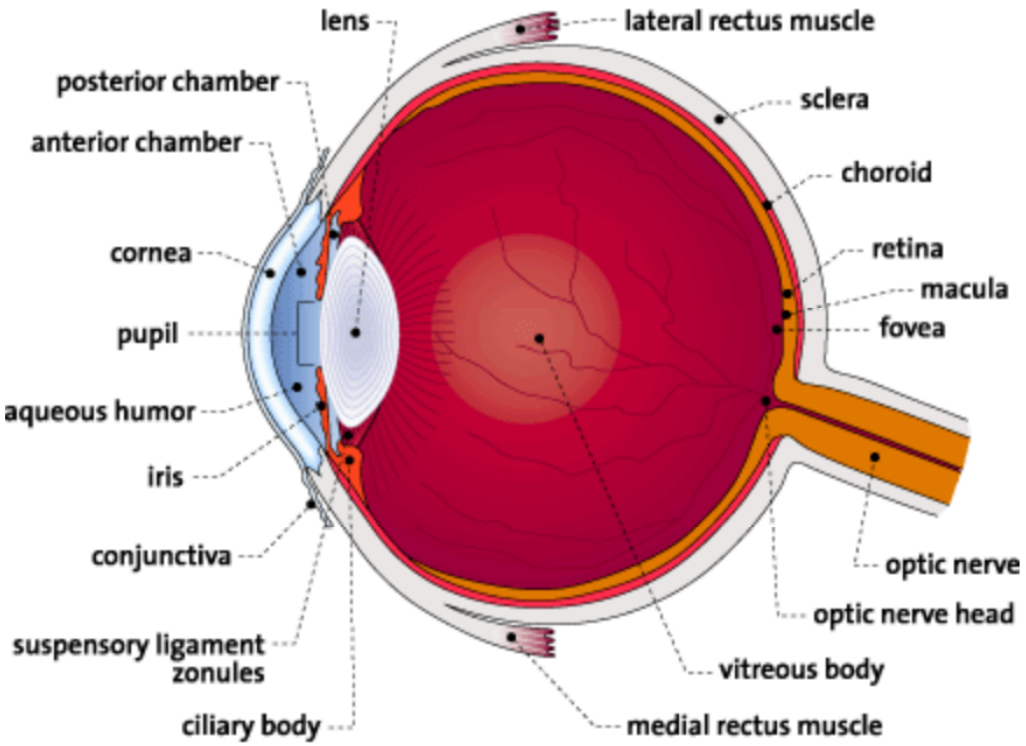

Figure 1: Sketch of the Eye – Showing the Vitreous Body and its Relations. About 80% of the eye is occupied by the vitreous cavity. It is composed of a clear gel-like fluid that is primarily composed of water. This image was taken from Bagi 2014. [1]

1. The Vitreous Body

Approximately 80% of the volume of the eye is occupied with the vitreous body, making it the largest single structure of the eye as shown in Figure 1. The anterior portion of the vitreous abuts the lens, and the posterior portion of the vitreous is joined to the retina. The vitreous is a semisolid transparent gel that is primarily composed of water, and approximately 1% of this gel is composed of collagen, hyaluronic acid, and other components. The vitreous body is composed of connective tissue that provides structural and metabolic support for the ocular tissues. [2]

2. The Retina

The posterior portion of the vitreous is attached to the retina. The retina is the innermost layer of the eyeball. It contains two microscopic photoreceptors: rods, which are receptors for nigh vision, and cones, which are receptors for day vision [3]. The tear in the retina can be instigated by many causes: structural changes in the vitreous humor, ocular injury, diabetes, inflammatory eye diseases, and many more [4].

B. Pars Plana Vitrectomy

Robert Machemer first developed pars plana vitrectomy in 1970, which allows the controlled access to the posterior segment of the eye [5, 6]. Currently, this surgery can by performed as an outpatient procedure [6]. Previously, this procedure was used for the purpose of extracting blood from the vitreous cavity; however, now it has many applications [6]. As stated earlier, pars plana vitrectomy is necessary to access the posterior portion of the eye in order to perform rhegmatogenous or tractional retinal detachment, vitreous hemorrhage, retained lens fragments after cataract surgery, endophthalmitis, epiretinal membrane, macular hole, vitreomacular traction, and intraocular foreign bodies [6]. A major indication for surgery of the retina and vitreous is retinal detachment. Rhegmatogeneous retinal detachment is caused by a tear in the neurosensory retina in association with the passage of liquid vitreous through the break and into the subretinal space, causing separation of the retina from the underlying retinal pigment epithelium [6]. The most frequent modality used to treat retinal detachment at present is 3-port pars plana vitrectomy. The vitreoretinal surgeon typically employs a cutting/aspirating instrument (the vitrectomy probe), a fiberoptic endoilluminator (the light source), and an infusion port to introduce fluids or gases thereby maintaining suitable intraocular pressure and volume as vitreous is aspirated [6].

Prior to the procedure, local anesthesia is given to the patient, followed by draping the surgical field appropriately. A 23-, 25-, or 27-guage system is used to penetrate through the sclera to access the vitreous. Three incisions using trocars are made that are located in the

inferotemporal, superotemporal, and superonasal quadrants as shown in Figure 2. The cannula, which is on the trocar, is penetrated into the sclera at an angle between 9° and 45°, which depended on the gauge. [6]

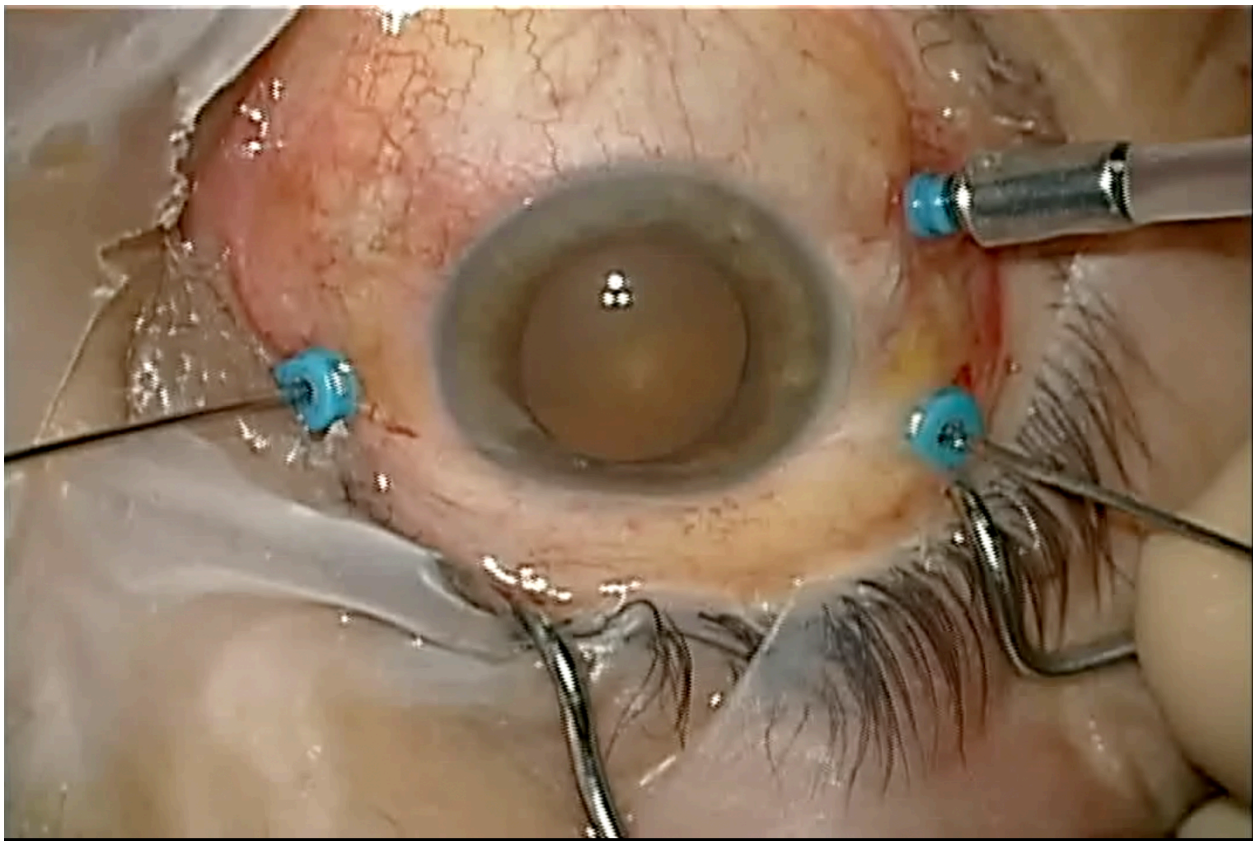

Figure 2: Incision Sites for pars plana vitrectomy. Three incisions are made using trocars in the in the inferotemporal, superotemporal, and superonasal quadrants. The infusion line is place in the inferotemporal region (upper right hand cannula), whereas the light source and the vitrector are rotated between the superotemporal and superonasal region (lower cannulas).

The trocar is inserted into the vitreous cavity until the hub of cannula was flush with the sclera. The trocar is then removed, leaving the cannula in place. This is done for the two other incisions as well. The infusion line is place in the inferotemporal region, where as the light source and the vitrector are rotated between the superotemporal and superonasal region. The

infusion line is used to maintain the pressure in the vitreous cavity, so the eye did not collapse. Using the vitrector probe, the vitreous fluid is aspirated starting from the anterior side. Once reaching close to the posterior side, the control will be based on the case. [6]

However, when aspiration reached closer to the region of the tear of the retina, the shaving of the vitreous base of often necessary [6]. It is noted that the strongest adherence between the vitreous body and the retina occurs at the base of the vitreous [2]. During the entire procedure, controlled excision and aspiration of vitreous and other intraocular tissues is performed by the surgeon via the modulation of several parameters including vacuum and/or flow rate, cut rate, and duty cycle. Commercially-available vitrectomy platforms employ peristaltic and/or Venturi pumps to allow for real-time modulation of flow and/or vacuum by the surgeon. Cut rate refers to the frequency of a guillotine blade within the vitrectomy probe that serves to shear tissue entering the port, an opening in the distal aspect of the vitrectomy probe lumen. Duty cycle refers to the ratio of port open- vs. closed time during a cutting cycle. For this thesis, the movement of the retina when the vitrector probe is close to the posterior side close to where the retinal tear occurred was analyzed.

Following the removal of the vitreous, the surgeon chooses to perform other intraocular procedures in order to repair the damage. Upon completion of this, to replace the vitreous fluid that is aspirated earlier, the surgeon chooses to replace with either gas-air exchange (sulfur hexafluoride [SF_6] or octafluoropropane [C_3F_8]) or silicone oil injection. Upon completion, the light source and the vitrector probe are removed followed by the infusion line. The 23-, 25, and

27-guage stents are designed to self-seal upon removal; therefore, after removing the cannula, pressure is applied using a cotton tip since no sutures were required. Finally, after antibiotics and steroids are administered, the eye is shielded. [6]

C. Vitreous Cutters Used for Pars Plana Vitrectomy

The surgeons today have numerous types of probes to select from when performing vitreoretinal surgery [7–9]. Over the years, these cutters have transformed into a smaller, safer, and faster with higher cut rates [10]; however a cutter to produce the lowest amount of shear force on the retinal tissue is still in need [9]. The common conclusion among the studies is that the cut rate, the vacuum pressure, cutter gauge, and distance the probe is away from the edge are factors that contribute the amount of traction being observed [9, 11–15]. Traction is defined to be the adhesive friction force that is used to generate motion between the body and the tangential surface [16].

Knowledge of the engineering concepts involved in vitrectomy surgery have facilitated in better selection of tools as well as the techniques to perform pars plana vitrectomy safely [10]. It is important to note that due to the complexity of the tissue in the eye, the cutting prevents an exact physics-based understand and mathematical representation [10].

Previous experiments have performed their analysis based on physiological parameters in *ex vivo*. However, the way the biological system works in ex vivo may not be the same for the

in vivo case. For this reason, it is important to perform the experiments *in vivo* in order to evaluate true effects on the physical motion.

D. In-Vivo Approach to Quantify Retinal Motion

The studies that were previously performed were based on the pressure, traction, cut rate, and distance the probe is from the retina. However, in this method, using imaging software, a novel approach has been established to quantitatively detect the movement of the retina during pars plana vitrectomy. This new approach has been performed *in vivo* after the surgery has been performed. To my knowledge, no quantitative method has been reported to determine the movement of the retina *in vivo* using ImageJ. This method can help compare different instruments and different parameters that different companies are claming to decrease the amount of shear that is acting on the retina. However, it also important to note not seem that it is necessary to determine the exact values as the estimates maybe enough to compare. Based on these estimates, the parameters and specifications can be determined to produce the lowest amount of shear force or traction on the retina during pars plana vitrectomy.

II. METHODS

A novel method to detect the movement of the retina is introduced. This approach can be performed *in vivo* following the pars plana vitrectomy. The method can quantitatively determine the motion of the retina when the probe is close to the retinal tear. Imaging software was used to assist in detecting the movement of the retina.

The goal of the experiment is to determine a method of measuring the motion of the retina during pars plana vitrectomy *in vivo*.

More on how the approach had been implemented will be explained in this chapter. Further, the assumptions and the constraints will also be explained. Finally, this approach is also compared to a manual frame-by-frame analysis.

A. Assumptions and Constraints

There were several assumptions that were taken into consideration before coming up with an approach to quantitatively identify the movement of the retinal tear. First of which is the movement of the video camera is assumed to be minimal. Because during the duration of the video that the motion of the retina is examined, the translation of the video camera is considered to be negligible. This assumption is proved in the results. Second, the line segment that is drawn on the image sequence in ImageJ is assumed to be as close to perpendicular to the movement of the retinal tear. Finally, the retinal tear flap is assumed to be moving in a linear fashion, meaning it is moving up and down along the perpendicular line segment on the image sequence.

In addition to the assumptions, there were also some constraints that were involved in the experiment. One of the constraints is the distance from the probe to the retinal tear is not controlled for this experiment as it is based on the surgeon's convenience. Another constraint is because of the high magnification of the video during the pars plana vitrectomy, it is impossible to detect a common anatomical reference point for all the videos. Further, based on every individual's lens and cornea, the magnification varies. For this reason, the edge of the camera frame is used as the reference point. Moreover, the analysis is based on a previously recorded surgery, so this converted the analysis to obtaining results in the Two-Dimension. Because of this, the movement happening in the z-direction is neglected, even though there is movement

happening in the z-direction. Finally, the brightness of the light source, vacuum pressure, cut rate were not controlled. All those were controlled based on surgeon's convenience.

B. Image Analysis Using ImageJ for Experimental Sections

In order to repair the damage of the retinal tear, it was necessary to perform a vitrectomy. During this procedure, the vitrectomy performed by the Retinal Surgeon was recorded. The video obtained from the vitrectomy was trimmed to where the movement of retinal motion occurred and was cropped to emphasize the movement using video editing software (iMovie, Apple Inc., Cupertino, CA). This trimmed and cropped video was converted into a series of images in the format of Tagged Image File Format (.tif) with a frame rate of 30 images per second using a video converter (Square 5 srl, Rome, Italy).

In order to analyze and determine the movement of the retinal tear, these images were imported as an image sequence into a Java-based image-processing program, ImageJ, developed by the National Institute of Health as shown in Figure 3. ImageJ is public domain software that is designed for image processing and analysis. This software has the capability of providing pixel value statistics, distances, angles, density histograms, and line profile plots. Most importantly, it supports image-processing functions such as edge detection. One of the advantages of this domain is that it is designed to be an open architecture that provides expandability via Java plugins, which can be built in the editor and Java compiler available within ImageJ. [17]

Figure 3: Image Sequence after importing into ImageJ. After cropping and trimming, the Vitrectomy video was converted to images with frame rate of 30 images per second. This image sequence was imported into ImageJ to analyze and help determine the movement of the retinal movement.

After importing the image sequence into ImageJ, an external plugin called Kymograph (time space plot) Plugin for ImageJ was installed. The purpose of this external plugin is to help determine the velocity of the moving structure in the image time series in a two-dimensional image series. The way this plugin works is a line is drawn through the first image, which is carried on to each frame in the sequence. The gray scale values along the line were displayed into another new image. The line produced by the first frame is recorded as the first row of this new image; the line produced by the second frame is recorded as the second row of this new image; and so forth. This process was continued until all the gray scale value of the line of each frame is recorded. Therefore, the new image will produce an image that has x-axis as the gray scale value along the line with units of pixels whereas the y-axis is the number of frames in the image sequence. The velocity can then be measured using the kymograph created; however,

for this experiment, velocity was not obtained using this method. This process will later be explained in detail. [18]

Following the installation of the plugin into ImageJ and importing the image sequence, the image sequence was converted from color into a 32-bit image type in order to convert to a monotone color. Using the stack images option, the images were stacked on each other creating a new image based on the maximum intensity of all the images in the series. Based on the intensity on this new image, the position where most of the movement was occurring was determined. On this image stack as shown in Figure 4, the white portions indicate the greatest intensity among all the frames in the image sequence.

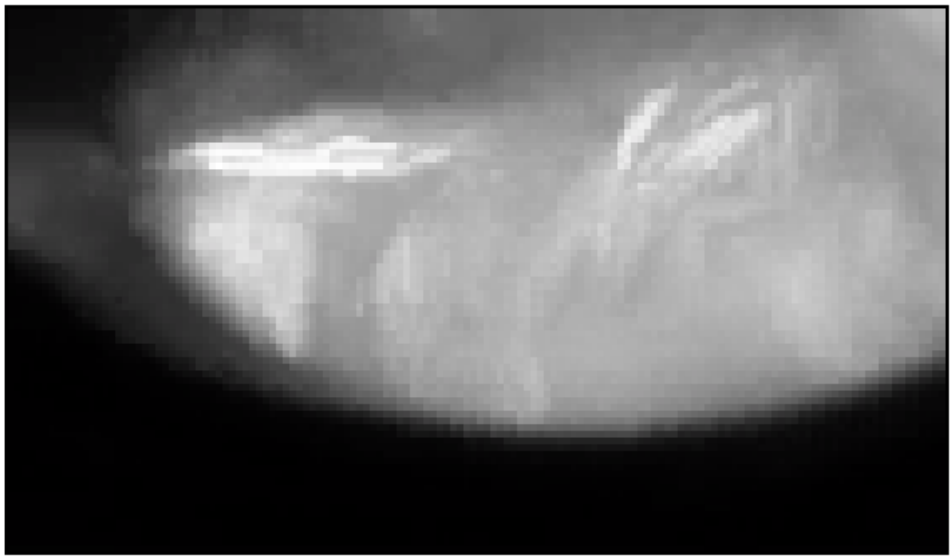

Figure 4: Image Stack based on Maximum Intensity on ImageJ. After importing the image sequence into ImageJ, using the stack images option, the images were then stacked on each other creating a new image based on the maximum intensity of all the images in the series. In this figure, the white portions indicate the location with the maximum intensity.

The corresponding line segment was drawn where there was the most intensity on the image stack based on maximum intensity image; the line was then restored to the image sequence file. The length of the line as well as its angle was modified manually, so the line was perpendicular to the movement of the retina. The reason for this was to detect the movement of the retinal tear, especially since there was no initial marker on the tear. Therefore, it was impossible to detect the actual movement of a specific point of the retinal tear. Hence, detecting a generalized motion by using the perpendicular line would result in the movement of the retina. Once the line was placed perpendicular to the movement of the retina, the kymograph was produced as shown in Figure 5.

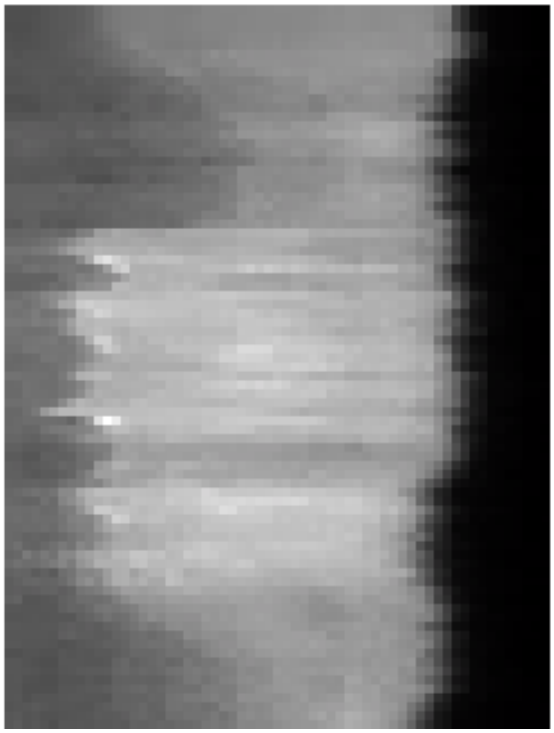

Figure 5: Kymograph Produced by the Image Sequence. After image sequence was imported to ImageJ, the kymograph was produced. It displayed the gray scale values along the line in the image sequence for all the images in the sequence. The x-axis of this image is the gray scale value along the line with units of pixels whereas the y-axis is the number of frames in the image sequence.

Following the assembly of the kymograph, the threshold level was adjusted in order to detect only the necessary portions of the kymograph. Since the brightness of each video was not consistent, the threshold level was adjusted manually in ImageJ to identify the motion of the retina as shown in Figure 6 (a). In this image, the red shows the region that the threshold detected. After detecting the portion, this image was converted into a binary image, based on the desired threshold level. The binary image as shown in Figure 6 (b) and was saved as XY coordinates, the x-coordinates were the pixel position, whereas y-coordinates were the frame number. This data was imported into Microsoft Excel for further analysis.

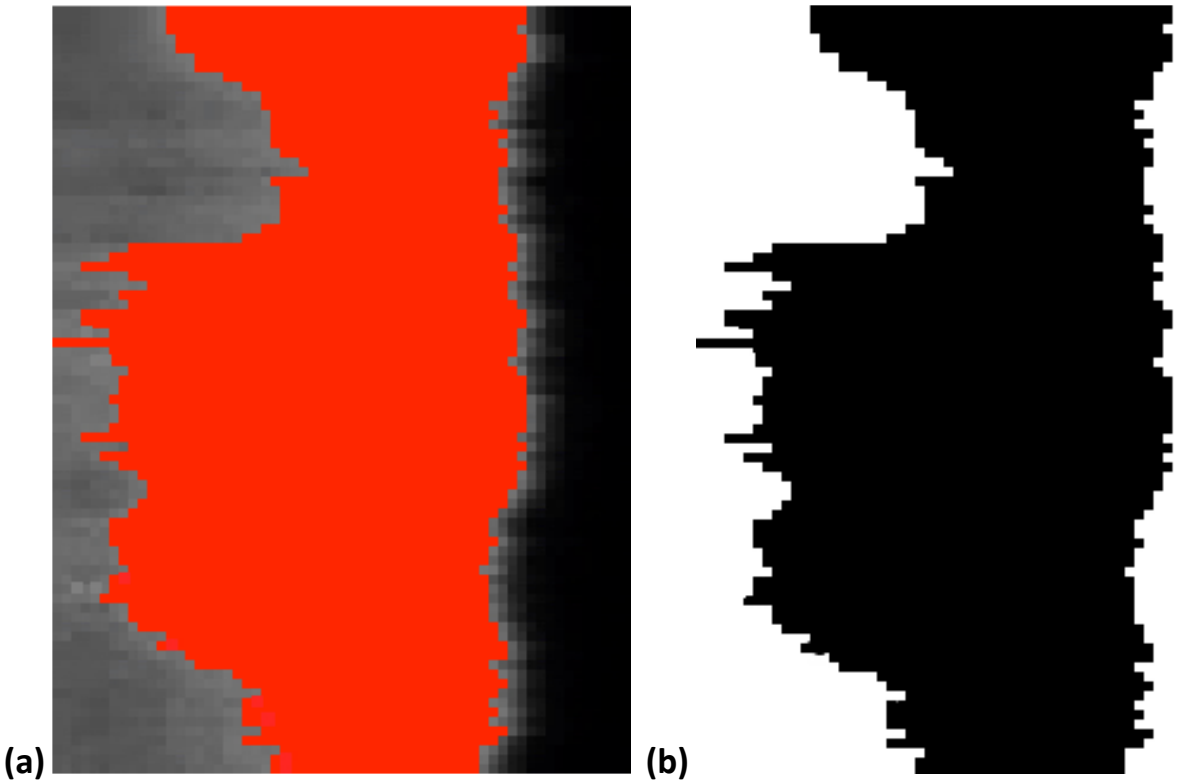

Figure 6: Applying Threshold to Image Sequence to Turn it into Binary. (a) Because the brightness of each video was not consistent, the threshold level was adjusted manually in order to identify the range of motion of the retinal movement. The essential portion of the kymograph is shown in red. (b) After applying the threshold level, the 8-bit images were converted into a binary image, which was exported as XY coordinates.

After the data was exported to Microsoft Excel, a Manual Pivot Table was designed, where the Row Labels were defined as the frame number (Y-Coordinates), and the Values were defined as the Maximum of the pixel position (X-Coordinates). In addition, another pivot table was made similarly, but the only difference was this time the Minimum of the pixel position (X-Coordinate) was determined. The Pivot Tables displayed the minimum value and the maximum pixel value for each frame; based on this, the length of the retina in each frame was estimated. The combination of all the frames can provide the movement of the retinal motion occurring in the video. In order to calculate the movement of the retina, the minimum value of the pixel position was subtracted from the maximum value of the pixel position within the frame. This produced the net movement within each frame.

Next, the distance between each frame was calculated based on the net position movement within each frame, and the all of these distances were added in order to produce a net distance traveled by the retina during the entire video. Finally, the net distance was divided by the number of frames and frame rate (30 pixels per second) in order to determine the velocity of the retinal movement. The reason to calculate the retinal motion was to compare the movement occurring between different video samples. The outcomes of this will be provided in the Results chapter.

This procedure was done eight times per video. However, the line segment was shifted two pixel values in the x-direction. Based on the eight sample segments, the average net

distance and velocity were determined. Since the brightness differed from location to location, the threshold level was also guaranteed to differ in some situations.

C. Image Analysis Using ImageJ for Control

In order to validate the movement occurring in the experimental portions of the retina, a control was needed. The control in this case was a location where the retina was not moving. Upon obtaining the desired location of the no movement of the retina, the same procedure was done as it was for the experimental sections: (1) the Kymograph was produced for the corresponding line segment; (2) the threshold was adjusted to detect the specific parts of the movement; (3) based on the threshold level, the kymographic image was turned into binary; (4) the binary image was saved as an XY coordinate system; (5) the XY coordinated system was imported into Microsoft Excel; (6) a pivot table was constructed, where the row labels were defined as the frame number (Y-Coordinates), and the Values were defined as the maximum/minimum of the pixel position (X-Coordinates); (7) the length of the retina in each frame was estimated by taking the minimum and subtracting it from the maximum pixel location within the frame for all the frames in the video; (8) the distances between each frame was calculated; (9) all the distances were added to measure the net distance traveled by the retina during the video; (10) the net distance was divided by the number of frames and frame rate (30 pixels per second) in order to determine the velocity of the retinal movement. This procedure was performed a total of eight times, where the line segments were shifted two pixel values in the x-direction. Based on this, the average net distance and average velocity

were calculated. In this situation also, since the brightness level for each position was not consistent, the threshold may have been adjusted to accommodate for the differences.

D. Validation – Using Camera Edge as Reference Point

As mentioned earlier, the high magnification of the video during the pars plana vitrectomy made it impossible to detect a common anatomical reference point for all the videos. The reason for this was that the tear in the retina could potentially occur anywhere in the back of eye. Therefore, another reference point was needed to be determined. Hence, the edge of the camera frame was used as a reference point. In order to validate this point, an arbitrary line was drawn so that it passed through the camera edge from the edge of the frame in the image sequence in ImageJ.

The Kymograph was produced for the corresponding line segment, and the threshold was adjusted to detect the edge of the camera to the edge of the frame as shown in Figure 7. After converting into a binary image and saving it an XY coordinate system, a pivot table was constructed on Microsoft Excel. The pivot table detected the maximum value only, since the minimum value for each of the frames was zero as it was the edge of the frame, for each frame. Following, the mean length of the segment for all frames was calculated; the distance away from this mean length was subtracted for each frame. Upon determining the distance away from the mean for each frame, the average change in distance was determined as well as its standard deviation fore each segment.

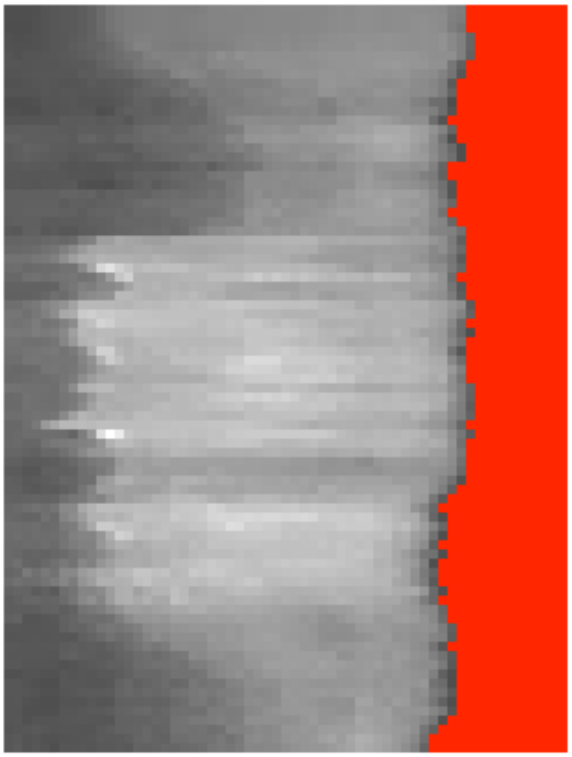

Figure 7: Portion of Kymograph Used to Determine Camera Edge as Reference Point. In order to confirm that the edge of the camera can be used for the reference point, an arbitrary line was drawn from the edge of the frame and crossed the camera edge. The kymograph was produced, and the threshold was adjusted so the distance between the edge of camera and the edge of the frame was detected.

This process was performed a total of eight times, where the distance between each line segment was two pixels apart. Based on this, the mean of the average of the distance away from the mean as well as the standard deviation were calculated. In addition, the average of the standard deviation and its standard deviation were also obtained. The reason for this was to accurately determine if using the camera edge was a valid assumption to make.

E. Validation – Frame-by-Frame Analysis

In order to validate this entire experiment, a manual frame-by-frame analysis was performed. After importing the image sequence into ImageJ, the same analysis to determine the location of the retinal motion was performed. Once the line was modified, the Plot Profile as shown in Figure 8 was used to determine the gray scale value for each pixel along the length of the line segment for each frame. The plot profile on ImageJ also has the capability to obtain the numerical value.

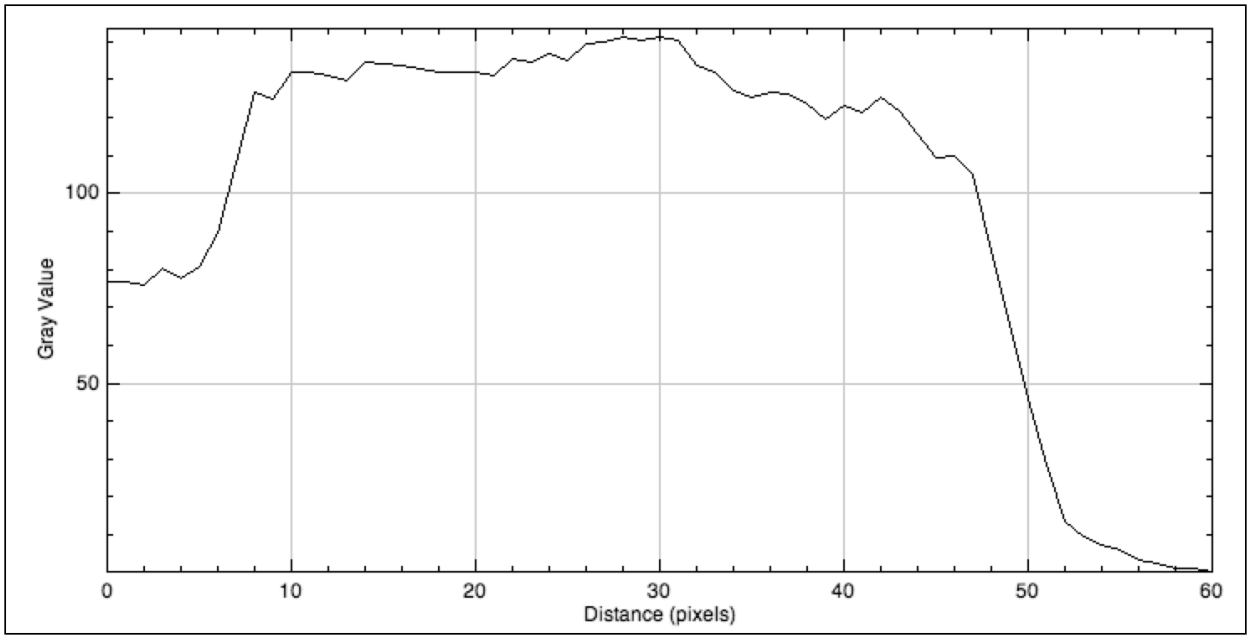

Figure 8: Plot Profile of Kymograph for Frame-by-Frame Analysis. After importing the image sequence into ImageJ, the same analysis done for the experimental sections in order to determine the location for the movement of the retina was applied. Upon confirming the location of the line, the Plot Profile of the line was displayed, where the x-axis represents the distance of the line in pixels and y-axis is the gray value (8-bit). On here, the distance with the maximum, positive slope was the location of the edge of retina, and the distance with the maximum, negative slope was the location of the edge of the camera.

This information was transferred to Microsoft Excel in order to determine the slope between the points. The pixel location where the maximum, positive slope occurred was the location of the edge of the retina. The pixel location where the maximum, negative slope occurred was the location of the edge of the camera. The difference of this was compared to the experimental value.

In order to obtain the kymograph, the same procedure that was done as stated in the Experimental section was performed. This was done for every five frames within the video segment. Based on this, the relative error between the experimental value and actual value was determined.

III. RESULTS

A novel method to detect the movement of the retina was introduced. This approach can be performed *in vivo* following the pars plana vitrectomy. This method can quantitatively determine the motion of the retina when the probe was close to the retinal tear. Imaging software was used to assist in detecting the movement of the retina.

The goal of the experiment was to determine a method of measuring the motion of the retina during pars plana vitrectomy *in vivo*.

More on the results that were obtained for each experiment will be presented in this chapter. The calculated portion of the raw data is provided in the in Appendix.

A. Image Analysis Using ImageJ for Experimental Sections

The experimental videos that showed movement in the retina was obtained and analyzed using ImageJ in order to obtain a kymograph of the motion of the retina. A threshold was adjusted in order to detect the specific parts of the motion since the brightness of the video was not constant for all the locations. The kymograph was converted into a binary image and outputted to Microsoft Excel in order to determine the length of the retina for each frame in the video. Based on the length of the retina, the distance between the retinal movements in each frame to another was calculated. These distances were added to measure the net distance traveled by the retina during the video. This net distance was divided by the time of the duration of the video in order to determine the velocity of the retinal motion. This process was performed 8 times with the line segment shifted by two pixels. The average net distance traveled as well as the average velocity were determined. This value can be used to compare to other videos since the length of the videos was not consistent

Information for Video 1 is shown in Table 1. The initial and final coordinates were measured. The distance between the segments was two pixels in length: The Y-Coordinate is kept constant, whereas the X-Coordinate was modified. The length of the line segment was measured to be 140.26 pixels with an angle of -131.53°. Furthermore, the threshold level for all the line segments were kept constant ranging from 120 to 255 after the kymograph was converted to an 8-bit image. The net distance and the velocity of the Video 1 were calculated and shown in Table 2. The number of frames in the video was 56 frames with a frame rate of 30

frames per second resulting in 1.87 seconds of video. The net distance travelled by the retina in Video 1 was 185 ± 8 pixels, and the velocity was calculated to be 99 ± 4 pixels/second.

Information for Video 2 is shown in Table 3. The initial and final coordinates were measured. The distance between the segments was two pixels in length: The Y-Coordinate is kept constant, whereas the X-Coordinate was modified. The length of the line segment was measured to be 112.45 pixels with an angle of -136.08°. Furthermore, the threshold level for all the line segments were kept constant ranging from 120 to 255 after the kymograph was converted to an 8-bit image. The net distance and the velocity of the Video 2 were calculated and shown in Table 4. The number of frames in the video was 109 frames with a frame rate of 30 frames per second resulting in 3.63 seconds of video. The net distance travelled by the retina in Video 2 was 353 ± 12 pixels, and the velocity was calculated to be 97 ± 3 pixels/second.

Information for Video 3 is shown in Table 5. The initial and final coordinates were measured. The distance between the segments was two pixels in length: The Y-Coordinate is kept constant, whereas the X-Coordinate was modified. The length of the line segment was measured to be 125 pixels with an angle of -90°. Furthermore, the threshold level for this video was not kept constant since the brightness of the portions of the video were not consistent; the range of the threshold after the kymograph was converted to an 8-bit image were from 120 to 255, 130 to 255, and 140 to 255. The net distance and the velocity of the Video 3 was calculated and shown in Table 6. The number of frames in the video was 66 frames with a frame rate of 30

frames per second resulting in 2.20 seconds of video. The net distance travelled by the retina in Video 3 were 203 ± 7 pixels, and the velocity was calculated to be 92 ± 3 pixels/second.

Information for Video 4 is shown in Table 7. The initial and final coordinates were measured. The distance between the segments was two pixels in length: The Y-Coordinate is kept constant, whereas the X-Coordinate was modified. The length of the line segment was measured to be 136.09 pixels with an angle of -87.89°. Furthermore, the threshold level for all the line segments were kept constant ranging from 110 to 255 after the kymograph was converted to an 8-bit image. The net distance and the velocity of the Video 4 were calculated and shown in Table 8. The number of frames in the video ranged from 126 to 139 frames with a frame rate of 30 frames per second resulting in 4.20 to 4.63 seconds of video. The reason for the change in frames between the video segment samples could be that the movement of the retinal tear was not moving during all the frames. The net distance travelled by the retina in Video 4 was 379 ± 11 pixels, and the velocity was calculated to be 83 ± 2 pixels/second.

Information for Video 5 is shown in Table 9. The initial and final coordinates were measured. The distance between the segments was two pixels in length: The Y-Coordinate is kept constant, whereas the X-Coordinate was modified. The length of the line segment was measured to be 126.91 pixels with an angle of -59.19°. Furthermore, the threshold level for this video was not kept constant; the ranges of the threshold after the kymograph was converted to an 8-bit image were from 110 to 255 and 120 to 255. The net distance and the velocity of the Video 5 were calculated and shown in Table 10. The number of frames in the video was 72

frames with a frame rate of 30 frames per second resulting in 2.40 seconds of video. The net distance travelled by the retina in Video 5 was 201 ± 8 pixels, and the velocity was calculated to be 84 ± 3 pixels/second.

Information for Video 6 is shown in Table 11. The initial and final coordinates were measured. The distance between the segments was two pixels in length: The Y-Coordinate is kept constant, whereas the X-Coordinate was modified. The length of the line segment was measured to be 138.32 pixels with an angle of -74.05°. Furthermore, the threshold level for all the line segments were kept constant ranging from 135 to 255 after the kymograph was converted to an 8-bit image. The net distance and the velocity of the Video 6 were calculated and shown in Table 12. The number of frames in the video was 68 frames with a frame rate of 30 frames per second resulting in 2.27 seconds of video. The net distance travelled by the retina in Video 6 was 165 ± 10 pixels, and the velocity was calculated to be 73 ± 4 pixels/second.

Information for Video 7 is shown in Table 13. The initial and final coordinates were measured. The distance between the segments was two pixels in length: The Y-Coordinate is kept constant, whereas the X-Coordinate was modified. The length of the line segment was measured to be 145.36 pixels with an angle of -115.68°. Furthermore, the threshold level for all the line segments were kept constant ranging from 111 to 255 after the kymograph was converted to an 8-bit image. The net distance and the velocity of the Video 7 were calculated and shown in Table 14. The number of frames in the video was 42 frames with a frame rate of

30 frames per second resulting in 1.40 seconds of video. The net distance travelled by the retina in Video 7 was 209 ± 3 pixels, and the velocity was calculated to be 149 ± 2 pixels/second.

B. Image Analysis Using ImageJ for Control

In order to validate the movement occurring in the experimental portions of the retina were valid, a control, where the retina was not moving, was needed. Upon determining a location of the no movement of the retina, the same procedure was done as it was for the experimental sections. Information for the Control video is shown in Table 15. The initial and final coordinates were measured. The distance between the segments was two pixels in length: The Y-Coordinate is kept constant, whereas the X-Coordinate was modified. The length of the line segment was measured to be 56.94 pixels with an angle of -121.62°. Furthermore, the threshold level for all the line segments were kept constant ranging from 50 to 255 after the kymograph was converted to an 8-bit image. The net distance and the velocity of the Control were calculated and shown in Table 16. The number of frames in the video was 79 frames with a frame rate of 30 frames per second resulting in 2.63 seconds of video. The net distance travelled by the retina in control was 96 ± 2 pixels, and the velocity was calculated to be 36 ± 1 pixels/second.

Segment	X_1	Y_1	X_2	Y_2	Angle	Length	Threshold
L1	179	24	86	129	-131.53°	140.26	120-255
L2	181	24	88	129	-131.53°	140.26	120-255
L3	183	24	90	129	-131.53°	140.26	120-255
L4	185	24	92	129	-131.53°	140.26	120-255
L5	187	24	94	129	-131.53°	140.26	120-255
L6	189	24	96	129	-131.53°	140.26	120-255
L7	191	24	98	129	-131.53°	140.26	120-255
L8	193	24	100	129	-131.53°	140.26	120-255

Table 1: Elementary Information of Video 1. Based on the initial and final coordinates shown for each sample line segment, a kymograph was produced using ImageJ. The line was 140.26 pixels in length and had an angle of -131.53°. The threshold ranged from 120-255 after converting the image of the kymograph to 8-bit in ImageJ.

Segment	Frames	Time (Seconds)	Net distance (Pixels)	Velocity (Pixels/Second)
L1	56	1.87	192	103
L2	56	1.87	188	101
L3	56	1.87	174	93
L4	56	1.87	194	104
L5	56	1.87	183	98
L6	56	1.87	180	96
L7	56	1.87	192	103
L8	56	1.87	173	93
AVERAGE	**56.00**	**1.87**	**185**	**99**
Std. Dev.	**---**	**---**	*8*	*4*

Table 2: Net Length and Velocity of Video 1. The number of frames on this segment that detected the movement of the retina based on the sample line segment was 56 frames with a frame rate of 30 frames per second, resulting in 1.87 seconds. The net distance traveled was an average of 185 ± 8 pixels. This results in a velocity of 99 ± 4 pixels/second.

Segment	X_1	Y_1	X_2	Y_2	Angle	Length	Threshold
L1	207	64	126	142	-136.08°	112.45	120-255
L2	209	64	128	142	-136.08°	112.45	120-255
L3	211	64	130	142	-136.08°	112.45	120-255
L4	213	64	132	142	-136.08°	112.45	120-255
L5	215	64	134	142	-136.08°	112.45	120-255
L6	217	64	136	142	-136.08°	112.45	120-255
L7	219	64	138	142	-136.08°	112.45	120-255
L8	221	64	140	142	-136.08°	112.45	120-255

Table 3: Elementary Information for Video 2. Based on the initial and final coordinates shown for each sample line segment, a kymograph was produced using ImageJ. The line was 112.45 pixels in length and had an angle of -136.08°. The threshold ranged from 120-255 after converting the image of the kymograph to 8-bit in ImageJ.

Segment	Frames	Time (Seconds)	Net distance (Pixels)	Velocity (Pixels/Second)
L1	109	3.63	362	100
L2	109	3.63	372	102
L3	109	3.63	355	98
L4	109	3.63	341	94
L5	109	3.63	353	97
L6	109	3.63	359	99
L7	109	3.63	343	94
L8	108	3.60	336	93
AVERAGE	**108.88**	**3.63**	**353**	**97**
Std. Dev.	**0.35**	**0.01**	*12*	*3*

Table 4: Net Length and Velocity of Video 2. The number of frames on this segment that detected the movement of the retina based on the sample line segment range from 108 to 109 frames with a frame rate of 30 frames per second, resulting in 3.60 to 3.63 seconds, respectively. The net distance traveled was an average of 353 ± 12 pixels. This results in a velocity of 97 ± 3 pixels/second.

Segment	X_1	Y_1	X_2	Y_2	Angle	Length	Threshold
L1	108	0	108	125	-90°	125	120-255
L2	110	0	110	125	-90°	125	120-255
L3	112	0	112	125	-90°	125	120-255
L4	114	0	114	125	-90°	125	130-255
L5	116	0	116	125	-90°	125	130-255
L6	118	0	118	125	-90°	125	140-255
L7	120	0	120	125	-90°	125	140-255
L8	122	0	122	125	-90°	125	140-255

Table 5: Elementary Information for Video 3. Based on the initial and final coordinates shown for each sample line segment, a kymograph was produced using ImageJ. The line was 125 pixels in length and had an angle of -90°. The threshold ranged from 120-255 to 140-255 after converting the image of the kymograph to 8-bit in ImageJ. The reason for the varying thresholds was the contrast level on the frame.

Segment	Frames	Time (Seconds)	Net distance (Pixels)	Velocity (Pixels/Second)
L1	66	2.20	205	93
L2	66	2.20	197	90
L3	66	2.20	199	90
L4	66	2.20	198	90
L5	66	2.20	195	88
L6	66	2.20	203	92
L7	66	2.20	212	96
L8	66	2.20	213	97
AVERAGE	**66.00**	**2.20**	**203**	**92**
Std. Dev.	**---**	**---**	*7*	*3*

Table 6: Net Length and Velocity of Video 3. The number of frames on this segment that detected the movement of the retina based on the sample line segment was 66 frames with a frame rate of 30 frames per second, resulting in 2.20 seconds. The net distance traveled was an average of 203 ± 7 pixels. This results in a velocity of 92 ± 3 pixels/second.

Segment	X_1	Y_1	X_2	Y_2	Angle	Length	Threshold
L1	107	40	113	176	-87.89°	136.09	110-255
L2	109	40	115	176	-87.89°	136.09	110-255
L3	111	40	117	176	-87.89°	136.09	110-255
L4	113	40	119	176	-87.89°	136.09	110-255
L5	115	40	121	176	-87.89°	136.09	110-255
L6	117	40	123	176	-87.89°	136.09	110-255
L7	119	40	125	176	-87.89°	136.09	110-255
L8	121	40	127	176	-87.89°	136.09	110-255

Table 7: Elementary Information for Video 4. Based on the initial and final coordinates shown for each sample line segment, a kymograph was produced using ImageJ. The line was 125 pixels in length and had an angle of -90°. The threshold ranged from 110-255 after converting the image of the kymograph to 8-bit in ImageJ.

Segment	Frames	Time (Seconds)	Net distance (Pixels)	Velocity (Pixels/Second)
L1	126	4.20	360	86
L2	132	4.40	377	86
L3	139	4.63	389	84
L4	139	4.63	366	79
L5	139	4.63	388	84
L6	139	4.63	383	83
L7	139	4.63	381	82
L8	139	4.63	388	84
AVERAGE	**136.50**	**4.55**	**379**	**83**
Std. Dev.	**4.90**	**0.16**	*11*	*2*

Table 8: Net Length and Velocity of Video 4. The number of frames on this segment that detected the movement of the retina based on the sample line segment range from 126 to 139 frames with a frame rate of 30 frames per second, resulting in 4.20 to 4.63 seconds, respectively. The net distance traveled was an average of 379 ± 11 pixels. This results in a velocity of 83 ± 2 pixels/second.

Segment	X_1	Y_1	X_2	Y_2	Angle	Length	Threshold
L1	62	127	127	236	-59.19°	126.91	110-255
L2	64	127	129	236	-59.19°	126.91	110-255
L3	66	127	131	236	-59.19°	126.91	110-255
L4	68	127	133	236	-59.19°	126.91	110-255
L5	70	127	135	236	-59.19°	126.91	120-255
L6	72	127	137	236	-59.19°	126.91	120-255
L7	74	127	139	236	-59.19°	126.91	120-255
L8	76	127	141	236	-59.19°	126.91	120-255

Table 9: Elementary Information for Video 5. Based on the initial and final coordinates shown for each sample line segment, a kymograph was produced using ImageJ. The line was 126.91 pixels in length and had an angle of -59.19°. The threshold ranged from 110-255 to 120-255 after converting the image of the kymograph to 8-bit in ImageJ. The reason for the varying thresholds was because of the contrast level on the frame.

Segment	Frames	Time (Seconds)	Net distance (Pixels)	Velocity (Pixels/Second)
L1	72	2.40	197	82
L2	72	2.40	214	89
L3	72	2.40	196	81
L4	72	2.40	207	86
L5	72	2.40	201	84
L6	72	2.40	189	79
L7	72	2.40	205	85
L8	72	2.40	197	82
AVERAGE	**72.00**	**2.40**	**201**	**84**
Std. Dev.	**---**	**---**	*8*	*3*

Table 10: Net Length and Velocity of Video 5. The number of frames on this segment that detected the movement of the retina based on the sample line segment range was 72 frames with a frame rate of 30 frames per second, resulting in 2.40 seconds. The net distance traveled was an average of 201 ± 8 pixels. This results in a velocity of 84 ± 3 pixels/second.

Segment	X_1	Y_1	X_2	Y_2	Angle	Length	Threshold
L1	68	149	106	282	-74.05°	138.32	135-225
L2	70	149	108	282	-74.05°	138.32	135-225
L3	72	149	110	282	-74.05°	138.32	135-225
L4	74	149	112	282	-74.05°	138.32	135-225
L5	76	149	114	282	-74.05°	138.32	135-225
L6	78	149	116	282	-74.05°	138.32	135-225
L7	80	149	118	282	-74.05°	138.32	135-225
L8	82	149	120	282	-74.05°	138.32	135-225

Table 11: Elementary Information for Video 6. Based on the initial and final coordinates shown for each sample line segment, a kymograph was produced using ImageJ. The line was 138.32 pixels in length and had an angle of -74.05°. The threshold ranged from 135-255 after converting the image of the kymograph to 8-bit in ImageJ.

Segment	Frames	Time (Seconds)	Net distance (Pixels)	Velocity (Pixels/Second)
L1	68	2.27	160	71
L2	68	2.27	170	75
L3	68	2.27	178	79
L4	68	2.27	177	78
L5	68	2.27	168	74
L6	68	2.27	152	67
L7	68	2.27	161	71
L8	68	2.27	155	68
AVERAGE	**68.00**	**2.27**	**165**	**73**
Std. Dev.	**---**	**---**	*10*	*4*

Table 12: Net Length and Velocity of Video 6. The number of frames on this segment that detected the movement of the retina based on the sample line segment range was 68 frames with a frame rate of 30 frames per second, resulting in 2.27 seconds. The net distance traveled was an average of 165 ± 10 pixels. This results in a velocity of 73 ± 4 pixels/second.

Segment	X_1	Y_1	X_2	Y_2	Angle	Length	Threshold
L1	105	74	42	195	-115.68°	145.36	111-255
L2	107	74	44	197	-115.68°	145.36	111-255
L3	109	74	46	199	-115.68°	145.36	111-255
L4	111	74	48	201	-115.68°	145.36	111-255
L5	113	74	50	203	-115.68°	145.36	111-255
L6	115	74	52	205	-115.68°	145.36	111-255
L7	117	74	54	207	-115.68°	145.36	111-255
L8	119	74	56	209	-115.68°	145.36	111-255

Table 13: Elementary Information for Video 7. Based on the initial and final coordinates shown for each sample line segment, a kymograph was produced using ImageJ. The line was 145.36 pixels in length and had an angle of -115.68°. The threshold ranged from 111-255 after converting the image of the kymograph to 8-bit in ImageJ.

Segment	Frames	Time (Seconds)	Net distance (Pixels)	Velocity (Pixels/Second)
L1	42	1.40	214	153
L2	42	1.40	213	152
L3	42	1.40	208	148
L4	42	1.40	205	147
L5	42	1.40	205	147
L6	42	1.40	208	149
L7	42	1.40	210	150
L8	42	1.40	209	149
AVERAGE	**42.00**	**1.40**	**209**	**149**
Std. Dev.	**---**	**---**	*3*	*2*

Table 14: Net Length and Velocity of Video 7. The number of frames on this segment that detected the movement of the retina based on the sample line segment range was 42 frames with a frame rate of 30 frames per second, resulting in 1.40 seconds. The net distance traveled was an average of 209 ± 3 pixels. This results in a velocity of 149 ± 2 pixels/second.

Segment	X_1	Y_1	X_2	Y_2	Angle	Length	Threshold
L1	77	16	48	65	-121.62	56.94	50-255
L2	79	16	50	65	-121.62	56.94	50-255
L3	81	16	52	65	-121.62	56.94	50-255
L4	83	16	54	65	-121.62	56.94	50-255
L5	85	16	56	65	-121.62	56.94	50-255
L6	87	16	58	65	-121.62	56.94	50-255
L7	89	16	60	65	-121.62	56.94	50-255
L8	91	16	62	65	-121.62	56.94	50-255

Table 15: Elementary Information for Control. Based on the initial and final coordinates shown for each sample line segment, a kymograph was produced using ImageJ. The line was 56.94 pixels in length and had an angle of -121.62°. The threshold ranged from 50-255 after converting the image of the kymograph to 8-bit in ImageJ.

Segment	Frames	Time (Seconds)	Net distance (Pixels)	Velocity (Pixels/Second)
L1	79	2.63	101	37
L2	79	2.63	95	35
L3	79	2.63	99	37
L4	79	2.63	96	36
L5	79	2.63	95	35
L6	79	2.63	94	35
L7	79	2.63	93	35
L8	79	2.63	96	35
AVERAGE	**79**	**2.63**	**96**	**36**
Std. Dev.	**---**	**---**	*2*	*1*

Table 16: Net Length and Velocity of Control. The number of frames on this segment that detected the movement of the retina based on the sample line segment range was 79 frames with a frame rate of 30 frames per second, resulting in 2.63 seconds. The net distance traveled was an average of 96 ± 2 pixels. This results in a velocity of 36 ± 1 pixels/second.

C. Validation – Using Camera Edge as Reference Point

Due to the high magnification for the video during pars plana vitrectomy, using an anatomical point as a reference was impossible. For this reason, the edge of the camera frame was used for the reference. In order to validate this, the movement of the edge of the camera was measured. A similar methodological approach was performed as the experimental sections. The distance between the edge of the camera frame to the edge of the actual frame was measured for each frame in the segment. The mean length of the segment was calculated. Next, the distance, between the edge of the frame to the edge of the camera display of each frame, away from the mean length was calculated, leading to finding the average distance and standard deviation away from the mean length for each segment.

Information for Edge detection is shown in Table 17. The initial and final coordinates were measured. The distance between the segments was two pixels in length: The Y-Coordinate is kept constant, whereas the X-Coordinate was modified. The length of the line segment was measured to be 50 pixels with an angle of -90°. Furthermore, the threshold level for all the line segments were kept constant ranging from 100 to 255 after the kymograph was converted to an 8-bit image. The average of the average distance away from the mean length was calculated and shown in Table 18. The number of frames in the video was 80 frames with a frame rate of 30 frames per second resulting in 2.67 seconds of video. The average of the average distance away from the mean length was 1 ± 0 pixels. The average of the standard deviation determined for each segment was calculated to be 1 ± 0 pixels

D. Validation – Frame-by-Frame Analysis

A manual frame-by-frame analysis was performed in order to validate this entire method. A similar methodological approach was performed for the detection of the retinal motion as the experimental sections. Using the Plot Profile on ImageJ, the gray scale values for the line segment in the frame were produced. Based on this, the maximum, positive slope was the location determined to the edge of the retina, whereas the maximum, negative slope was the location of the edge of the camera. The difference of this was compared to the kymograph, experimental. Based on the difference, the relative error value was calculated by find the quantity of subtracting the actual value from the experimental value and dividing it by the actual value. This analysis was performed for every five frames within the image sequence.

Information for the frame-by-frame analysis is shown in Table 19. The initial and final coordinates were measured. The length of the line segment was measured to be 60.03 pixels with an angle of -91.91°. Furthermore, the threshold level for the line segment was ranged from 120 to 255 after the kymograph was converted to an 8-bit image. The relative error for the frame-by-frame analysis is shown in Table 20. The average actual value was 35 ± 7 pixels, and the average experimental was 36 ± 8 pixels. The average relative error was calculated to be 0.369 ± 6.911%. The analysis of what this information means will be explained in the Discussion chapter.

Segment	X_1	Y_1	X_2	Y_2	Angle	Length	Threshold
L1	107	27	107	77	-90°	50	100-255
L2	109	27	109	77	-90°	50	100-255
L3	111	27	111	77	-90°	50	100-255
L4	113	27	113	77	-90°	50	100-255
L5	115	27	115	77	-90°	50	100-255
L6	117	27	117	77	-90°	50	100-255
L7	119	27	119	77	-90°	50	100-255
L8	121	27	121	77	-90°	50	100-255

Table 17: Elementary Information for Edge Detection. Based on the initial and final coordinates shown for each sample line segment, a kymograph was produced using ImageJ. The line was 50 pixels in length and had an angle of -90°. The threshold ranged from 100-255 after converting the image of the kymograph to 8-bit in ImageJ.

Segment	Frames	Time (Seconds)	Average Distance Away from Mean (Pixels)	Standard Deviation
L1	80	2.67	1	1
L2	80	2.67	1	1
L3	80	2.67	1	1
L4	80	2.67	1	1
L5	80	2.67	1	1
L6	80	2.67	1	1
L7	80	2.67	1	1
L8	80	2.67	1	1
AVERAGE	**80.00**	**2.67**	**1**	**1**
Std. Dev.	**---**	**---**	*0*	*0*

Table 18: Average Distance Away from Mean of Edge Detection. The distance between the edge of the frame to the edge of the camera display portion was determined using ImageJ for each frame in the segment. The mean length of the segment was calculated. Next, the distance away from this mean length of each frame was calculated, leading to finding the average distance and standard deviation away from the mean length for each segment. The average of the average distance away from mean length was 1 ± 0 pixels. The average of the standard deviation determined for each segment was calculated to be 1 ± 0 pixels.

X_1	Y_1	X_2	Y_2	Angle	Length	Threshold
64	10	62	70	-91.91	60.03	120-255

Table 19: Elementary Information for Frame-by-Frame Analysis. Based on the initial and final coordinates shown for the sample line segment, a kymograph was produced using ImageJ. The line was 60.53 pixels in length and had an angle of -91.91°. The threshold ranged from 120-255 after converting the image of the kymograph to 8-bit in ImageJ.

Frame	Initial	Final	Difference	Experimental	Relative Error
5	22	46	24	24	0.000%
10	18	50	32	30	6.667%
15	7	41	34	31	9.677%
20	24	48	24	24	0.000%
25	20	50	30	30	0.000%
30	10	48	38	42	-9.524%
35	8	50	42	48	-12.500%
40	4	50	46	45	2.222%
45	7	51	44	49	-10.204%
50	9	50	41	41	0.000%
55	6	46	40	42	-4.762%
60	8	47	39	39	0.000%
65	8	47	39	38	2.632%
70	13	47	34	32	6.250%
75	18	48	30	29	3.448%
80	18	46	28	25	12.000%
AVERAGE			**35**	**36**	**0.369%**
Std. Dev.			**7**	**8**	**6.911%**

Table 20: Relative Error for Frame-by-Frame Analysis. Using the Plot Profile on ImageJ, the gray scale value for each pixel along the length of the line was determined. Based on these values, the slope of the line was calculated. The pixel location where the maximum, positive slope occurred was the location of the edge of the retina. The pixel location where the maximum, negative slope occurred was the location of the edge of the camera. The difference of this was compared to the experimental value that was obtained through the kymograph. This was done for every five frames within the video segment. The average relative error was calculated to be 0.369 ± 6.911%.

IV. DISCUSSION

A novel method to detect the movement of the retina was introduced. This approach can be performed *in vivo* following the pars Plana vitrectomy. This method can quantitatively determine the motion of the retina when the probe was close to the retinal tear. An imaging software was used to assist in detecting the movement of the retina.

The goal of the experiment was to determine a method of measuring the motion of the retina during pars plana vitrectomy *in vivo*.

In this section, the results will be analyzed for the experimental sections and compare to the control. In addition, the analysis for using the camera edge as the reference will be defended. Furthermore, the frame-by-frame analysis will prove that this approach was a valid method of analysis. Finally, the sources of error will be explained.

A. Image Analysis Using ImageJ for Experimental Sections

The kymograph was generated based on the motion of the retina on the experimental video that was analyzed using ImageJ. The adjustment of the threshold was performed to sample out the portions where the motion occurred as the brightness was not consistent in all the video segments. Upon producing a binary image and analyzing it in Microsoft Excel, the distance between the retinal movements in each frame was calculated. Based on these measurements, the average net distance and velocity were calculated for each video, and the summary results is as shown in Table 21.

	Net Distance Traveled (Pixels)	Velocity (Pixels/Seconds)
Video 1	184.583 ± 8.211	98.884 ± 4.399
Video 2	352.569 ± 12.144	97.144 ± 3.183
Video 3	202.801 ± 6.937	92.182 ± 3.153
Video 4	379.022 ± 10.671	83.345 ± 2.130
Video 5	200.606 ± 7.614	83.586 ± 3.173
Video 6	165.155 ± 9.632	72.862 ± 4.247
Video 7	208.871 ± 3.054	149.194 ± 2.181
Control	96.196 ± 2.462	35.628 ± 0.912

Table 21: Summary of Net Distance Traveled and Velocity. The net distance was not consistent for each video. For this reason, the velocity was used to compare between the movements of the retinal motion. It is evident that the velocity was not consistent between the videos. The reason for this was that the distance of the Vitrectomy probe and the edge of the retina was not consistent. A greater velocity means that the probe was close to the retinal tear whereas lesser velocity means that the probe was far from the retinal tear.

There was significant variation in the retinal displacement values among the surgical videos. The experimental videos had net distance movement ranging from 152 to 389 pixels, and 93 to 101 pixels for the control. The results obtained for all of the experimental values

differed and did not seem to have any correlation, especially since the only information initially measured were the net distance traveled. For this reason, the velocity was determined by taking the quotient of the net distance traveled and the distance in order to compare movements between the videos. Similarly there was variation among velocity measurements. Nevertheless, after taking into considerations the constraints and the assumptions, a potential reason for the difference in values in determined. The reason for the inconsistency was believed to be the difference in distance between the retinal tear and the probe, which made a difference in the occurrence of the movement of the retina. Teixeria et al proved that one of the factors of retinal traction was the distance from the retina, where the closer the probe was to the retina, the greater the amount of traction [16]. It is clearly evident that the distance between the probe and the retinal tear made an impact on the movement of the retinal tear. As shown in Table 21, the velocity with the lowest values in the experimental videos, Video 6, was believed to have had the probe farther away in distance than the retinal tear than the videos with the highest values for the velocity, Video 7. Based on this analysis, it is evident that the use of ImageJ was an appropriate way to measure the motion of the retina during pars plana vitrectomy surgery.

The reason why this method of using ImageJ as a viable source to determine the movement of the retina could be considered worthwhile was since the results were consistent when the line segments that were sampled two pixels apart within the video showed little deviation from the average. This was consistent with the net distance traveled as well as the velocity of the video. The standard deviation for those resulted in a low number ensuring that

the movement along the lines was consistent. Another reason to validate this method was because the control.

B. Image Analysis Using ImageJ for Control

The kymograph for the control was obtained in a similar fashion as the experimental videos. The control was where there was no movement in the retina. The threshold was adjusted to detect the movement of the retina. Upon producing a binary image and analyzing it in Microsoft Excel, the distance between the retinal movements in each frame was calculated. Based on these measurements, the average net distance and velocity were calculated for the control video and shown in Table 21.

Theoretically, the motion of the retinal tear for the control when there was no movement occurring should be zero pixels per second. However, due to the the assumptions made as well as the constraints placed upon experiment, this had not resulted in a perfect control. Nevertheless, comparing the control to the experimental values, it is evident that even the lowest velocity of the experimental was twice as great as the velocity of the control. Therefore, there is a clear distinction between the experimental and the control.

As mentioned earlier, the approach of using ImageJ as a method to determine the movement of the retina was plausible because comparing the velocity of the control to the velocity of the experimental video can validate that the movement of the retina was much

lower in the control than in the experimental videos. This was the case even with the experimental video where the probe was farther away from the retina. The control resulted in a lower velocity than the lowest of experimental video, but the experimental still was twice as greater velocity than the control.

Therefore, another explanation that the velocities vary based on the distance was explained. As defined earlier, the control was supposed to be the location where there was no movement of the retinal tear. This was happening when the probe was not close to the tear. However, when the probe was close to the retina, there was the movement in the retina that causes the retina to move and produce a velocity of the motion.

C. Validation – Using Camera Edge as Reference Point

During pars plana vitrectomy, the magnification into the eye was very high that it was impossible to detect a specific anatomical point as a reference. Therefore, to use the edge of the camera as the reference point, the motion of the edge of the camera was analyzed. The distance between the edge of the frame to the edge of the camera display was measured. With the mean length of the segment calculated, the distance between the edge of the frame to the edge of the camera display of each frame away from the mean length was calculated, leading to finding the average distance and standard deviation away from the mean length for each segment.

Based on the results, the average distance away from the mean length was significantly less than the motion of the retinal tear ($p<0.0001$). In addition, the average of the standard deviation obtained for the combination of the eight video segments was low. Around 95% of the standard deviation was ranged within 5% of the value of the average. In addition, the length of the line segment was much longer than the deviation of the distance of the edge of the camera moving. Therefore, it is satisfactory to assume that the edge of the camera can be a viable reference point. Furthermore, because the retinal movement experimental videos were short, using the edge for reference based on the data looked feasible.

D. Validation – Frame-by-Frame

In order to validate the method of using the kymograph and ImageJ in order to analyze the motion of the retinal tear, a manual frame-by-frame analysis was performed. The Plot Profile in ImageJ was used to determine the gray scale values of the line segment for each frame. Based on the maximum, positive slope and maximum, negative slope, the location was determined for the edge of the retina and the edge of the camera, respectively. This result was compared to the experimental data obtained from the kymograph. Based on this, the relative error value was calculated.

The results showed that the average of the actual value obtained from the Plot Profile on ImageJ was close to the average of the experimental value obtained from the kymograph. The relative error between them of 0.369% articulates that the kymograph provides results

very close to the actual results. However, the standard deviation from the mean was about 7% difference. Nonetheless, this could be due to the sources of error, constraints, and the assumptions that were made.

E. Sources of Error

Because of the constraints and the assumptions that were made in the experiment, the raise to errors was introduced. First of which was since there was no specific marker placed on the retinal tear prior to evaluating the motion, it was impossible to detect, using ImageJ, the movement of a particular point of the retina during the entire motion when the probe was close to the edge of the retinal tear. For this reason, a line perpendicular to the motion was used to detect the motion. The error that was associated with this would be calculated based on the comparision between the results obtained in this experiment and the new experiments based on the surgically implemented tag on the retina.

Another error was the line perpendicular to the motion. Because of this assumption, two more errors may rise. One was the line that was produced may not be precisely perpendicular to the motion of the retinal tear. This could result in the kymograph detecting the movement fluctuating between one point to other neighboring points. This can produce sudden fluctuating results. In addition, another error was that the line may be perpendicular in the beginning of the motion. However, since this was performed *in vivo*, as mentioned earlier, it was important to note that due to the complexity of the tissue in the eye, the cutting prevents

an exact physics-based understand and mathematical representation [10]. This could result in a different angle of motion in the middle of motion, meaning the angle of movement in the beginning of the video may not the same angle at the end of the video. The error that was associated with this would be calculated based on the comparision between the results obtained in this experiment and the new experiments based on the surgically implemented tag on the retina. However, if the retina was surgically tagged, the need for determining a perpendicular line along the motion of the retina was not necessary.

Furthermore, as mentioned earlier, the velocity of the control was not zero pixels per second. However, due to the assumptions made as well as the constraints placed upon experiment, this had not resulted in a perfect control. Therefore, a potential reason could be because of the distance the probe was away from the retina was changing. Even though the probe was considered farther away from the retina, due to the size of the eye and the physiological properties, the probe may still have an affect on the vibrations and the movement of the retina. The error that was associated with this would be calculated based on the comparision between the results obtained in this experiment and when the vitrector was not turned on.

In addition, during the experiment, the threshold was manually altered. The error that could have been brought by this was that during detecting the portion of the video that was necessary, the threshold might have detected more of the movement or less based on the user's selection. The source of error resulted with this was approximately 4%, which was based

on adjusting the pixel value of 10 pixels when detecting the range of motion. In addition, since the video was converted from color to 32-bit, there may be other parts in the video that may have the same pixel value as the ones that detected as part of the movement, but were not actually part of the movement of the retinal tear. The source of error resulted with this was less than 1% as the amount of pixels that were detected that were not part of the image was lesser than the portions that were detected. However, this was based entirely on the amount of light source acting on it. Due to this, the error of detecting other points could result in the wrong minimum and maximum value of the position of the retina in the frame. The error that was associated with this based entirely on where the particular region was detected.

Finally, the edge of camera was not straight. The surgical microscopic was stationary. Therefore, there should not had been any movement in the camera movement for the edge of the camera. However, the reason for the movement could be because of the external momement from the outside, resulting from the vibrations from footsteps or movement from the outside, etc. Because of this movement, the edge of the camera was not consistent and was fluctuating. This was why the kymograph image did not produce a straight line of the camera edge. The error that was associated with this would be calculated based on the flexuation of the distance based on the edge detection resulting in an average of approximately 4%.

Based on these errors, there was an error associated with it. Therefore, combining all these errors resulted in an estimated cummalative error of 10% with a deviation of 7%. The deviation was based on based on the actual and experimental value determined by the frame-

by-frame analysis. This value was based on the errors that could be measured. Although this may be a greater error value, eliminating the errors would result in better determining the movement of the retina.

V. FUTURE ENHANCEMENTS

There were many limitiations that were learned from this project. Most of them were addressed in the Sources of Error section in the Discussion. Eliminating these obstacles will help better determine the movement of the retina.

The next steps would be to validate the approach by minimizing some of the constraints and assumptions made. Therefore, the first step would be to first surgically tag a location of the retina where there was tear and detect the movement based on the tag. This could measure the absolute net movement of that specific tag. Another constrain that would be to controlled was the distance the probe was located from the edge of the retina. Furthermore, the vacuum rate as well as the cut rate was going to be kept constant and controlled for the entire experiment. Finally, the light source will be kept constant, so there will be not need to adjust the threshold value between experiments. The independent variable in this case was the distance of the probe from the retinal tear, and the dependent variable was the movement of the retinal tear, which was going to be monitored using the surgically implemented tag.

With these future enhancements, the movement of the retina could be detected accurately *in vivo*. This method can help compare different instruments and different parameters. However, it does not seem that it is necessary to determine the exact values as the estimates maybe enough to compare. Based on these estimates, the parameters and

specifications can be determined to produce the lowest amount of shear force or traction on the retina during pars plana vitrectomy.

VI. REFERENCES

[1] S. Bagi, "Parts of the Eye," *Human Eye Anatomy: Parts of the Eye*, 2014. [Online]. Available: http://www.allaboutvision.com/resources/anatomy.htm.

[2] H. Lund-Andersen and B. Sander, "The Vitreous," in *Adler's Physiology of the Eye*, Elsevier Inc., 2011, pp. 164–181.

[3] G. A. Thibodeau and K. T. Patton, *Structure & Function of the Body*. Elsevier Health Sciences, 2013.

[4] A. H. Rogers and J. S. Duker, *Retina*. Elsevier Health Sciences, 2008.

[5] R. Machemer, "The development of pars plana vitrectomy: a personal account.," *Graefes Arch. Clin. Exp. Ophthalmol.*, vol. 233, no. 8, pp. 453–68, Aug. 1995.

[6] C. C. Patel, S. C. Oliver, N. Mandava, J. Olson, and H. Quiroz-Mercado, "Pars Plana Vitrectomy," *Medscape*. 2015.

[7] T. Sato, S. Kusaka, Y. Oshima, and T. Fujikado, "Analyses of cutting and aspirating properties of vitreous cutters with high-speed camera.," *Retina*, vol. 28, no. 5, pp. 749–54, May 2008.

[8] G. Y. Fujii, E. De Juan, M. S. Humayun, D. J. Pieramici, T. S. Chang, C. Awh, E. Ng, A. Barnes, S. L. Wu, and D. N. Sommerville, "A new 25-gauge instrument system for transconjunctival sutureless vitrectomy surgery.," *Ophthalmology*, vol. 109, no. 10, pp. 1807–12; discussion 1813, Oct. 2002.

[9] A. Teixeira, L. P. Chong, N. Matsuoka, L. Arana, R. Kerns, P. Bhadri, and M. Humayun, "Vitreoretinal Traction Created by Conventional Cutters during Vitrectomy," *Ophthalmology*, vol. 117, no. 7, pp. 1387–1392.e2, Jul. 2010.

[10] S. Charles, "An engineering approach to vitreoretinal surgery.," *Retina*, vol. 24, no. 3, pp. 435–44, Jun. 2004.

[11] C. DeBoer, S. Fang, L. H. Lima, M. McCormick, P. Bhadri, R. Kerns, and M. S. Humayun, "Port Geometery and its influcne on vitrectomy," *Retina*, vol. 28, no. 8, pp. 1061–1067, Sep. 2008.

[12] T. Rossi, G. Querzoli, G. Angelini, C. Malvasi, M. Iossa, L. Placentino, and G. Ripandelli, "Introducing New Vitreous Cutter Blade Shapes," *Retina*, vol. 34, no. 9, pp. 1896–1904, Sep. 2014.

[13] B. Diniz, R. B. Fernandes, R. M. Ribeiro, J.-C. Lue, A. G. Teixeira, O. Magalhães, M. Maia, and M. S. Humayun, "Analysis of a 23-gauge ultra high-speed cutter with duty cycle

control.," *Retina*, vol. 33, no. 5, pp. 933–8, May 2013.

[14] R. M. Ribeiro, A. G. Teixeira, B. Diniz, R. B. Fernandes, Y. Zhong, R. Kerns, and M. S. Humayun, "Performance analysis of ultrahigh-speed vitreous cutter system.," *Retina*, vol. 33, no. 5, pp. 928–32, May 2013.

[15] O. Magalhães, L. P. Chong, C. DeBoer, P. Bhadri, R. Kerns, A. Barnes, S. Fang, and M. S. Humayun, "Vitreous Dynamics," *Retina*, vol. 28, no. 2, pp. 236–241, Feb. 2008.

[16] A. Teixeira, L. Chong, N. Matsuoka, L. Arana, J.-C. Lue, M. McCormick, R. Kerns, P. Bhadri, and M. Humayun, "An Experimental Protocol of the Model to Quantify Traction Applied to the Retina by Vitreous Cutters," *Investig. Opthalmology Vis. Sci.*, vol. 51, no. 8, p. 4181, Aug. 2010.

[17] T. Ferreira and W. Rasband, *ImageJ User Guide*, IJ 1.46r. 2012.

[18] J. Rietdorf and A. Seitz, "Kymograph Plugin for ImageJ," *2008*. [Online]. Available: http://www.embl.de/eamnet/html/body_kymograph.html.

VII. APPENDIX

A. Image Analysis Using ImageJ for Experimental Sections

1. Video 1

a) Kymograph 1

Frame	Maximum	Minimum	Difference	Length
0	106	74	32	
1	106	73	33	1
2	105	70	35	2
3	106	68	38	3
4	106	65	41	3
5	106	65	41	1
6	108	61	47	6
7	108	58	50	3
8	108	55	53	3
9	108	52	56	3
10	109	51	58	2
11	110	50	60	2
12	110	47	63	3
13	110	46	64	1
14	109	43	66	2
15	108	42	66	1
16	108	40	68	2
17	108	40	68	1
18	107	42	65	3
19	107	42	65	1
20	108	43	65	1
21	107	43	64	1
22	109	46	63	1
23	109	47	62	1
24	107	44	63	1
25	107	42	65	2
26	106	40	66	1
27	107	38	69	3
28	108	35	73	4
29	107	34	73	1
30	106	31	75	2
31	106	32	74	1
32	106	39	67	7
33	106	44	62	5
34	107	40	67	5
35	107	38	69	2
36	107	36	71	2
37	106	35	71	1
38	106	32	74	3
39	105	30	75	1
40	105	27	78	3
41	105	31	74	4
42	103	38	65	9
43	103	38	65	1
44	105	32	73	8
45	105	30	75	2
46	105	32	73	2
47	105	32	73	1
48	105	31	74	1
49	105	30	75	1
50	105	23	82	7
51	103	29	74	8
52	102	34	68	6
53	100	36	64	4
54	100	48	52	12
55	97	70	27	25

b) Kymograph 2

Frame	Maximum	Minimum	Difference	Length
0	108	76	32	
1	108	75	33	1
2	106	73	33	1
3	108	68	40	7
4	108	68	40	1
5	108	66	42	2
6	109	64	45	3
7	109	60	49	4
8	109	58	51	2
9	109	55	54	3
10	111	53	58	4
11	111	50	61	3
12	111	48	63	2
13	111	46	65	2
14	110	44	66	1
15	109	43	66	1
16	110	41	69	3
17	109	43	66	3
18	109	43	66	1
19	109	43	66	1
20	109	44	65	1

21	109	44	65	1
22	109	47	62	3
23	109	47	62	1
24	109	44	65	3
25	108	42	66	1
26	108	40	68	2
27	109	40	69	1
28	109	35	74	5
29	109	32	77	3
30	108	31	77	1
31	108	34	74	3
32	108	40	68	6
33	109	44	65	3
34	109	42	67	2
35	109	36	73	6
36	109	36	73	1
37	108	35	73	1
38	107	32	75	2
39	106	30	76	1
40	106	29	77	1
41	106	32	74	3
42	105	39	66	8
43	106	39	67	1
44	107	34	73	6
45	107	32	75	2
46	106	31	75	1
47	106	34	72	3
48	106	32	74	2
49	106	31	75	1
50	106	27	79	4
51	105	28	77	2
52	103	34	69	8
53	102	36	66	3
54	102	50	52	14
55	95	71	24	28

c) Kymograph 3

Frame	Maximum	Minimum	Difference	Length
0	109	78	31	
1	109	77	32	1
2	109	75	34	2
3	109	71	38	4
4	110	71	39	1
5	110	68	42	3
6	111	65	46	4
7	111	62	49	3
8	111	59	52	3
9	111	54	57	5
10	112	55	57	1
11	112	52	60	3
12	113	51	62	2
13	112	47	65	3
14	112	46	66	1
15	111	44	67	1
16	111	44	67	1
17	111	44	67	1
18	111	44	67	1
19	111	44	67	1
20	111	43	68	1
21	111	46	65	3
22	111	47	64	1
23	111	47	64	1
24	110	44	66	2
25	109	42	67	1
26	109	40	69	2
27	110	39	71	2
28	110	36	74	3
29	110	35	75	1
30	110	34	76	1
31	109	34	75	1
32	109	40	69	6
33	110	46	64	5
34	110	40	70	6
35	110	38	72	2
36	110	37	73	1
37	110	37	73	1
38	109	34	75	2
39	108	32	76	1
40	108	31	77	1
41	108	32	76	1
42	106	39	67	9
43	107	39	68	1
44	109	36	73	5
45	109	34	75	2
46	108	34	74	1
47	108	34	74	1
48	108	34	74	1
49	108	31	77	3
50	108	30	78	1
51	106	31	75	3
52	105	35	70	5
53	103	36	67	3
54	103	50	53	14
55	97	72	25	28

d) Kymograph 4

Frame	Maximum	Minimum	Difference	Length
0	110	78	32	
1	111	77	34	2
2	111	75	36	2
3	111	73	38	2
4	111	70	41	3
5	112	70	42	1
6	112	68	44	2
7	113	63	50	6
8	112	59	53	3
9	114	56	58	5
10	114	58	56	2
11	114	53	61	5
12	114	52	62	1

13	114	50	64	2
14	113	50	63	1
15	113	46	67	4
16	113	46	67	1
17	113	46	67	1
18	113	44	69	2
19	113	44	69	1
20	112	44	68	1
21	113	44	69	1
22	113	48	65	4
23	113	47	66	1
24	112	42	70	4
25	111	42	69	1
26	111	41	70	1
27	112	40	72	2
28	112	35	77	5
29	111	35	76	1
30	111	34	77	1
31	111	35	76	1
32	111	43	68	8
33	111	46	65	3
34	112	40	72	7

35	112	38	74	2
36	111	39	72	2
37	111	36	75	3
38	111	35	76	1
39	110	32	78	2
40	110	31	79	1
41	109	31	78	1
42	108	40	68	10
43	109	39	70	2
44	111	37	74	4
45	110	34	76	2
46	109	34	75	1
47	109	35	74	1
48	109	35	74	1
49	110	32	78	4
50	111	30	81	3
51	108	34	74	7
52	106	35	71	3
53	106	35	71	1
54	105	50	55	16
55	97	70	27	28

e) Kymograph 5

Frame	Maximum	Minimum	Difference	Length
0	112	79	33	
1	113	79	34	1
2	113	77	36	2
3	112	74	38	2
4	114	73	41	3
5	113	71	42	1
6	114	70	44	2
7	114	65	49	5
8	114	62	52	3
9	114	59	55	3
10	115	56	59	4
11	115	56	59	1
12	115	53	62	3
13	115	52	63	1
14	115	48	67	4
15	114	47	67	1
16	114	41	73	6
17	114	44	70	3
18	114	44	70	1
19	114	44	70	1
20	114	46	68	2
21	114	46	68	1
22	114	46	68	1
23	114	46	68	1
24	114	44	70	2
25	113	42	71	1
26	112	41	71	1
27	113	40	73	2

28	114	38	76	3
29	114	35	79	3
30	113	35	78	1
31	113	36	77	1
32	113	44	69	8
33	113	47	66	3
34	113	40	73	7
35	113	38	75	2
36	113	40	73	2
37	112	37	75	2
38	112	36	76	1
39	111	34	77	1
40	111	31	80	3
41	111	34	77	3
42	110	41	69	8
43	111	37	74	5
44	112	38	74	1
45	111	35	76	2
46	110	35	75	1
47	111	35	76	1
48	111	36	75	1
49	111	31	80	5
50	112	31	81	1
51	110	34	76	5
52	108	36	72	4
53	107	37	70	2
54	107	51	56	14
55	99	68	31	25

f) Kymograph 6

Frame	Maximum	Minimum	Difference	Length
0	113	81	32	
1	115	81	34	2

2	113	80	33	1
3	113	77	36	3
4	115	74	41	5

5	115	72	43	2
6	115	69	46	3
7	116	67	49	3
8	116	64	52	3
9	116	61	55	3
10	116	58	58	3
11	116	56	60	2
12	116	55	61	1
13	116	54	62	1
14	117	49	68	6
15	116	46	70	2
16	115	46	69	1
17	116	46	70	1
18	116	45	71	1
19	115	45	70	1
20	116	48	68	2
21	116	48	68	1
22	116	48	68	1
23	116	46	70	2
24	115	45	70	1
25	115	43	72	2
26	115	42	73	1
27	115	41	74	1
28	115	39	76	2
29	115	36	79	3
30	115	36	79	1
31	113	37	76	3
32	113	44	69	7
33	115	48	67	2
34	116	41	75	8
35	115	39	76	1
36	115	41	74	2
37	115	39	76	2
38	113	34	79	3
39	113	34	79	1
40	112	33	79	1
41	112	34	78	1
42	112	42	70	8
43	112	39	73	3
44	113	40	73	1
45	113	37	76	3
46	112	36	76	1
47	113	37	76	1
48	112	37	75	1
49	113	36	77	2
50	113	30	83	6
51	111	36	75	8
52	109	37	72	3
53	108	38	70	2
54	108	52	56	14
55	101	69	32	24

g) Kymograph 7

Frame	Maximum	Minimum	Difference	Length
0	117	83	34	
1	115	80	35	1
2	115	78	37	2
3	115	76	39	2
4	115	75	40	1
5	115	73	42	2
6	117	71	46	4
7	117	67	50	4
8	117	64	53	3
9	117	62	55	2
10	118	60	58	3
11	118	59	59	1
12	118	56	62	3
13	118	55	63	1
14	117	55	62	1
15	117	50	67	5
16	117	50	67	1
17	117	47	70	3
18	117	48	69	1
19	117	49	68	1
20	115	50	65	3
21	117	49	68	3
22	117	49	68	1
23	117	48	69	1
24	115	47	68	1
25	115	46	69	1
26	115	44	71	2
27	117	43	74	3
28	117	43	74	1
29	117	40	77	3
30	115	38	77	1
31	115	38	77	1
32	115	46	69	8
33	115	50	65	4
34	115	41	74	9
35	115	40	75	1
36	115	43	72	3
37	115	41	74	2
38	114	38	76	2
39	114	35	79	3
40	114	34	80	1
41	114	36	78	2
42	113	42	71	7
43	113	39	74	3
44	114	42	72	2
45	114	38	76	4
46	113	39	74	2
47	114	36	78	4
48	114	39	75	3
49	114	37	77	2
50	114	31	83	6
51	112	35	77	6
52	111	38	73	4
53	110	36	74	1
54	109	55	54	20
55	98	64	34	20

h) Kymograph 8

Frame	Maximum	Minimum	Difference	Length
0	118	83	35	
1	118	80	38	3
2	117	79	38	1
3	117	76	41	3
4	117	75	42	1
5	117	74	43	1
6	117	72	45	2
7	118	68	50	5
8	118	66	52	2
9	118	63	55	3
10	119	62	57	2
11	120	60	60	3
12	119	61	58	2
13	119	59	60	2
14	118	56	62	2
15	118	53	65	3
16	118	50	68	3
17	118	50	68	1
18	118	50	68	1
19	118	50	68	1
20	118	50	68	1
21	117	51	66	2
22	118	50	68	2
23	118	50	68	1
24	117	49	68	1
25	117	47	70	2
26	117	46	71	1
27	117	44	73	2
28	118	43	75	2
29	117	43	74	1
30	117	40	77	3
31	115	39	76	1
32	117	47	70	6
33	117	48	69	1
34	117	43	74	5
35	117	43	74	1
36	117	44	73	1
37	115	43	72	1
38	115	40	75	3
39	115	37	78	3
40	115	35	80	2
41	115	38	77	3
42	114	43	71	6
43	114	40	74	3
44	115	44	71	3
45	115	40	75	4
46	114	40	74	1
47	114	37	77	3
48	115	41	74	3
49	115	39	76	2
50	115	32	83	7
51	113	35	78	5
52	112	38	74	4
53	111	39	72	2
54	111	55	56	16
55	102	64	38	18

2. Video 2

a) Kymograph 1

Frame	Maximum	Minimum	Difference	Length
120	52	51	1	
121	62	50	12	11
122	64	46	18	6
123	67	43	24	6
124	68	41	27	3
125	68	39	29	2
126	68	35	33	4
127	69	34	35	2
128	69	32	37	2
129	70	31	39	2
130	69	31	38	1
131	81	20	61	23
132	72	27	45	16
133	72	26	46	1
134	73	24	49	3
135	73	28	45	4
136	72	26	46	1
137	74	26	48	2
138	73	23	50	2
139	75	20	55	5
140	76	17	59	4
141	74	26	48	11
142	73	24	49	1
143	73	21	52	3
144	74	20	54	2
145	74	17	57	3
146	76	16	60	3
147	76	12	64	4
148	76	11	65	1
149	76	9	67	2
150	77	9	68	1
151	78	5	73	5
152	78	4	74	1
153	78	3	75	1
154	79	3	76	1
155	80	6	74	2
156	78	14	64	10
157	76	18	58	6
158	76	20	56	2
159	77	16	61	5
160	77	7	70	9

161	78	3	75	5
162	79	3	76	1
163	80	5	75	1
164	80	11	69	6
165	81	10	71	2
166	79	14	65	6
167	77	20	57	8
168	73	18	55	2
169	74	18	56	1
170	75	20	55	1
171	75	20	55	1
172	75	21	54	1
173	75	23	52	2
174	74	24	50	2
175	74	24	50	1
176	74	24	50	1
177	74	24	50	1
178	74	23	51	1
179	75	24	51	1
180	76	24	52	1
181	76	25	51	1
182	75	24	51	1
183	75	24	51	1
184	75	25	50	1
185	76	23	53	3
186	76	21	55	2
187	76	21	55	1
188	76	21	55	1
189	75	20	55	1
190	75	18	57	2
191	76	16	60	3
192	76	14	62	2
193	76	13	63	1
194	76	10	66	3
195	76	10	66	1
196	77	10	67	1
197	77	8	69	2
198	77	7	70	1
199	77	9	68	2
200	78	7	71	3
201	78	6	72	1
202	80	3	77	5
203	78	2	76	1
204	77	1	76	1
205	76	3	73	3
206	74	9	65	8
207	71	17	54	11
208	73	20	53	1
209	73	20	53	1
210	72	20	52	1
211	71	20	51	1
212	69	27	42	9
213	67	30	37	5
214	67	29	38	1
215	66	30	36	2
216	67	29	38	2
217	66	25	41	3
218	66	24	42	1
219	69	23	46	4
220	69	16	53	7
221	69	9	60	7
222	69	6	63	3
223	69	6	63	1
224	69	5	64	1
225	71	5	66	2
226	71	7	64	2
227	71	3	68	4
228	71	2	69	1

b) Kymograph 2

Frame	Maximum	Minimum	Difference	Length
120	55	53	2	
121	67	50	17	15
122	69	46	23	6
123	69	44	25	2
124	70	42	28	3
125	69	39	30	2
126	70	36	34	4
127	71	34	37	3
128	72	34	38	1
129	73	33	40	2
130	72	31	41	1
131	82	21	61	20
132	74	28	46	15
133	74	27	47	1
134	75	26	49	2
135	73	27	46	3
136	74	27	47	1
137	76	27	49	2
138	76	24	52	3
139	76	20	56	4
140	77	18	59	3
141	76	27	49	10
142	75	24	51	2
143	75	21	54	3
144	76	18	58	4
145	76	18	58	1
146	78	16	62	4
147	78	12	66	4
148	78	8	70	4
149	79	7	72	2
150	80	6	74	2
151	79	3	76	2
152	80	3	77	1
153	80	3	77	1
154	81	3	78	1
155	82	3	79	1
156	81	16	65	14
157	78	20	58	7
158	78	20	58	1
159	79	11	68	10
160	79	6	73	5
161	80	2	78	5
162	81	6	75	3

163	82	6	76	1
164	82	7	75	1
165	82	10	72	3
166	81	12	69	3
167	79	14	65	4
168	76	20	56	9
169	77	20	57	1
170	77	20	57	1
171	76	20	56	1
172	76	23	53	3
173	76	23	53	1
174	76	24	52	1
175	76	23	53	1
176	76	24	52	1
177	76	24	52	1
178	76	23	53	1
179	77	25	52	1
180	77	25	52	1
181	77	27	50	2
182	77	24	53	3
183	77	24	53	1
184	77	24	53	1
185	78	23	55	2
186	77	23	54	1
187	77	20	57	3
188	77	21	56	1
189	77	18	59	3
190	77	18	59	1
191	78	16	62	3
192	77	14	63	1
193	78	11	67	4
194	78	12	66	1
195	78	12	66	1
196	78	12	66	1

197	78	10	68	2
198	79	9	70	2
199	78	10	68	2
200	80	9	71	3
201	81	6	75	4
202	81	5	76	1
203	81	3	78	2
204	80	2	78	1
205	78	3	75	3
206	76	11	65	10
207	73	17	56	9
208	75	23	52	4
209	74	21	53	1
210	73	21	52	1
211	74	17	57	5
212	70	26	44	13
213	70	31	39	5
214	69	31	38	1
215	69	32	37	1
216	69	32	37	1
217	68	28	40	3
218	68	25	43	3
219	70	20	50	7
220	70	17	53	3
221	71	9	62	9
222	71	9	62	1
223	70	9	61	1
224	71	7	64	3
225	72	6	66	2
226	73	7	66	1
227	73	6	67	1
228	72	3	69	2

c) Kymograph 3

Frame	Maximum	Minimum	Difference	Length
120	63	54	9	
121	70	51	19	10
122	70	49	21	2
123	71	46	25	4
124	71	43	28	3
125	71	41	30	2
126	72	39	33	3
127	73	36	37	4
128	73	35	38	1
129	74	34	40	2
130	73	33	40	1
131	84	21	63	23
132	76	30	46	17
133	76	28	48	2
134	76	27	49	1
135	75	28	47	2
136	76	29	47	1
137	78	30	48	1
138	78	26	52	4
139	78	21	57	5
140	78	18	60	3
141	76	26	50	10

142	77	24	53	3
143	77	23	54	1
144	78	20	58	4
145	78	18	60	2
146	79	17	62	2
147	81	16	65	3
148	81	9	72	7
149	80	8	72	1
150	82	7	75	3
151	81	5	76	1
152	82	3	79	3
153	82	5	77	2
154	84	5	79	2
155	82	4	78	1
156	82	14	68	10
157	80	18	62	6
158	81	18	63	1
159	81	11	70	7
160	81	4	77	7
161	81	6	75	2
162	81	6	75	1
163	84	7	77	2
164	84	9	75	2

165	85	10	75	1
166	82	14	68	7
167	81	14	67	1
168	78	18	60	7
169	78	20	58	2
170	78	20	58	1
171	78	21	57	1
172	78	21	57	1
173	78	23	55	2
174	78	23	55	1
175	77	24	53	2
176	78	24	54	1
177	78	24	54	1
178	78	24	54	1
179	78	24	54	1
180	78	26	52	2
181	79	27	52	1
182	79	27	52	1
183	78	26	52	1
184	78	26	52	1
185	79	24	55	3
186	79	24	55	1
187	78	23	55	1
188	78	21	57	2
189	80	20	60	3
190	79	20	59	1
191	79	16	63	4
192	80	16	64	1
193	79	13	66	2
194	80	12	68	2
195	80	12	68	1
196	80	11	69	1
197	80	12	68	1

198	80	10	70	2
199	81	10	71	1
200	81	10	71	1
201	81	7	74	3
202	82	5	77	3
203	82	4	78	1
204	81	4	77	1
205	79	4	75	2
206	78	10	68	7
207	74	18	56	12
208	76	24	52	4
209	76	24	52	1
210	76	21	55	3
211	76	18	58	3
212	72	23	49	9
213	71	32	39	10
214	70	33	37	2
215	70	35	35	2
216	71	34	37	2
217	69	30	39	2
218	70	27	43	4
219	71	24	47	4
220	72	23	49	2
221	73	21	52	3
222	73	12	61	9
223	72	12	60	1
224	72	10	62	2
225	74	9	65	3
226	74	10	64	1
227	74	8	66	2
228	73	7	66	1

d) Kymograph 4

Frame	Maximum	Minimum	Difference	Length
120	62	61	1	
121	71	54	17	16
122	71	50	21	4
123	71	49	22	1
124	71	46	25	3
125	72	44	28	3
126	73	41	32	4
127	72	39	33	1
128	72	38	34	1
129	74	37	37	3
130	74	36	38	1
131	84	28	56	18
132	76	32	44	12
133	78	30	48	4
134	77	30	47	1
135	77	31	46	1
136	75	30	45	1
137	76	31	45	1
138	76	28	48	3
139	78	24	54	6
140	79	20	59	5
141	77	27	50	9
142	78	27	51	1

143	78	24	54	3
144	78	23	55	1
145	78	21	57	2
146	80	17	63	6
147	81	16	65	2
148	81	13	68	3
149	81	11	70	2
150	81	12	69	1
151	82	9	73	4
152	82	8	74	1
153	82	8	74	1
154	82	7	75	1
155	85	7	78	3
156	84	16	68	10
157	82	21	61	7
158	81	20	61	1
159	82	14	68	7
160	81	9	72	4
161	82	8	74	2
162	81	8	73	1
163	82	9	73	1
164	84	11	73	1
165	85	13	72	1
166	84	16	68	4

167	81	16	65	3
168	78	21	57	8
169	80	23	57	1
170	79	21	58	1
171	78	21	57	1
172	78	26	52	5
173	78	26	52	1
174	78	26	52	1
175	76	26	50	2
176	78	27	51	1
177	79	27	52	1
178	79	27	52	1
179	79	27	52	1
180	79	27	52	1
181	80	29	51	1
182	79	30	49	2
183	78	29	49	1
184	78	29	49	1
185	80	27	53	4
186	80	26	54	1
187	80	24	56	2
188	80	24	56	1
189	80	23	57	1
190	79	23	56	1
191	80	20	60	4
192	80	17	63	3
193	80	16	64	1
194	81	14	67	3
195	81	14	67	1
196	81	13	68	1
197	81	14	67	1
198	81	14	67	1

199	82	12	70	3
200	82	12	70	1
201	82	9	73	3
202	84	8	76	3
203	82	7	75	1
204	82	6	76	1
205	80	7	73	3
206	78	11	67	6
207	75	20	55	12
208	77	27	50	5
209	76	27	49	1
210	75	24	51	2
211	76	23	53	2
212	73	27	46	7
213	72	34	38	8
214	71	34	37	1
215	71	37	34	3
216	72	36	36	2
217	71	32	39	3
218	71	31	40	1
219	72	28	44	4
220	73	26	47	3
221	73	23	50	3
222	73	18	55	5
223	73	16	57	2
224	73	14	59	2
225	75	14	61	2
226	76	13	63	2
227	76	12	64	1
228	75	10	65	1

e) Kymograph 5

Frame	Maximum	Minimum	Difference	Length
120	69	59	10	
121	73	56	17	7
122	73	53	20	3
123	73	50	23	3
124	73	48	25	2
125	74	45	29	4
126	75	43	32	3
127	76	41	35	3
128	76	39	37	2
129	76	38	38	1
130	76	36	40	2
131	85	25	60	20
132	77	34	43	17
133	78	31	47	4
134	80	30	50	3
135	78	31	47	3
136	76	31	45	2
137	78	33	45	1
138	79	30	49	4
139	80	26	54	5
140	81	21	60	6
141	79	27	52	8
142	79	27	52	1
143	80	24	56	4

144	79	23	56	1
145	81	21	60	4
146	82	17	65	5
147	82	14	68	3
148	82	13	69	1
149	82	9	73	4
150	84	9	75	2
151	84	9	75	1
152	85	8	77	2
153	85	8	77	1
154	85	8	77	1
155	85	7	78	1
156	86	14	72	6
157	84	21	63	9
158	85	21	64	1
159	85	12	73	9
160	84	8	76	3
161	85	9	76	1
162	84	10	74	2
163	85	10	75	1
164	88	12	76	1
165	88	14	74	2
166	84	14	70	4
167	82	14	68	2
168	81	21	60	8

169	82	21	61	1
170	81	20	61	1
171	81	21	60	1
172	80	23	57	3
173	80	24	56	1
174	80	26	54	2
175	78	24	54	1
176	78	25	53	1
177	80	25	55	2
178	80	25	55	1
179	81	26	55	1
180	81	29	52	3
181	81	24	57	5
182	81	30	51	6
183	81	29	52	1
184	81	28	53	1
185	81	27	54	1
186	81	27	54	1
187	81	25	56	2
188	81	25	56	1
189	82	24	58	2
190	82	23	59	1
191	82	21	61	2
192	82	18	64	3
193	82	17	65	1
194	82	16	66	1
195	82	16	66	1
196	82	14	68	2
197	82	13	69	1
198	82	13	69	1
199	82	11	71	2

200	84	13	71	1
201	84	10	74	3
202	85	10	75	1
203	85	8	77	2
204	84	8	76	1
205	82	8	74	2
206	81	10	71	3
207	78	18	60	11
208	79	25	54	6
209	78	25	53	1
210	78	21	57	4
211	78	17	61	4
212	75	21	54	7
213	74	31	43	11
214	73	36	37	6
215	73	38	35	2
216	74	38	36	1
217	73	35	38	2
218	73	31	42	4
219	73	30	43	1
220	75	28	47	4
221	76	24	52	5
222	74	21	53	1
223	74	17	57	4
224	75	16	59	2
225	77	14	63	4
226	77	14	63	1
227	77	13	64	1
228	77	11	66	2

f) Kymograph 6

Frame	Maximum	Minimum	Difference	Length
120	63	61	2	
121	69	60	9	7
122	74	56	18	9
123	74	53	21	3
124	73	50	23	2
125	76	48	28	5
126	74	45	29	1
127	75	42	33	4
128	76	40	36	3
129	76	40	36	1
130	76	38	38	2
131	86	31	55	17
132	78	36	42	13
133	78	34	44	2
134	81	33	48	4
135	78	33	45	3
136	77	34	43	2
137	78	35	43	1
138	78	31	47	4
139	81	27	54	7
140	81	21	60	6
141	78	28	50	10
142	79	27	52	2
143	79	26	53	1
144	80	24	56	3

145	81	23	58	2
146	82	20	62	4
147	82	18	64	2
148	82	14	68	4
149	84	14	70	2
150	84	13	71	1
151	84	12	72	1
152	85	10	75	3
153	86	12	74	1
154	85	11	74	1
155	86	10	76	2
156	86	14	72	4
157	84	23	61	11
158	85	23	62	1
159	85	14	71	9
160	84	12	72	1
161	85	12	73	1
162	86	14	72	1
163	87	13	74	2
164	88	14	74	1
165	88	16	72	2
166	87	16	71	1
167	85	17	68	3
168	80	23	57	11
169	81	24	57	1
170	82	21	61	4

171	81	26	55	6
172	80	26	54	1
173	80	26	54	1
174	78	29	49	5
175	78	27	51	2
176	80	27	53	2
177	80	27	53	1
178	81	27	54	1
179	81	27	54	1
180	81	27	54	1
181	82	29	53	1
182	81	31	50	3
183	81	31	50	1
184	82	30	52	2
185	82	29	53	1
186	82	28	54	1
187	82	30	52	2
188	81	30	51	1
189	82	27	55	4
190	82	26	56	1
191	82	23	59	3
192	82	20	62	3
193	82	18	64	2
194	82	18	64	1
195	82	16	66	2
196	82	17	65	1
197	82	14	68	3
198	84	16	68	1
199	84	14	70	2
200	84	13	71	1

201	85	13	72	1
202	85	11	74	2
203	86	8	78	4
204	85	11	74	4
205	84	10	74	1
206	82	13	69	5
207	78	20	58	11
208	80	27	53	5
209	79	28	51	2
210	78	24	54	3
211	78	24	54	1
212	76	27	49	5
213	75	37	38	11
214	74	36	38	1
215	74	40	34	4
216	75	41	34	1
217	74	39	35	1
218	76	32	44	9
219	75	31	44	1
220	75	30	45	1
221	76	27	49	4
222	76	24	52	3
223	76	20	56	4
224	76	20	56	1
225	78	17	61	5
226	78	17	61	1
227	78	16	62	1
228	78	13	65	3

g) Kymograph 7

Frame	Maximum	Minimum	Difference	Length
120	69	65	4	
121	70	62	8	4
122	75	59	16	8
123	76	56	20	4
124	76	53	23	3
125	77	50	27	4
126	77	47	30	3
127	77	43	34	4
128	77	42	35	1
129	77	41	36	1
130	77	39	38	2
131	88	31	57	19
132	79	37	42	15
133	79	35	44	2
134	81	34	47	3
135	79	35	44	3
136	78	36	42	2
137	80	36	44	2
138	79	33	46	2
139	81	29	52	6
140	82	24	58	6
141	81	29	52	6
142	79	30	49	3
143	81	28	53	4
144	81	25	56	3
145	82	24	58	2

146	84	21	63	5
147	82	17	65	2
148	84	16	68	3
149	84	16	68	1
150	85	14	71	3
151	86	14	72	1
152	86	13	73	1
153	86	13	73	1
154	87	13	74	1
155	88	12	76	2
156	87	16	71	5
157	85	23	62	9
158	88	21	67	5
159	85	14	71	4
160	85	16	69	2
161	87	14	73	4
162	88	14	74	1
163	88	16	72	2
164	89	16	73	1
165	89	17	72	1
166	88	16	72	1
167	87	18	69	3
168	81	23	58	11
169	81	23	58	1
170	81	25	56	2
171	81	26	55	1
172	81	27	54	1

173	81	27	54	1
174	81	27	54	1
175	80	28	52	2
176	81	30	51	1
177	80	30	50	1
178	80	28	52	2
179	81	28	53	1
180	81	31	50	3
181	82	32	50	1
182	81	31	50	1
183	81	30	51	1
184	81	31	50	1
185	82	30	52	2
186	82	29	53	1
187	82	29	53	1
188	82	30	52	1
189	82	27	55	3
190	82	27	55	1
191	84	24	60	5
192	84	21	63	3
193	84	20	64	1
194	84	20	64	1
195	85	18	67	3
196	85	17	68	1
197	85	18	67	1
198	85	18	67	1
199	85	13	72	5
200	86	16	70	2
201	86	12	74	4

202	86	10	76	2
203	87	10	77	1
204	85	11	74	3
205	84	12	72	2
206	82	14	68	4
207	80	20	60	8
208	81	29	52	8
209	81	29	52	1
210	80	26	54	2
211	79	23	56	2
212	77	26	51	5
213	76	36	40	11
214	77	38	39	1
215	77	41	36	3
216	76	40	36	1
217	76	37	39	3
218	76	34	42	3
219	76	34	42	1
220	76	32	44	2
221	78	30	48	4
222	78	26	52	4
223	78	23	55	3
224	78	21	57	2
225	79	20	59	2
226	79	18	61	2
227	80	16	64	3
228	79	16	63	1

h) Kymograph 8

Frame	Maximum	Minimum	Difference	Length
121	71	65	6	
122	69	63	6	1
123	76	59	17	11
124	76	56	20	3
125	76	54	22	2
126	76	51	25	3
127	76	48	28	3
128	78	44	34	6
129	78	45	33	1
130	78	43	35	2
131	89	34	55	20
132	79	41	38	17
133	79	37	42	4
134	79	37	42	1
135	79	39	40	2
136	78	39	39	1
137	79	39	40	1
138	79	36	43	3
139	81	30	51	8
140	80	24	56	5
141	78	30	48	8
142	78	31	47	1
143	79	30	49	2
144	80	29	51	2
145	82	26	56	5
146	82	23	59	3
147	83	21	62	3

148	84	18	66	4
149	85	17	68	2
150	85	18	67	1
151	85	15	70	3
152	87	14	73	3
153	87	16	71	2
154	87	15	72	1
155	87	14	73	1
156	86	17	69	4
157	85	24	61	8
158	85	23	62	1
159	86	18	68	6
160	84	18	66	2
161	86	17	69	3
162	86	16	70	1
163	87	16	71	1
164	88	17	71	1
165	90	18	72	1
166	87	18	69	3
167	84	20	64	5
168	79	26	53	11
169	82	27	55	2
170	81	27	54	1
171	80	29	51	3
172	80	29	51	1
173	79	29	50	1
174	79	29	50	1
175	79	30	49	1

176	80	31	49	1
177	80	31	49	1
178	80	33	47	2
179	80	33	47	1
180	80	33	47	1
181	80	34	46	1
182	81	36	45	1
183	80	34	46	1
184	81	34	47	1
185	82	33	49	2
186	80	32	48	1
187	81	32	49	1
188	82	32	50	1
189	82	33	49	1
190	82	30	52	3
191	84	27	57	5
192	83	26	57	1
193	84	24	60	3
194	83	23	60	1
195	82	21	61	1
196	83	21	62	1
197	85	21	64	2
198	85	19	66	2
199	84	18	66	1
200	85	16	69	3
201	86	14	72	3
202	86	12	74	2

203	86	12	74	1
204	85	14	71	3
205	84	14	70	1
206	81	16	65	5
207	79	23	56	9
208	81	30	51	5
209	81	30	51	1
210	79	27	52	1
211	79	25	54	2
212	76	29	47	7
213	76	37	39	8
214	76	41	35	4
215	76	43	33	2
216	76	41	35	2
217	76	39	37	2
218	76	37	39	2
219	78	36	42	3
220	76	34	42	1
221	78	31	47	5
222	78	29	49	2
223	78	26	52	3
224	78	23	55	3
225	79	22	57	2
226	79	21	58	1
227	79	20	59	1
228	79	18	61	2

3. Video 3

a) Kymograph 1

Frame	Maximum	Minimum	Difference	Length
0	98	54	44	
1	96	54	42	2
2	96	54	42	1
3	94	54	40	2
4	96	52	44	4
5	96	53	43	1
6	95	53	42	1
7	96	53	43	1
8	95	52	43	1
9	95	51	44	1
10	98	49	49	5
11	98	48	50	1
12	98	47	51	1
13	98	44	54	3
14	99	41	58	4
15	99	40	59	1
16	100	36	64	5
17	100	36	64	1
18	100	37	63	1
19	100	34	66	3
20	102	34	68	2
21	102	34	68	1
22	102	33	69	1
23	103	32	71	2

24	102	31	71	1
25	103	33	70	1
26	103	31	72	2
27	103	30	73	1
28	103	29	74	1
29	104	30	74	1
30	104	28	76	2
31	104	26	78	2
32	104	25	79	1
33	104	24	80	1
34	104	21	83	3
35	103	20	83	1
36	102	18	84	1
37	104	18	86	2
38	104	16	88	2
39	104	17	87	1
40	104	12	92	5
41	104	8	96	4
42	104	10	94	2
43	102	10	92	2
44	102	4	98	6
45	103	3	100	2
46	103	7	96	4
47	102	13	89	7
48	102	6	96	7

49	102	5	97	1
50	102	6	96	1
51	102	12	90	6
52	101	12	89	1
53	101	17	84	5
54	100	23	77	7
55	98	28	70	7
56	96	34	62	8
57	95	36	59	3
58	95	36	59	1
59	95	36	59	1
60	96	36	60	1
61	97	42	55	5
62	93	58	35	20
63	91	70	21	14
64	91	70	21	1
65	94	70	24	3

b) Kymograph 2

Frame	Maximum	Minimum	Difference	Length
0	97	43	54	
1	96	43	53	1
2	96	43	53	1
3	95	43	52	1
4	95	43	52	1
5	97	43	54	2
6	96	43	53	1
7	95	42	53	1
8	96	42	54	1
9	96	41	55	1
10	97	41	56	1
11	98	40	58	2
12	98	38	60	2
13	98	37	61	1
14	98	35	63	2
15	99	35	64	1
16	99	32	67	3
17	100	29	71	4
18	101	29	72	1
19	101	27	74	2
20	103	28	75	1
21	103	27	76	1
22	102	27	75	1
23	103	24	79	4
24	102	25	77	2
25	102	25	77	1
26	103	26	77	1
27	104	25	79	2
28	104	25	79	1
29	105	25	80	1
30	104	24	80	1
31	104	22	82	2
32	104	21	83	1
33	103	20	83	1
34	105	17	88	5
35	105	15	90	2
36	105	15	90	1
37	104	13	91	1
38	104	9	95	4
39	105	9	96	1
40	105	10	95	1
41	105	5	100	5
42	104	6	98	2
43	103	7	96	2
44	102	4	98	2
45	103	0	103	5
46	103	0	103	1
47	102	8	94	9
48	103	2	101	7
49	102	1	101	1
50	103	1	102	1
51	102	9	93	9
52	101	6	95	2
53	101	12	89	6
54	100	20	80	9
55	99	22	77	3
56	96	29	67	10
57	95	32	63	4
58	95	29	66	3
59	96	27	69	3
60	96	27	69	1
61	96	37	59	10
62	95	51	44	15
63	92	55	37	7
64	93	54	39	2
65	94	54	40	1

c) Kymograph 3

Frame	Maximum	Minimum	Difference	Length
0	98	38	60	
1	97	37	60	1
2	97	36	61	1
3	96	37	59	2
4	96	40	56	3
5	97	39	58	2
6	97	39	58	1
7	96	40	56	2
8	97	40	57	1
9	97	38	59	2
10	98	37	61	2
11	99	37	62	1
12	99	36	63	1
13	99	35	64	1
14	100	31	69	5
15	100	32	68	1
16	100	28	72	4
17	101	26	75	3
18	101	26	75	1
19	101	22	79	4
20	102	21	81	2

21	103	25	78	3
22	103	25	78	1
23	103	22	81	3
24	103	24	79	2
25	103	24	79	1
26	104	24	80	1
27	105	23	82	2
28	105	21	84	2
29	106	20	86	2
30	105	20	85	1
31	105	19	86	1
32	104	18	86	1
33	105	19	86	1
34	105	16	89	3
35	105	15	90	1
36	105	13	92	2
37	105	7	98	6
38	105	5	100	2
39	105	7	98	2
40	105	7	98	1
41	105	0	105	7
42	105	1	104	1
43	103	7	96	8
44	102	0	102	6
45	103	0	103	1
46	103	1	102	1
47	103	5	98	4
48	103	3	100	2
49	103	0	103	3
50	103	4	99	4
51	103	7	96	3
52	102	5	97	1
53	101	7	94	3
54	101	18	83	11
55	99	19	80	3
56	97	22	75	5
57	96	26	70	5
58	96	26	70	1
59	96	25	71	1
60	96	26	70	1
61	97	35	62	8
62	96	48	48	14
63	94	54	40	8
64	95	53	42	2
65	96	49	47	5

d) Kymograph 4

Frame	Maximum	Minimum	Difference	Length
0	98	35	63	
1	97	36	61	2
2	97	35	62	1
3	96	40	56	6
4	97	40	57	1
5	98	40	58	1
6	98	39	59	1
7	97	39	58	1
8	97	38	59	1
9	97	38	59	1
10	98	36	62	3
11	99	37	62	1
12	99	35	64	2
13	100	33	67	3
14	100	30	70	3
15	100	30	70	1
16	100	28	72	2
17	101	25	76	4
18	102	25	77	1
19	102	22	80	3
20	103	22	81	1
21	103	22	81	1
22	103	22	81	1
23	103	22	81	1
24	103	24	79	2
25	103	22	81	2
26	104	21	83	2
27	104	20	84	1
28	105	20	85	1
29	105	21	84	1
30	105	20	85	1
31	105	20	85	1
32	105	20	85	1
33	105	19	86	1
34	105	17	88	2
35	106	12	94	6
36	105	10	95	1
37	105	7	98	3
38	105	7	98	1
39	105	11	94	4
40	105	9	96	2
41	105	3	102	6
42	105	4	101	1
43	103	11	92	9
44	103	5	98	6
45	103	0	103	5
46	104	1	103	1
47	103	9	94	9
48	103	4	99	5
49	102	3	99	1
50	103	1	102	3
51	103	9	94	8
52	102	7	95	1
53	102	10	92	3
54	101	18	83	9
55	100	17	83	1
56	97	22	75	8
57	96	26	70	5
58	96	27	69	1
59	96	25	71	2
60	96	27	69	2
61	97	35	62	7
62	96	47	49	13
63	95	50	45	4
64	95	50	45	1
65	96	51	45	1

e) Kymograph 5

Frame	Maximum	Minimum	Difference	Length
0	99	37	62	
1	98	37	61	1
2	97	37	60	1
3	97	37	60	1
4	97	37	60	1
5	99	37	62	2
6	98	39	59	3
7	97	39	58	1
8	97	39	58	1
9	98	37	61	3
10	99	37	62	1
11	100	35	65	3
12	100	34	66	1
13	100	31	69	3
14	101	28	73	4
15	100	27	73	1
16	101	24	77	4
17	102	23	79	2
18	102	21	81	2
19	102	20	82	1
20	104	22	82	1
21	104	23	81	1
22	103	20	83	2
23	104	21	83	1
24	103	20	83	1
25	103	20	83	1
26	104	20	84	1
27	105	19	86	2
28	105	21	84	2
29	105	20	85	1
30	105	18	87	2
31	105	16	89	2
32	104	15	89	1
33	105	14	91	2
34	105	14	91	1
35	106	13	93	2
36	104	12	92	1
37	105	7	98	6
38	105	7	98	1
39	106	13	93	5
40	105	10	95	2
41	105	1	104	9
42	105	2	103	1
43	104	7	97	6
44	103	6	97	1
45	103	2	101	4
46	104	1	103	2
47	103	9	94	9
48	103	3	100	6
49	103	0	103	3
50	103	1	102	1
51	103	8	95	7
52	102	6	96	1
53	102	7	95	1
54	101	16	85	10
55	100	19	81	4
56	98	22	76	5
57	97	25	72	4
58	96	25	71	1
59	96	24	72	1
60	96	25	71	1
61	97	33	64	7
62	96	43	53	11
63	95	50	45	8
64	95	48	47	2
65	97	47	50	3

f) Kymograph 6

Frame	Maximum	Minimum	Difference	Length
0	99	36	63	
1	98	37	61	2
2	98	37	61	1
3	96	36	60	1
4	98	37	61	1
5	98	38	60	1
6	98	37	61	1
7	97	38	59	2
8	98	37	61	2
9	99	38	61	1
10	100	38	62	1
11	101	33	68	6
12	100	34	66	2
13	101	30	71	5
14	101	29	72	1
15	101	28	73	1
16	102	26	76	3
17	102	22	80	4
18	103	21	82	2
19	102	21	81	1
20	103	21	82	1
21	104	22	82	1
22	103	22	81	1
23	103	22	81	1
24	103	22	81	1
25	103	23	80	1
26	104	21	83	3
27	105	19	86	3
28	105	19	86	1
29	105	19	86	1
30	105	17	88	2
31	105	17	88	1
32	105	16	89	1
33	106	15	91	2
34	106	17	89	2
35	105	13	92	3
36	105	15	90	2
37	105	15	90	1
38	105	14	91	1

39	105	14	91	1
40	105	13	92	1
41	105	3	102	10
42	105	5	100	2
43	103	11	92	8
44	102	12	90	2
45	104	6	98	8
46	104	3	101	3
47	103	8	95	6
48	103	4	99	4
49	103	3	100	1
50	103	0	103	3
51	103	9	94	9
52	102	5	97	3
53	102	11	91	6
54	101	17	84	7
55	100	17	83	1
56	97	22	75	8
57	96	27	69	6
58	97	28	69	1
59	96	27	69	1
60	96	26	70	1
61	97	31	66	4
62	97	44	53	13
63	96	53	43	10
64	96	53	43	1
65	97	50	47	4

g) Kymograph 7

Frame	Maximum	Minimum	Difference	Length
0	100	32	68	
1	98	31	67	1
2	98	33	65	2
3	97	34	63	2
4	97	35	62	1
5	99	37	62	1
6	99	35	64	2
7	98	37	61	3
8	98	37	61	1
9	98	35	63	2
10	100	34	66	3
11	101	36	65	1
12	100	33	67	2
13	101	30	71	4
14	101	27	74	3
15	101	27	74	1
16	102	21	81	7
17	103	20	83	2
18	103	20	83	1
19	103	19	84	1
20	103	18	85	1
21	104	20	84	1
22	103	20	83	1
23	104	19	85	2
24	104	20	84	1
25	104	21	83	1
26	105	20	85	2
27	105	21	84	1
28	106	20	86	2
29	106	20	86	1
30	106	18	88	2
31	105	15	90	2
32	104	16	88	2
33	105	15	90	2
34	106	13	93	3
35	106	13	93	1
36	106	15	91	2
37	106	14	92	1
38	106	13	93	1
39	106	13	93	1
40	105	14	91	2
41	105	0	105	14
42	104	2	102	3
43	104	11	93	9
44	103	10	93	1
45	104	1	103	10
46	104	0	104	1
47	103	7	96	8
48	103	0	103	7
49	103	1	102	1
50	104	1	103	1
51	103	9	94	9
52	102	4	98	4
53	102	5	97	1
54	102	14	88	9
55	100	16	84	4
56	97	20	77	7
57	97	25	72	5
58	97	25	72	1
59	96	26	70	2
60	97	25	72	2
61	97	28	69	3
62	96	41	55	14
63	96	48	48	7
64	96	48	48	1
65	97	46	51	3

h) Kymograph 8

Frame	Maximum	Minimum	Difference	Length
0	100	35	65	
1	99	36	63	2
2	98	36	62	1
3	98	35	63	1
4	98	35	63	1
5	99	37	62	1
6	99	36	63	1
7	98	39	59	4
8	98	38	60	1
9	99	36	63	3
10	100	34	66	3

11	101	35	66	1
12	101	32	69	3
13	101	31	70	1
14	101	30	71	1
15	101	29	72	1
16	102	27	75	3
17	103	22	81	6
18	103	22	81	1
19	103	21	82	1
20	105	21	84	2
21	104	22	82	2
22	104	22	82	1
23	105	23	82	1
24	105	21	84	2
25	105	21	84	1
26	105	21	84	1
27	106	23	83	1
28	106	23	83	1
29	106	21	85	2
30	106	19	87	2
31	106	15	91	4
32	105	14	91	1
33	105	14	91	1
34	104	14	90	1
35	105	12	93	3
36	106	13	93	1
37	106	15	91	2
38	106	13	93	2

39	106	13	93	1
40	105	15	90	3
41	105	1	104	14
42	105	4	101	3
43	104	12	92	9
44	103	11	92	1
45	104	7	97	5
46	104	0	104	7
47	103	0	103	1
48	103	3	100	3
49	103	5	98	2
50	103	0	103	5
51	103	10	93	10
52	102	1	101	8
53	102	6	96	5
54	101	13	88	8
55	100	15	85	3
56	98	23	75	10
57	97	27	70	5
58	96	27	69	1
59	97	24	73	4
60	97	24	73	1
61	96	28	68	5
62	96	40	56	12
63	96	47	49	7
64	96	46	50	1
65	97	46	51	1

4. Video 4

a) Kymograph 1

Frame	Maximum	Minimum	Difference	Length
0	95	62	33	
1	95	59	36	3
2	93	55	38	2
3	92	55	37	1
4	94	53	41	4
5	96	54	42	1
6	98	50	48	6
7	96	49	47	1
8	98	48	50	3
9	95	44	51	1
10	95	43	52	1
11	95	42	53	1
12	95	40	55	2
13	94	39	55	1
14	93	35	58	3
15	93	35	58	1
16	93	34	59	1
17	93	34	59	1
18	93	34	59	1
19	94	34	60	1
20	93	31	62	2
21	91	28	63	1
22	90	28	62	1

23	90	30	60	2
24	91	30	61	1
25	90	30	60	1
26	90	31	59	1
27	90	31	59	1
28	91	33	58	1
29	93	34	59	1
30	92	31	61	2
31	91	31	60	1
32	93	31	62	2
33	91	31	60	2
34	92	30	62	2
35	92	28	64	2
36	92	28	64	1
37	90	29	61	3
38	91	27	64	3
39	91	26	65	1
40	91	26	65	1
41	90	29	61	4
42	89	30	59	2
43	94	34	60	1
44	96	37	59	1
45	94	36	58	1
46	95	35	60	2

47	97	36	61	1
48	98	36	62	1
49	97	38	59	3
50	98	40	58	1
51	97	41	56	2
52	97	41	56	1
53	100	39	61	5
54	101	36	65	4
55	98	33	65	1
56	99	33	66	1
57	99	31	68	2
58	97	30	67	1
59	98	29	69	2
60	99	27	72	3
61	97	29	68	4
62	97	24	73	5
63	97	14	83	10
64	98	20	78	5
65	98	21	77	1
66	98	25	73	4
67	97	26	71	2
68	96	26	70	1
69	99	28	71	1
70	99	28	71	1
71	98	28	70	1
72	98	28	70	1
73	99	22	77	7
74	99	24	75	2
75	99	27	72	3
76	99	30	69	3
77	97	33	64	5
78	98	33	65	1
79	97	30	67	2
80	98	28	70	3
81	97	27	70	1
82	97	25	72	2
83	97	22	75	3
84	99	22	77	2
85	101	24	77	1
86	99	21	78	1
87	99	23	76	2
88	99	23	76	1
89	99	23	76	1
90	99	21	78	2
91	99	20	79	1
92	100	19	81	2
93	100	14	86	5

94	100	18	82	4
95	100	25	75	7
96	100	32	68	7
97	98	34	64	4
98	99	35	64	1
99	98	36	62	2
100	96	36	60	2
101	94	33	61	1
102	95	34	61	1
103	95	33	62	1
104	96	31	65	3
105	95	32	63	2
106	97	25	72	9
107	95	22	73	1
108	95	27	68	5
109	95	31	64	4
110	97	33	64	1
111	97	27	70	6
112	97	32	65	5
113	93	40	53	12
114	95	41	54	1
115	97	53	44	10
116	97	83	14	30
117	97	86	11	3
118	97	83	14	3
119	95	83	12	2
120	95	82	13	1
121	96	84	12	1
122	96	87	9	3
123	95	88	7	2
124	97	95	2	5
125	89	89	0	2
126	95	62	33	3
127	95	59	36	2
128	93	55	38	1
129	92	55	37	4
130	94	53	41	1
131	96	54	42	6
132	98	50	48	1
133	96	49	47	3
134	98	48	50	1
135	95	44	51	1
136	95	43	52	1
137	95	42	53	2
138	95	40	55	1

b) Kymograph 2

Frame	Maximum	Minimum	Difference	Length
0	97	57	40	
1	97	56	41	1
2	97	55	42	1
3	97	54	43	1
4	96	51	45	2
5	97	50	47	2
6	99	47	52	5
7	99	45	54	2
8	97	44	53	1

9	97	44	53	1
10	97	42	55	2
11	97	41	56	1
12	97	39	58	2
13	95	38	57	1
14	94	36	58	1
15	93	34	59	1
16	94	33	61	2
17	95	33	62	1
18	95	32	63	1

19	95	32	63	1
20	94	29	65	2
21	94	28	66	1
22	93	29	64	2
23	93	29	64	1
24	93	29	64	1
25	92	31	61	3
26	92	30	62	1
27	93	30	63	1
28	92	32	60	3
29	94	32	62	2
30	94	30	64	2
31	94	30	64	1
32	95	30	65	1
33	94	29	65	1
34	95	28	67	2
35	94	26	68	1
36	93	27	66	2
37	92	28	64	2
38	92	26	66	2
39	92	24	68	2
40	92	26	66	2
41	92	29	63	3
42	92	29	63	1
43	97	32	65	2
44	97	35	62	3
45	97	35	62	1
46	98	34	64	2
47	99	35	64	1
48	99	36	63	1
49	99	37	62	1
50	98	39	59	3
51	99	39	60	1
52	98	39	59	1
53	100	37	63	4
54	101	36	65	2
55	102	32	70	5
56	102	31	71	1
57	101	31	70	1
58	99	29	70	1
59	101	28	73	3
60	101	28	73	1
61	99	29	70	3
62	100	23	77	7
63	101	14	87	10
64	101	19	82	5
65	101	20	81	1
66	100	24	76	5
67	101	27	74	2
68	101	28	73	1
69	100	28	72	1
70	99	28	71	1
71	99	28	71	1
72	101	28	73	2
73	101	21	80	7
74	102	22	80	1
75	99	26	73	7
76	99	28	71	2
77	99	30	69	2
78	100	30	70	1

79	100	30	70	1
80	101	27	74	4
81	99	26	73	1
82	98	23	75	2
83	99	22	77	2
84	101	22	79	2
85	101	23	78	1
86	101	21	80	2
87	101	19	82	2
88	100	19	81	1
89	101	19	82	1
90	100	20	80	2
91	100	20	80	1
92	101	19	82	2
93	101	13	88	6
94	102	18	84	4
95	101	24	77	7
96	102	31	71	6
97	102	34	68	3
98	101	32	69	1
99	100	35	65	4
100	100	35	65	1
101	97	32	65	1
102	95	32	63	2
103	95	32	63	1
104	97	31	66	3
105	99	32	67	1
106	95	22	73	6
107	95	20	75	2
108	95	26	69	6
109	96	31	65	4
110	97	33	64	1
111	97	25	72	8
112	96	32	64	8
113	95	39	56	8
114	99	40	59	3
115	100	49	51	8
116	95	66	29	22
117	97	82	15	14
118	97	74	23	8
119	97	77	20	3
120	96	78	18	2
121	96	80	16	2
122	97	81	16	1
123	98	82	16	1
124	97	82	15	1
125	97	83	14	1
126	95	84	11	3
127	96	84	12	1
128	95	89	6	6
129	95	91	4	2
130	93	87	6	2
131	94	89	5	1
132	97	57	40	1
133	97	56	41	1
134	97	55	42	1
135	97	54	43	2
136	96	51	45	2
137	97	50	47	5
138	99	47	52	2

c) Kymograph 3

Frame	Maximum	Minimum	Difference	Length
0	99	56	43	
1	99	55	44	1
2	99	54	45	1
3	98	50	48	3
4	98	49	49	1
5	98	48	50	1
6	99	46	53	3
7	101	46	55	2
8	100	42	58	3
9	99	42	57	1
10	98	38	60	3
11	98	38	60	1
12	97	36	61	1
13	97	36	61	1
14	95	35	60	1
15	94	34	60	1
16	96	32	64	4
17	96	31	65	1
18	97	31	66	1
19	97	30	67	1
20	96	28	68	1
21	96	27	69	1
22	94	27	67	2
23	95	28	67	1
24	95	27	68	1
25	94	28	66	2
26	94	28	66	1
27	95	28	67	1
28	94	30	64	3
29	96	30	66	2
30	96	29	67	1
31	96	28	68	1
32	96	29	67	1
33	96	29	67	1
34	97	28	69	2
35	96	25	71	2
36	95	26	69	2
37	94	27	67	2
38	94	25	69	2
39	94	23	71	2
40	95	24	71	1
41	95	28	67	4
42	94	28	66	1
43	98	30	68	2
44	98	33	65	3
45	98	33	65	1
46	99	32	67	2
47	99	34	65	2
48	99	34	65	1
49	98	36	62	3
50	99	38	61	1
51	99	37	62	1
52	102	37	65	3
53	102	35	67	2
54	101	33	68	1
55	103	30	73	5
56	104	29	75	2
57	104	28	76	1
58	101	27	74	2
59	102	28	74	1
60	103	26	77	3
61	102	28	74	3
62	101	21	80	6
63	102	14	88	8
64	102	17	85	3
65	102	20	82	3
66	103	23	80	2
67	102	24	78	2
68	101	24	77	1
69	103	27	76	1
70	103	26	77	1
71	101	27	74	3
72	103	26	77	3
73	103	23	80	3
74	103	22	81	1
75	102	24	78	3
76	102	28	74	4
77	101	28	73	1
78	102	28	74	1
79	103	28	75	1
80	102	28	74	1
81	101	24	77	3
82	100	21	79	2
83	101	19	82	3
84	103	20	83	1
85	104	19	85	2
86	103	21	82	3
87	102	17	85	3
88	102	18	84	1
89	101	18	83	1
90	101	22	79	4
91	102	18	84	5
92	102	16	86	2
93	104	13	91	5
94	104	16	88	3
95	104	23	81	7
96	104	31	73	8
97	104	32	72	1
98	103	33	70	2
99	102	34	68	2
100	101	32	69	1
101	101	29	72	3
102	100	31	69	3
103	98	30	68	1
104	97	31	66	2
105	99	32	67	1
106	101	23	78	11
107	98	19	79	1
108	99	25	74	5
109	99	29	70	4
110	99	34	65	5
111	99	26	73	8
112	99	29	70	3

113	99	38	61	9
114	100	39	61	1
115	101	47	54	7
116	98	61	37	17
117	101	66	35	2
118	100	68	32	3
119	99	66	33	1
120	98	66	32	1
121	98	66	32	1
122	98	67	31	1
123	99	72	27	4
124	99	74	25	2
125	99	75	24	1
126	99	76	23	1
127	97	76	21	2
128	96	81	15	6
129	95	81	14	1
130	94	79	15	1
131	95	82	13	2
132	98	92	6	7
133	98	93	5	1
134	100	82	18	13
135	99	80	19	1
136	100	79	21	2
137	100	72	28	7
138	99	70	29	1

d) Kymograph 4

Frame	Maximum	Minimum	Difference	Length
0	99	53	46	
1	101	51	50	4
2	99	50	49	1
3	99	47	52	3
4	98	45	53	1
5	99	44	55	2
6	101	42	59	4
7	102	41	61	2
8	101	39	62	1
9	100	38	62	1
10	99	37	62	1
11	99	37	62	1
12	98	35	63	1
13	98	32	66	3
14	97	33	64	2
15	96	31	65	1
16	96	30	66	1
17	97	30	67	1
18	98	30	68	1
19	98	29	69	1
20	98	27	71	2
21	97	25	72	1
22	96	25	71	1
23	96	26	70	1
24	96	26	70	1
25	96	28	68	2
26	96	27	69	1
27	97	28	69	1
28	97	29	68	1
29	97	28	69	1
30	97	27	70	1
31	97	27	70	1
32	98	28	70	1
33	98	27	71	1
34	98	27	71	1
35	98	25	73	2
36	98	25	73	1
37	96	26	70	3
38	97	23	74	4
39	97	21	76	2
40	97	22	75	1
41	97	27	70	5
42	97	26	71	1
43	98	29	69	2
44	100	30	70	1
45	101	31	70	1
46	101	31	70	1
47	100	32	68	2
48	100	32	68	1
49	101	34	67	1
50	102	35	67	1
51	103	35	68	1
52	104	35	69	1
53	104	31	73	4
54	104	30	74	1
55	104	29	75	1
56	104	28	76	1
57	105	26	79	3
58	104	26	78	1
59	105	25	80	2
60	105	26	79	1
61	103	27	76	3
62	103	21	82	6
63	103	13	90	8
64	103	16	87	3
65	105	20	85	2
66	105	22	83	2
67	104	23	81	2
68	104	22	82	1
69	105	26	79	3
70	105	25	80	1
71	104	26	78	2
72	105	24	81	3
73	104	18	86	5
74	104	18	86	1
75	104	20	84	2
76	104	24	80	4
77	104	27	77	3
78	104	27	77	1
79	104	26	78	1
80	103	22	81	3
81	103	21	82	1
82	102	19	83	1
83	103	17	86	3
84	105	17	88	2
85	104	20	84	4
86	104	16	88	4

87	104	15	89	1
88	104	15	89	1
89	104	16	88	1
90	104	18	86	2
91	103	17	86	1
92	104	16	88	2
93	105	13	92	4
94	105	14	91	1
95	105	21	84	7
96	105	28	77	7
97	104	28	76	1
98	103	29	74	2
99	103	30	73	1
100	103	31	72	1
101	103	27	76	4
102	102	28	74	2
103	101	28	73	1
104	101	30	71	2
105	103	31	72	1
106	102	22	80	8
107	101	17	84	4
108	101	24	77	7
109	99	30	69	8
110	101	33	68	1
111	101	22	79	11
112	101	28	73	6
113	101	37	64	9

114	101	38	63	1
115	102	44	58	5
116	100	57	43	15
117	101	59	42	1
118	102	61	41	1
119	100	61	39	2
120	99	61	38	1
121	99	61	38	1
122	100	62	38	1
123	101	63	38	1
124	101	64	37	1
125	101	66	35	2
126	100	66	34	1
127	99	66	33	1
128	98	66	32	1
129	95	66	29	3
130	96	66	30	1
131	99	66	33	3
132	99	80	19	14
133	100	74	26	7
134	100	71	29	3
135	100	70	30	1
136	101	69	32	2
137	101	66	35	3
138	101	65	36	1

e) Kymograph 5

Frame	Maximum	Minimum	Difference	Length
0	102	47	55	
1	102	45	57	2
2	101	46	55	2
3	100	43	57	2
4	100	41	59	2
5	101	40	61	2
6	103	39	64	3
7	103	37	66	2
8	103	35	68	2
9	101	33	68	1
10	101	32	69	1
11	101	30	71	2
12	101	28	73	2
13	100	27	73	1
14	99	26	73	1
15	97	28	69	4
16	98	28	70	1
17	98	27	71	1
18	99	27	72	1
19	99	28	71	1
20	98	23	75	4
21	99	23	76	1
22	98	23	75	1
23	98	23	75	1
24	98	24	74	1
25	97	25	72	2
26	98	25	73	1
27	99	25	74	1
28	98	27	71	3

29	99	27	72	1
30	99	25	74	2
31	99	24	75	1
32	99	25	74	1
33	100	25	75	1
34	101	24	77	2
35	100	22	78	1
36	99	23	76	2
37	98	24	74	2
38	98	21	77	3
39	99	19	80	3
40	99	18	81	1
41	98	24	74	7
42	99	24	75	1
43	99	28	71	4
44	100	29	71	1
45	102	28	74	3
46	102	29	73	1
47	102	30	72	1
48	101	30	71	1
49	103	31	72	1
50	103	31	72	1
51	104	29	75	3
52	105	28	77	2
53	105	26	79	2
54	105	25	80	1
55	106	25	81	1
56	106	25	81	1
57	106	24	82	1
58	106	23	83	1

59	106	21	85	2
60	106	21	85	1
61	105	21	84	1
62	105	18	87	3
63	105	10	95	8
64	105	13	92	3
65	106	19	87	5
66	106	20	86	1
67	106	23	83	3
68	106	21	85	2
69	106	20	86	1
70	107	22	85	1
71	107	25	82	3
72	106	23	83	1
73	107	18	89	6
74	107	14	93	4
75	106	15	91	2
76	105	21	84	7
77	106	20	86	2
78	106	22	84	2
79	106	16	90	6
80	106	13	93	3
81	105	13	92	1
82	103	12	91	1
83	104	12	92	1
84	106	12	94	2
85	106	13	93	1
86	106	14	92	1
87	105	10	95	3
88	105	11	94	1
89	105	12	93	1
90	105	16	89	4
91	105	14	91	2
92	106	15	91	1
93	106	0	106	15
94	107	11	96	10
95	107	16	91	5
96	107	24	83	8
97	105	24	81	2
98	104	24	80	1
99	104	27	77	3

100	104	24	80	3
101	104	20	84	4
102	104	20	84	1
103	103	20	83	1
104	103	20	83	1
105	104	22	82	1
106	104	18	86	4
107	104	13	91	5
108	103	18	85	6
109	103	28	75	10
110	104	30	74	1
111	104	18	86	12
112	104	25	79	7
113	103	34	69	10
114	102	34	68	1
115	103	42	61	7
116	105	47	58	3
117	105	53	52	6
118	104	52	52	1
119	102	52	50	2
120	101	54	47	3
121	101	54	47	1
122	102	55	47	1
123	102	55	47	1
124	102	55	47	1
125	102	56	46	1
126	101	56	45	1
127	101	56	45	1
128	100	56	44	1
129	99	56	43	1
130	98	56	42	1
131	101	57	44	2
132	101	67	34	10
133	101	68	33	1
134	102	65	37	4
135	102	62	40	3
136	103	60	43	3
137	103	57	46	3
138	102	56	46	1

f) Kymograph 6

Frame	Maximum	Minimum	Difference	Length
0	102	47	55	
1	102	45	57	2
2	101	41	60	3
3	101	41	60	1
4	100	42	58	2
5	102	41	61	3
6	103	39	64	3
7	103	37	66	2
8	103	36	67	1
9	102	34	68	1
10	101	32	69	1
11	101	30	71	2
12	101	29	72	1
13	101	27	74	2
14	100	25	75	1

15	98	25	73	2
16	99	25	74	1
17	99	26	73	1
18	99	26	73	1
19	100	24	76	3
20	99	21	78	2
21	99	21	78	1
22	97	22	75	3
23	97	21	76	1
24	98	23	75	1
25	98	25	73	2
26	98	24	74	1
27	99	24	75	1
28	99	26	73	2
29	99	26	73	1
30	99	24	75	2

31	99	24	75	1
32	100	24	76	1
33	100	24	76	1
34	100	22	78	2
35	100	21	79	1
36	100	22	78	1
37	100	23	77	1
38	100	21	79	2
39	100	17	83	4
40	99	18	81	2
41	99	23	76	5
42	99	22	77	1
43	100	26	74	3
44	102	28	74	1
45	102	29	73	1
46	102	28	74	1
47	103	28	75	1
48	103	29	74	1
49	104	32	72	2
50	104	31	73	1
51	105	29	76	3
52	106	28	78	2
53	106	25	81	3
54	106	24	82	1
55	106	23	83	1
56	107	25	82	1
57	106	23	83	1
58	106	20	86	3
59	107	24	83	3
60	107	24	83	1
61	106	23	83	1
62	106	20	86	3
63	105	4	101	15
64	105	10	95	6
65	107	10	97	2
66	106	21	85	12
67	107	23	84	1
68	107	22	85	1
69	107	24	83	2
70	107	24	83	1
71	108	25	83	1
72	108	25	83	1
73	107	21	86	3
74	108	18	90	4
75	107	18	89	1
76	106	23	83	6
77	106	24	82	1
78	107	24	83	1
79	107	22	85	2
80	106	16	90	5
81	105	15	90	1
82	105	13	92	2
83	105	12	93	1
84	107	13	94	1
85	107	13	94	1
86	106	15	91	3

87	105	12	93	2
88	105	12	93	1
89	106	13	93	1
90	106	15	91	2
91	106	15	91	1
92	106	15	91	1
93	107	1	106	15
94	107	8	99	7
95	107	16	91	8
96	107	26	81	10
97	105	24	81	1
98	105	26	79	2
99	104	26	78	1
100	104	27	77	1
101	105	23	82	5
102	104	23	81	1
103	104	22	82	1
104	103	24	79	3
105	105	29	76	3
106	105	22	83	7
107	104	14	90	7
108	104	17	87	3
109	104	28	76	11
110	105	30	75	1
111	105	20	85	10
112	105	23	82	3
113	104	32	72	10
114	103	32	71	1
115	104	40	64	7
116	105	47	58	6
117	104	52	52	6
118	104	52	52	1
119	102	52	50	2
120	102	53	49	1
121	102	54	48	1
122	102	55	47	1
123	102	55	47	1
124	103	55	48	1
125	102	55	47	1
126	101	56	45	2
127	102	55	47	2
128	101	56	45	2
129	100	56	44	1
130	100	56	44	1
131	102	58	44	1
132	102	65	37	7
133	102	64	38	1
134	102	61	41	3
135	102	60	42	1
136	103	59	44	2
137	103	57	46	2
138	102	56	46	1

g) Kymograph 7

Frame	Maximum	Minimum	Difference	Length
0	102	46	56	
1	101	45	56	1
2	100	44	56	1
3	99	42	57	1
4	99	41	58	1
5	100	40	60	2
6	102	38	64	4
7	103	37	66	2
8	102	36	66	1
9	101	34	67	1
10	101	33	68	1
11	102	32	70	2
12	102	31	71	1
13	101	30	71	1
14	99	25	74	3
15	99	25	74	1
16	99	23	76	2
17	100	23	77	1
18	100	24	76	1
19	100	23	77	1
20	99	22	77	1
21	99	22	77	1
22	98	21	77	1
23	99	22	77	1
24	98	23	75	2
25	98	24	74	1
26	99	24	75	1
27	99	24	75	1
28	99	27	72	3
29	100	26	74	2
30	100	24	76	2
31	99	24	75	1
32	100	24	76	1
33	100	25	75	1
34	101	25	76	1
35	101	21	80	4
36	100	22	78	2
37	100	22	78	1
38	100	20	80	2
39	100	17	83	3
40	99	18	81	2
41	100	22	78	3
42	99	22	77	1
43	102	25	77	1
44	103	26	77	1
45	103	26	77	1
46	103	25	78	1
47	104	28	76	2
48	103	28	75	1
49	104	31	73	2
50	104	33	71	2
51	105	28	77	6
52	106	27	79	2
53	106	26	80	1
54	106	25	81	1
55	106	23	83	2
56	106	24	82	1
57	106	20	86	4
58	106	19	87	1
59	107	23	84	3
60	107	24	83	1
61	106	25	81	2
62	106	21	85	4
63	105	12	93	8
64	106	16	90	3
65	107	19	88	2
66	107	22	85	3
67	107	22	85	1
68	107	22	85	1
69	107	25	82	3
70	107	24	83	1
71	107	24	83	1
72	107	24	83	1
73	107	19	88	5
74	107	21	86	2
75	106	21	85	1
76	106	22	84	1
77	106	24	82	2
78	107	24	83	1
79	107	21	86	3
80	107	24	83	3
81	106	24	82	1
82	105	14	91	9
83	106	20	86	5
84	107	15	92	6
85	107	20	87	5
86	106	16	90	3
87	106	17	89	1
88	106	17	89	1
89	106	3	103	14
90	107	20	87	16
91	106	18	88	1
92	106	17	89	1
93	106	13	93	4
94	106	10	96	3
95	107	17	90	6
96	106	24	82	8
97	106	26	80	2
98	105	25	80	1
99	105	26	79	1
100	104	26	78	1
101	105	23	82	4
102	104	26	78	4
103	104	26	78	1
104	105	28	77	1
105	105	29	76	1
106	105	23	82	6
107	104	16	88	6
108	104	22	82	6
109	105	28	77	5
110	105	31	74	3
111	105	21	84	10
112	104	26	78	6
113	103	33	70	8
114	103	33	70	1

115	104	39	65	5
116	105	50	55	10
117	104	54	50	5
118	104	55	49	1
119	102	54	48	1
120	101	54	47	1
121	102	52	50	3
122	102	53	49	1
123	103	53	50	1
124	103	54	49	1
125	102	58	44	5
126	102	53	44	1
127	102	55	45	1
128	99	56	42	3
129	98	55	41	1
130	98	55	41	1
131	99	54	42	1
132	102	62	40	2
133	101	62	39	1
134	101	58	39	1
135	102	57	42	3
136	102	57	42	1
137	102	55	44	2
138	102	53	46	2

h) Kymograph 8

Frame	Maximum	Minimum	Difference	Length
0	102	43	59	
1	102	42	60	1
2	102	42	60	1
3	101	40	61	1
4	102	39	63	2
5	102	39	63	1
6	104	37	67	4
7	103	36	67	1
8	103	33	70	3
9	101	32	69	1
10	101	30	71	2
11	102	29	73	2
12	101	28	73	1
13	101	27	74	1
14	100	24	76	2
15	100	23	77	1
16	100	23	77	1
17	101	22	79	2
18	101	22	79	1
19	101	20	81	2
20	101	19	82	1
21	100	20	80	2
22	99	18	81	1
23	99	18	81	1
24	99	18	81	1
25	99	23	76	5
26	99	23	76	1
27	100	23	77	1
28	101	26	75	2
29	101	22	79	4
30	101	22	79	1
31	100	22	78	1
32	101	23	78	1
33	101	22	79	1
34	101	22	79	1
35	101	20	81	2
36	101	21	80	1
37	101	22	79	1
38	100	19	81	2
39	101	16	85	4
40	100	16	84	1
41	100	21	79	5
42	100	19	81	2
43	102	25	77	4
44	103	25	78	1
45	104	25	79	1
46	104	25	79	1
47	104	27	77	2
48	104	28	76	1
49	105	30	75	1
50	105	32	73	2
51	107	28	79	6
52	107	26	81	2
53	107	23	84	3
54	107	22	85	1
55	107	21	86	1
56	107	22	85	1
57	107	21	86	1
58	107	20	87	1
59	107	22	85	2
60	109	24	85	1
61	106	25	81	4
62	106	20	86	5
63	106	13	93	7
64	106	15	91	2
65	107	17	90	1
66	108	19	89	1
67	108	21	87	2
68	108	20	88	1
69	107	24	83	5
70	108	24	84	1
71	108	24	84	1
72	108	25	83	1
73	108	22	86	3
74	108	20	88	2
75	107	20	87	1
76	107	22	85	2
77	107	24	83	2
78	108	25	83	1
79	107	18	89	6
80	107	14	93	4
81	106	14	92	1
82	106	10	96	4
83	106	9	97	1
84	108	10	98	1
85	108	6	102	4
86	107	6	101	1
87	106	4	102	1
88	107	4	103	1

89	107	4	103	1
90	107	16	91	12
91	106	16	90	1
92	106	17	89	1
93	107	4	103	14
94	107	4	103	1
95	107	12	95	8
96	107	23	84	11
97	106	24	82	2
98	106	24	82	1
99	105	25	80	2
100	105	24	81	1
101	105	18	87	6
102	105	24	81	6
103	105	26	79	2
104	105	28	77	2
105	106	29	77	1
106	106	23	83	6
107	105	14	91	8
108	105	21	84	7
109	105	27	78	6
110	106	30	76	2
111	106	18	88	12
112	106	25	81	7
113	103	31	72	9
114	104	32	72	1

115	105	34	71	1
116	105	48	57	14
117	105	52	53	4
118	105	52	53	1
119	103	51	52	1
120	102	52	50	2
121	102	52	50	1
122	103	53	50	1
123	103	54	49	1
124	103	54	49	1
125	103	55	48	1
126	103	53	50	2
127	103	55	48	2
128	102	56	46	2
129	101	55	46	1
130	100	55	45	1
131	101	54	47	2
132	101	62	39	8
133	101	62	39	1
134	102	58	44	5
135	104	57	47	3
136	104	57	47	1
137	104	55	49	2
138	103	53	50	1

5. Video 5

a) Kymograph 1

Frame	Maximum	Minimum	Difference	Length
0	86	39	47	
1	86	39	47	1
2	85	38	47	1
3	85	38	47	1
4	82	39	43	4
5	84	41	43	1
6	87	41	46	3
7	89	39	50	4
8	89	41	48	2
9	85	41	44	4
10	84	41	43	1
11	86	43	43	1
12	87	41	46	3
13	86	42	44	2
14	82	43	39	5
15	82	43	39	1
16	85	43	42	3
17	85	43	42	1
18	85	42	43	1
19	82	41	41	2
20	83	41	42	1
21	82	40	42	1
22	82	39	43	1
23	83	37	46	3
24	82	37	45	1

25	82	35	47	2
26	85	34	51	4
27	86	33	53	2
28	87	31	56	3
29	85	31	54	2
30	83	31	52	2
31	82	29	53	1
32	82	27	55	2
33	87	25	62	7
34	89	27	62	1
35	90	29	61	1
36	87	30	57	4
37	89	28	61	4
38	90	27	63	2
39	91	26	65	2
40	91	25	66	1
41	90	23	67	1
42	89	19	70	3
43	89	19	70	1
44	91	19	72	2
45	90	23	67	5
46	91	24	67	1
47	90	23	67	1
48	90	25	65	2
49	92	24	68	3
50	96	23	73	5

51	93	27	66	7
52	93	29	64	2
53	94	29	65	1
54	97	26	71	6
55	99	21	78	7
56	100	17	83	5
57	99	15	84	1
58	99	13	86	2
59	99	13	86	1
60	99	10	89	3
61	101	9	92	3
62	103	7	96	4
63	103	8	95	1
64	101	8	93	2
65	103	11	92	1
66	104	21	83	9
67	105	23	82	1
68	105	29	76	6
69	105	35	70	6
70	104	35	69	1
71	105	33	72	3

b) Kymograph 2

Frame	Maximum	Minimum	Difference	Length
0	87	37	50	
1	87	38	49	1
2	87	36	51	2
3	86	36	50	1
4	83	38	45	5
5	85	38	47	2
6	87	38	49	2
7	88	39	49	1
8	89	37	52	3
9	86	39	47	5
10	85	40	45	2
11	88	40	48	3
12	88	38	50	2
13	87	38	49	1
14	82	39	43	6
15	82	40	42	1
16	85	40	45	3
17	86	40	46	1
18	86	40	46	1
19	83	38	45	1
20	83	38	45	1
21	82	38	44	1
22	85	36	49	5
23	85	35	50	1
24	85	34	51	1
25	85	33	52	1
26	86	31	55	3
27	87	30	57	2
28	87	30	57	1
29	87	28	59	2
30	85	26	59	1
31	82	26	56	3
32	85	22	63	7
33	87	22	65	2
34	88	25	63	2
35	89	26	63	1
36	88	28	60	3
37	89	24	65	5
38	91	24	67	2
39	92	24	68	1
40	92	23	69	1
41	92	20	72	3
42	89	17	72	1
43	88	17	71	1
44	92	16	76	5
45	90	20	70	6
46	92	20	72	2
47	89	20	69	3
48	89	23	66	3
49	93	21	72	6
50	95	20	75	3
51	94	25	69	6
52	94	27	67	2
53	95	26	69	2
54	96	25	71	2
55	100	21	79	8
56	100	14	86	7
57	97	12	85	1
58	99	11	88	3
59	97	10	87	1
60	99	10	89	2
61	100	7	93	4
62	103	4	99	6
63	102	7	95	4
64	101	6	95	1
65	102	10	92	3
66	103	20	83	9
67	104	20	84	1
68	103	26	77	7
69	103	32	71	6
70	103	33	70	1
71	103	32	71	1

c) Kymograph 3

Frame	Maximum	Minimum	Difference	Length
0	89	30	59	
1	89	30	59	1
2	88	32	56	3
3	88	31	57	1
4	86	33	53	4
5	88	33	55	2
6	89	34	55	1
7	92	32	60	5
8	92	34	58	2

9	88	34	54	4
10	88	36	52	2
11	89	35	54	2
12	90	35	55	1
13	88	35	53	2
14	86	36	50	3
15	85	36	49	1
16	88	36	52	3
17	88	36	52	1
18	87	35	52	1
19	86	36	50	2
20	86	34	52	2
21	86	32	54	2
22	86	32	54	1
23	86	32	54	1
24	87	30	57	3
25	86	30	56	1
26	87	26	61	5
27	89	25	64	3
28	89	24	65	1
29	88	24	64	1
30	87	20	67	3
31	86	20	66	1
32	86	18	68	2
33	89	16	73	5
34	90	20	70	3
35	92	23	69	1
36	90	24	66	3
37	90	20	70	4
38	92	19	73	3
39	93	18	75	2
40	93	18	75	1

41	92	18	74	1
42	90	14	76	2
43	92	16	76	1
44	93	13	80	4
45	92	14	78	2
46	93	18	75	3
47	92	17	75	1
48	92	20	72	3
49	94	18	76	4
50	96	19	77	1
51	96	21	75	2
52	95	24	71	4
53	96	24	72	1
54	97	22	75	3
55	100	20	80	5
56	100	13	87	7
57	99	11	88	1
58	100	9	91	3
59	100	7	93	2
60	100	6	94	1
61	102	4	98	4
62	103	2	101	3
63	103	4	99	2
64	102	6	96	3
65	103	7	96	1
66	103	17	86	10
67	106	16	90	4
68	104	21	83	7
69	104	25	79	4
70	104	27	77	2
71	104	25	79	2

d) Kymograph 4

Frame	Maximum	Minimum	Difference	Length
0	90	26	64	
1	90	24	66	2
2	90	28	62	4
3	88	28	60	2
4	87	30	57	3
5	89	30	59	2
6	90	30	60	1
7	93	27	66	6
8	92	31	61	5
9	89	31	58	3
10	89	34	55	3
11	90	34	56	1
12	92	33	59	3
13	89	33	56	3
14	86	34	52	4
15	87	34	53	1
16	88	34	54	1
17	89	34	55	1
18	88	32	56	1
19	88	32	56	1
20	87	30	57	1
21	86	30	56	1
22	88	30	58	2
23	87	28	59	1

24	88	26	62	3
25	87	26	61	1
26	88	24	64	3
27	90	22	68	4
28	89	20	69	1
29	89	18	71	2
30	88	18	70	1
31	86	16	70	1
32	87	14	73	3
33	90	12	78	5
34	92	16	76	2
35	92	18	74	2
36	92	21	71	3
37	92	18	74	3
38	93	16	77	3
39	94	16	78	1
40	94	16	78	1
41	94	14	80	2
42	92	12	80	1
43	92	13	79	1
44	93	12	81	2
45	93	12	81	1
46	94	14	80	1
47	93	16	77	3
48	93	16	77	1

49	96	14	82	5
50	96	17	79	3
51	95	20	75	4
52	96	18	78	3
53	97	22	75	3
54	99	18	81	6
55	100	18	82	1
56	100	13	87	5
57	99	9	90	3
58	100	7	93	3
59	100	6	94	1
60	101	5	96	2
61	101	3	98	2
62	102	0	102	4
63	103	3	100	2
64	102	6	96	4
65	103	6	97	1
66	103	16	87	10
67	106	12	94	7
68	106	19	87	7
69	104	23	81	6
70	104	26	78	3
71	104	22	82	4

e) Kymograph 5

Frame	Maximum	Minimum	Difference	Length
0	90	31	59	
1	90	32	58	1
2	89	28	61	3
3	89	32	57	4
4	87	32	55	2
5	89	32	57	2
6	90	33	57	1
7	92	33	59	2
8	92	33	59	1
9	89	33	56	3
10	89	33	56	1
11	89	34	55	1
12	90	33	57	2
13	89	34	55	2
14	86	34	52	3
15	86	33	53	1
16	89	33	56	3
17	88	32	56	1
18	88	32	56	1
19	87	30	57	1
20	87	28	59	2
21	86	28	58	1
22	87	28	59	1
23	87	27	60	1
24	87	26	61	1
25	87	24	63	2
26	88	22	66	3
27	89	21	68	2
28	90	18	72	4
29	90	16	74	2
30	88	16	72	2
31	87	14	73	1
32	87	11	76	3
33	90	10	80	4
34	92	16	76	4
35	92	19	73	3
36	92	22	70	3
37	92	14	78	8
38	93	14	79	1
39	94	14	80	1
40	94	14	80	1
41	93	14	79	1
42	92	12	80	1
43	90	12	78	2
44	93	11	82	4
45	92	10	82	1
46	94	12	82	1
47	92	13	79	3
48	92	17	75	4
49	95	14	81	6
50	96	18	78	3
51	95	23	72	6
52	95	22	73	1
53	96	23	73	1
54	97	20	77	4
55	100	20	80	3
56	99	14	85	5
57	99	10	89	4
58	99	6	93	4
59	99	4	95	2
60	100	4	96	1
61	100	2	98	2
62	102	0	102	4
63	101	2	99	3
64	101	6	95	4
65	102	6	96	1
66	103	14	89	7
67	103	10	93	4
68	103	20	83	10
69	103	26	77	6
70	103	28	75	2
71	103	26	77	2

f) Kymograph 6

Frame	Maximum	Minimum	Difference	Length
0	92	25	67	
1	92	26	66	1
2	90	25	65	1
3	89	26	63	2
4	88	30	58	5

5	89	27	62	4
6	91	31	60	2
7	92	32	60	1
8	92	28	64	4
9	90	31	59	5
10	89	31	58	1
11	90	31	59	1
12	93	32	61	2
13	90	31	59	2
14	88	32	56	3
15	88	31	57	1
16	89	31	58	1
17	90	30	60	2
18	89	30	59	1
19	89	28	61	2
20	88	27	61	1
21	88	26	62	1
22	89	24	65	3
23	89	24	65	1
24	88	22	66	1
25	88	21	67	1
26	90	18	72	5
27	92	17	75	3
28	92	16	76	1
29	92	14	78	2
30	90	12	78	1
31	88	10	78	1
32	88	8	80	2
33	90	9	81	1
34	93	14	79	2
35	93	14	79	1
36	92	17	75	4
37	93	10	83	8
38	94	10	84	1

39	95	11	84	1
40	95	11	84	1
41	94	10	84	1
42	92	8	84	1
43	92	8	84	1
44	94	10	84	1
45	93	6	87	3
46	94	10	84	3
47	93	12	81	3
48	94	13	81	1
49	96	10	86	5
50	97	16	81	5
51	96	19	77	4
52	97	20	77	1
53	97	20	77	1
54	99	17	82	5
55	101	16	85	3
56	100	14	86	1
57	99	10	89	3
58	99	5	94	5
59	99	3	96	2
60	100	3	97	1
61	101	0	101	4
62	102	0	102	1
63	103	0	103	1
64	101	6	95	8
65	102	6	96	1
66	103	11	92	4
67	104	8	96	4
68	104	14	90	6
69	104	20	84	6
70	104	24	80	4
71	104	20	84	4

g) Kymograph 7

Frame	Maximum	Minimum	Difference	Length
0	92	23	69	
1	92	24	68	1
2	92	25	67	1
3	89	30	59	8
4	89	30	59	1
5	90	30	60	1
6	92	30	62	2
7	93	30	63	1
8	93	30	63	1
9	90	31	59	4
10	89	31	58	1
11	90	32	58	1
12	92	30	62	4
13	90	30	60	2
14	87	30	57	3
15	88	30	58	1
16	89	30	59	1
17	90	30	60	1
18	89	28	61	1
19	88	27	61	1
20	88	26	62	1
21	88	26	62	1

22	89	23	66	4
23	88	22	66	1
24	89	20	69	3
25	89	18	71	2
26	89	16	73	2
27	92	14	78	5
28	92	13	79	1
29	92	12	80	1
30	89	11	78	2
31	88	10	78	1
32	89	7	82	4
33	90	6	84	2
34	92	12	80	4
35	93	16	77	3
36	93	17	76	1
37	93	8	85	9
38	94	8	86	1
39	94	9	85	1
40	94	10	84	1
41	94	8	86	2
42	93	6	87	1
43	92	6	86	1
44	94	8	86	1

45	94	6	88	2
46	94	9	85	3
47	93	12	81	4
48	94	10	84	3
49	96	8	88	4
50	96	17	79	9
51	96	18	78	1
52	96	18	78	1
53	96	19	77	1
54	99	17	82	5
55	101	17	84	2
56	100	12	88	4
57	100	10	90	2
58	99	5	94	4
59	99	2	97	3
60	99	2	97	1
61	100	0	100	3
62	102	0	102	2
63	101	0	101	1
64	100	6	94	7
65	102	4	98	4
66	103	9	94	4
67	104	6	98	4
68	104	13	91	7
69	103	20	83	8
70	103	25	78	5
71	103	20	83	5

h) Kymograph 8

Frame	Maximum	Minimum	Difference	Length
0	92	21	71	
1	92	23	69	2
2	92	24	68	1
3	90	26	64	4
4	89	23	66	2
5	92	24	68	2
6	93	28	65	3
7	94	28	66	1
8	94	28	66	1
9	92	24	68	2
10	90	30	60	8
11	92	28	64	4
12	92	28	64	1
13	92	30	62	2
14	89	30	59	3
15	89	30	59	1
16	90	28	62	3
17	92	27	65	3
18	92	27	65	1
19	88	26	62	3
20	88	25	63	1
21	89	24	65	2
22	89	22	67	2
23	89	20	69	2
24	89	18	71	2
25	89	16	73	2
26	90	14	76	3
27	92	13	79	3
28	93	11	82	3
29	92	11	81	1
30	90	10	80	1
31	89	8	81	1
32	89	6	83	2
33	92	6	86	3
34	93	8	85	1
35	94	13	81	4
36	93	14	79	2
37	93	6	87	8
38	94	6	88	1
39	96	7	89	1
40	95	6	89	1
41	94	5	89	1
42	93	4	89	1
43	93	5	88	1
44	95	4	91	3
45	94	4	90	1
46	94	6	88	2
47	93	10	83	5
48	94	8	86	3
49	96	6	90	4
50	97	12	85	5
51	96	16	80	5
52	97	16	81	1
53	97	16	81	1
54	99	14	85	4
55	100	11	89	4
56	100	11	89	1
57	100	9	91	2
58	100	5	95	4
59	99	2	97	2
60	100	0	100	3
61	101	0	101	1
62	103	0	103	2
63	101	0	101	2
64	101	6	95	6
65	102	4	98	3
66	103	7	96	2
67	104	5	99	3
68	104	10	94	5
69	104	16	88	6
70	103	19	84	4
71	103	16	87	3

6. *Video 6*

a) *Kymograph 1*

Frame	Maximum	Minimum	Difference	Length
0	115	44	71	
1	116	46	70	1
2	115	46	69	1
3	115	46	69	1
4	116	44	72	3
5	117	46	71	1
6	116	46	70	1
7	115	45	70	1
8	114	49	65	5
9	114	49	65	1
10	115	49	66	1
11	114	48	66	1
12	113	49	64	2
13	113	49	64	1
14	113	49	64	1
15	113	49	64	1
16	113	48	65	1
17	114	50	64	1
18	114	48	66	2
19	114	47	67	1
20	115	46	69	2
21	114	46	68	1
22	114	47	67	1
23	114	47	67	1
24	114	50	64	3
25	114	48	66	2
26	114	48	66	1
27	115	48	67	1
28	116	46	70	3
29	115	46	69	1
30	114	45	69	1
31	114	43	71	2
32	115	40	75	4
33	115	36	79	4
34	115	42	73	6
35	115	39	76	3
36	115	40	75	1
37	117	42	75	1
38	117	41	76	1
39	116	40	76	1
40	117	39	78	2
41	117	37	80	2
42	118	35	83	3
43	117	33	84	1
44	118	31	87	3
45	116	23	93	6
46	119	19	100	7
47	118	20	98	2
48	119	16	103	5
49	120	21	99	4
50	119	27	92	7
51	119	26	93	1
52	120	31	89	4
53	121	31	90	1
54	122	34	88	2
55	120	34	86	2
56	121	33	88	2
57	122	36	86	2
58	122	47	75	11
59	122	50	72	3
60	121	52	69	3
61	121	52	69	1
62	122	53	69	1
63	123	53	70	1
64	123	53	70	1
65	123	54	69	1
66	123	54	69	1
67	123	54	69	1

b) *Kymograph 2*

Frame	Maximum	Minimum	Difference	Length
0	115	45	70	
1	115	42	73	3
2	115	42	73	1
3	114	42	72	1
4	116	43	73	1
5	116	44	72	1
6	116	45	71	1
7	115	46	69	2
8	114	46	68	1
9	115	46	69	1
10	115	47	68	1
11	113	47	66	2
12	114	49	65	1
13	112	48	64	1
14	113	49	64	1
15	113	49	64	1
16	115	48	67	3
17	115	49	66	1
18	114	49	65	1
19	114	45	69	4
20	115	48	67	2
21	115	45	70	3
22	114	48	66	4
23	113	47	66	1
24	113	45	68	2
25	115	45	70	2
26	115	47	68	2
27	116	47	69	1
28	115	45	70	1
29	115	45	70	1
30	115	44	71	1
31	114	44	70	1
32	115	41	74	4

33	115	38	77	3
34	116	42	74	3
35	116	37	79	5
36	115	39	76	3
37	117	42	75	1
38	117	39	78	3
39	117	39	78	1
40	117	39	78	1
41	117	38	79	1
42	117	36	81	2
43	117	33	84	3
44	118	33	85	1
45	116	23	93	8
46	120	19	101	8
47	118	19	99	2
48	120	16	104	5
49	122	20	102	2
50	120	26	94	8
51	119	24	95	1
52	118	31	87	8
53	120	30	90	3
54	121	34	87	3
55	120	32	88	1
56	121	33	88	1
57	121	35	86	2
58	123	44	79	7
59	122	50	72	7
60	120	48	72	1
61	122	51	71	1
62	122	53	69	2
63	123	53	70	1
64	123	52	71	1
65	123	51	72	1
66	123	51	72	1
67	123	51	72	1

c) Kymograph 3

Frame	Maximum	Minimum	Difference	Length
0	114	45	69	
1	114	46	68	1
2	115	46	69	1
3	115	45	70	1
4	115	46	69	1
5	115	46	69	1
6	115	46	69	1
7	114	45	69	1
8	113	48	65	4
9	113	47	66	1
10	114	48	66	1
11	114	50	64	2
12	112	50	62	2
13	111	50	61	1
14	112	49	63	2
15	112	50	62	1
16	113	49	64	2
17	112	50	62	2
18	112	48	64	2
19	114	48	66	2
20	114	49	65	1
21	114	48	66	1
22	114	49	65	1
23	113	49	64	1
24	113	50	63	1
25	114	48	66	3
26	114	48	66	1
27	114	49	65	1
28	114	46	68	3
29	114	46	68	1
30	114	46	68	1
31	114	43	71	3
32	114	42	72	1
33	114	42	72	1
34	114	42	72	1
35	113	37	76	4
36	112	42	70	6
37	112	42	70	1
38	114	39	75	5
39	116	39	77	2
40	114	40	74	3
41	114	39	75	1
42	115	38	77	2
43	115	36	79	2
44	115	35	80	1
45	114	27	87	7
46	118	20	98	11
47	119	19	100	2
48	118	16	102	2
49	120	20	100	2
50	119	28	91	9
51	119	23	96	5
52	116	31	85	11
53	119	31	88	3
54	120	35	85	3
55	119	35	84	1
56	120	35	85	1
57	120	36	84	1
58	119	47	72	12
59	122	52	70	2
60	120	53	67	3
61	121	54	67	1
62	120	58	62	5
63	120	58	62	1
64	121	58	63	1
65	122	57	65	2
66	122	57	65	1
67	121	57	64	1

d) Kymograph 4

Frame	Maximum	Minimum	Difference	Length
0	115	43	72	
1	115	43	72	1
2	115	43	72	1
3	114	43	71	1
4	116	42	74	3
5	116	43	73	1
6	116	44	72	1
7	115	44	71	1
8	114	46	68	3
9	115	44	71	3
10	115	45	70	1
11	113	48	65	5
12	113	46	67	2
13	113	45	68	1
14	113	46	67	1
15	113	47	66	1
16	113	46	67	1
17	113	46	67	1
18	113	47	66	1
19	114	46	68	2
20	114	45	69	1
21	114	46	68	1
22	114	47	67	1
23	113	46	67	1
24	114	45	69	2
25	114	46	68	1
26	114	46	68	1
27	115	46	69	1
28	116	44	72	3
29	116	44	72	1
30	115	42	73	1
31	114	41	73	1
32	114	39	75	2
33	115	39	76	1
34	115	41	74	2
35	115	37	78	4
36	116	42	74	4
37	116	39	77	3
38	117	37	80	3
39	117	37	80	1
40	115	38	77	3
41	116	37	79	2
42	116	39	77	2
43	116	34	82	5
44	116	32	84	2
45	115	27	88	4
46	119	19	100	12
47	118	18	100	1
48	119	15	104	4
49	119	19	100	4
50	120	25	95	5
51	120	21	99	4
52	117	29	88	11
53	121	28	93	5
54	121	32	89	4
55	119	31	88	1
56	120	32	88	1
57	120	35	85	3
58	121	42	79	6
59	122	50	72	7
60	120	50	70	2
61	121	50	71	1
62	121	52	69	2
63	123	52	71	2
64	123	52	71	1
65	123	53	70	1
66	123	53	70	1
67	123	53	70	1

e) Kymograph 5

Frame	Maximum	Minimum	Difference	Length
0	116	39	77	
1	116	42	74	3
2	115	40	75	1
3	115	41	74	1
4	116	42	74	1
5	116	42	74	1
6	116	41	75	1
7	116	42	74	1
8	116	42	74	1
9	116	42	74	1
10	115	42	73	1
11	114	42	72	1
12	114	46	68	4
13	113	46	67	1
14	113	45	68	1
15	113	45	68	1
16	114	45	69	1
17	113	46	67	2
18	114	39	75	8
19	115	45	70	5
20	116	44	72	2
21	116	44	72	1
22	114	43	71	1
23	114	44	70	1
24	114	44	70	1
25	115	44	71	1
26	115	45	70	1
27	115	43	72	2
28	115	41	74	2
29	117	42	75	1
30	116	42	74	1
31	116	39	77	3
32	116	39	77	1
33	115	37	78	1
34	115	39	76	2
35	115	35	80	4
36	116	40	76	4
37	116	37	79	3
38	116	37	79	1

39	116	35	81	2
40	118	37	81	1
41	118	35	83	2
42	118	35	83	1
43	116	32	84	1
44	116	31	85	1
45	116	27	89	4
46	118	21	97	8
47	118	19	99	2
48	120	14	106	7
49	119	17	102	4
50	119	22	97	5
51	119	20	99	2
52	119	28	91	8
53	120	25	95	4
54	121	27	94	1
55	121	29	92	2
56	121	29	92	1
57	120	32	88	4
58	123	40	83	5
59	123	44	79	4
60	121	44	77	2
61	121	46	75	2
62	121	50	71	4
63	123	47	76	5
64	123	47	76	1
65	123	47	76	1
66	123	47	76	1
67	123	47	76	1

f) Kymograph 6

Frame	Maximum	Minimum	Difference	Length
0	115	42	73	
1	115	41	74	1
2	115	41	74	1
3	115	40	75	1
4	117	42	75	1
5	116	42	74	1
6	117	44	73	1
7	115	45	70	3
8	115	45	70	1
9	115	45	70	1
10	115	43	72	2
11	114	46	68	4
12	114	46	68	1
13	113	46	67	1
14	112	44	68	1
15	113	45	68	1
16	114	45	69	1
17	114	46	68	1
18	115	46	69	1
19	115	46	69	1
20	115	45	70	1
21	115	45	70	1
22	115	45	70	1
23	114	45	69	1
24	114	45	69	1
25	115	44	71	2
26	115	44	71	1
27	115	44	71	1
28	115	43	72	1
29	116	42	74	2
30	116	40	76	2
31	115	39	76	1
32	116	38	78	2
33	116	37	79	1
34	116	38	78	1
35	115	37	78	1
36	115	40	75	3
37	115	38	77	2
38	117	39	78	1
39	117	36	81	3
40	115	37	78	3
41	115	35	80	2
42	116	36	80	1
43	116	32	84	4
44	115	31	84	1
45	116	29	87	3
46	117	22	95	8
47	117	19	98	3
48	118	15	103	5
49	118	19	99	4
50	119	24	95	4
51	119	19	100	5
52	118	25	93	7
53	120	24	96	3
54	121	26	95	1
55	119	27	92	3
56	120	30	90	2
57	120	32	88	2
58	121	39	82	6
59	121	45	76	6
60	120	46	74	2
61	121	48	73	1
62	121	52	69	4
63	121	50	71	2
64	122	50	72	1
65	122	50	72	1
66	122	50	72	1
67	122	50	72	1

g) Kymograph 7

Frame	Maximum	Minimum	Difference	Length
0	116	39	77	
1	116	38	78	1
2	115	37	78	1
3	116	37	79	1
4	116	39	77	2
5	116	39	77	1
6	117	42	75	2

7	115	42	73	2
8	115	42	73	1
9	114	43	71	2
10	115	43	72	1
11	114	44	70	2
12	114	44	70	1
13	113	44	69	1
14	113	43	70	1
15	113	43	70	1
16	115	43	72	2
17	115	42	73	1
18	116	42	74	1
19	116	42	74	1
20	116	43	73	1
21	116	43	73	1
22	115	39	76	3
23	114	43	71	5
24	114	43	71	1
25	115	42	73	2
26	115	43	72	1
27	115	43	72	1
28	115	42	73	1
29	115	41	74	1
30	115	40	75	1
31	116	37	79	4
32	116	36	80	1
33	116	35	81	1
34	115	37	78	3
35	116	40	76	2
36	114	38	76	1
37	116	37	79	3

38	118	38	80	1
39	116	38	78	2
40	118	35	83	5
41	118	34	84	1
42	118	36	82	2
43	118	31	87	5
44	115	30	85	2
45	117	27	90	5
46	117	23	94	4
47	118	24	94	1
48	117	16	101	7
49	116	16	100	1
50	119	23	96	4
51	117	18	99	3
52	119	26	93	6
53	119	22	97	4
54	120	24	96	1
55	120	25	95	1
56	120	31	89	6
57	120	35	85	4
58	120	39	81	4
59	121	43	78	3
60	120	45	75	3
61	120	46	74	1
62	120	50	70	4
63	122	47	75	5
64	122	46	76	1
65	122	46	76	1
66	122	46	76	1
67	122	46	76	1

h) Kymograph 8

Frame	Maximum	Minimum	Difference	Length
0	115	37	78	
1	115	35	80	2
2	115	35	80	1
3	116	35	81	1
4	117	39	78	3
5	117	37	80	2
6	117	38	79	1
7	115	39	76	3
8	115	39	76	1
9	115	40	75	1
10	115	40	75	1
11	114	42	72	3
12	114	42	72	1
13	113	42	71	1
14	113	42	71	1
15	113	42	71	1
16	114	42	72	1
17	114	42	72	1
18	114	42	72	1
19	114	42	72	1
20	114	39	75	3
21	115	40	75	1
22	114	42	72	3
23	114	41	73	1
24	114	41	73	1

25	115	42	73	1
26	116	42	74	1
27	116	42	74	1
28	116	41	75	1
29	117	40	77	2
30	116	39	77	1
31	115	39	76	1
32	115	38	77	1
33	115	37	78	1
34	113	36	77	1
35	115	39	76	1
36	116	37	79	3
37	115	38	77	2
38	117	36	81	4
39	115	37	78	3
40	116	35	81	3
41	117	33	84	3
42	116	34	82	2
43	117	31	86	4
44	115	31	84	2
45	114	25	89	5
46	116	24	92	3
47	119	26	93	1
48	117	22	95	2
49	119	18	101	6
50	117	22	95	6

51	117	19	98	3
52	117	24	93	5
53	118	24	94	1
54	120	23	97	3
55	118	26	92	5
56	119	26	93	1
57	119	30	89	4
58	121	38	83	6
59	119	42	77	6
60	118	44	74	3
61	118	44	74	1
62	120	46	74	1
63	122	46	76	2
64	122	46	76	1
65	122	44	78	2
66	122	44	78	1
67	122	44	78	1

7. Video 7

a) Kymograph 1

Frame	Maximum	Minimum	Difference	Length
0	105	61	44	
1	105	61	44	1
2	108	59	49	5
3	110	50	60	11
4	110	50	60	1
5	110	49	61	1
6	110	46	64	3
7	110	44	66	2
8	110	43	67	1
9	111	41	70	3
10	112	46	66	4
11	112	46	66	1
12	111	46	65	1
13	110	39	71	6
14	110	34	76	5
15	112	33	79	3
16	112	31	81	2
17	112	33	79	2
18	111	40	71	8
19	110	31	79	8
20	111	37	74	5
21	112	39	73	1
22	112	37	75	2
23	112	45	67	8
24	114	44	70	3
25	112	30	82	12
26	115	27	88	6
27	116	39	77	11
28	116	36	80	3
29	116	36	80	1
30	116	39	77	3
31	115	31	84	7
32	115	31	84	1
33	116	34	82	2
34	116	29	87	5
35	115	24	91	4
36	115	25	90	1
37	115	40	75	15
38	111	39	72	3
39	101	46	55	17
40	98	58	40	15
41	95	70	25	15

b) Kymograph 2

Frame	Maximum	Minimum	Difference	Length
0	108	61	47	
1	108	61	47	1
2	111	57	54	7
3	111	51	60	6
4	111	51	60	1
5	111	49	62	2
6	110	46	64	2
7	111	44	67	3
8	112	40	72	5
9	112	40	72	1
10	114	45	69	3
11	114	44	70	1
12	112	47	65	5
13	112	37	75	10
14	112	35	77	2
15	114	34	80	3
16	114	31	83	3
17	114	33	81	2
18	114	37	77	4
19	112	33	79	2
20	112	36	76	3
21	114	38	76	1
22	115	35	80	4
23	115	45	70	10
24	115	42	73	3
25	115	29	86	13
26	116	25	91	5
27	118	38	80	11
28	117	35	82	2
29	117	36	81	1
30	118	40	78	3
31	117	30	87	9
32	117	31	86	1
33	117	33	84	2
34	117	28	89	5

35	117	22	95	6
36	116	25	91	4
37	117	35	82	9
38	116	38	78	4
39	105	45	60	18
40	102	60	42	18
41	100	70	30	12

c) Kymograph 3

Frame	Maximum	Minimum	Difference	Length
0	112	60	52	
1	112	60	52	1
2	111	57	54	2
3	112	51	61	7
4	112	51	61	1
5	112	46	66	5
6	114	45	69	3
7	114	41	73	4
8	115	41	74	1
9	115	39	76	2
10	115	45	70	6
11	115	44	71	1
12	115	47	68	3
13	114	33	81	13
14	114	33	81	1
15	115	31	84	3
16	115	33	82	2
17	115	35	80	2
18	115	37	78	2
19	114	33	81	3
20	115	36	79	2
21	115	36	79	1
22	116	34	82	3
23	117	46	71	11
24	117	40	77	6
25	116	31	85	8
26	117	26	91	6
27	119	39	80	11
28	118	36	82	2
29	119	36	83	1
30	119	39	80	3
31	119	33	86	6
32	119	31	88	2
33	118	33	85	3
34	118	29	89	4
35	118	20	98	9
36	118	27	91	7
37	118	38	80	11
38	117	40	77	3
39	110	44	66	11
40	108	60	48	18
41	103	67	36	12

d) Kymograph 4

Frame	Maximum	Minimum	Difference	Length
0	112	61	51	
1	112	60	52	1
2	112	57	55	3
3	115	49	66	11
4	115	49	66	1
5	116	47	69	3
6	116	45	71	2
7	115	41	74	3
8	115	40	75	1
9	116	39	77	2
10	117	44	73	4
11	117	47	70	3
12	116	47	69	1
13	116	35	81	12
14	115	34	81	1
15	116	30	86	5
16	117	33	84	2
17	116	34	82	2
18	116	37	79	3
19	116	33	83	4
20	116	36	80	3
21	117	38	79	1
22	117	35	82	3
23	118	46	72	10
24	118	39	79	7
25	117	33	84	5
26	118	26	92	8
27	120	38	82	10
28	119	37	82	1
29	119	37	82	1
30	119	40	79	3
31	119	33	86	7
32	119	33	86	1
33	119	33	86	1
34	117	28	89	3
35	120	19	101	12
36	120	28	92	9
37	119	38	81	11
38	117	41	76	5
39	117	45	72	4
40	115	65	50	22
41	108	67	41	9

e) Kymograph 5

Frame	Maximum	Minimum	Difference	Length
0	110	60	50	
1	110	61	49	1
2	112	57	55	6
3	115	48	67	12
4	115	48	67	1
5	116	46	70	3
6	116	44	72	2

7	116	43	73	1
8	117	41	76	3
9	117	38	79	3
10	117	45	72	7
11	116	49	67	5
12	117	50	67	1
13	117	34	83	16
14	116	33	83	1
15	117	31	86	3
16	117	35	82	4
17	117	34	83	1
18	117	39	78	5
19	117	37	80	2
20	117	37	80	1
21	118	38	80	1
22	117	36	81	1
23	119	47	72	9
24	118	38	80	8
25	117	37	80	1
26	118	28	90	10
27	120	37	83	7
28	119	36	83	1
29	120	37	83	1
30	120	40	80	3
31	120	35	85	5
32	119	33	86	1
33	118	33	85	1
34	119	30	89	4
35	119	20	99	10
36	119	31	88	11
37	120	38	82	6
38	116	44	72	10
39	110	45	65	7
40	111	68	43	22
41	110	70	40	3

f) Kymograph 6

Frame	Maximum	Minimum	Difference	Length
0	116	59	57	
1	116	60	56	1
2	115	56	59	3
3	116	48	68	9
4	116	48	68	1
5	118	45	73	5
6	118	45	73	1
7	118	44	74	1
8	118	41	77	3
9	118	38	80	3
10	120	44	76	4
11	118	49	69	7
12	118	46	72	3
13	118	34	84	12
14	117	33	84	1
15	118	31	87	3
16	118	33	85	2
17	118	36	82	3
18	118	39	79	3
19	117	34	83	4
20	118	36	82	1
21	118	34	84	2
22	120	33	87	3
23	121	48	73	14
24	120	35	85	12
25	120	36	84	1
26	120	28	92	8
27	122	35	87	5
28	122	36	86	1
29	122	35	87	1
30	122	41	81	6
31	123	35	88	7
32	121	33	88	1
33	122	34	88	1
34	121	28	93	5
35	120	21	99	6
36	120	33	87	12
37	122	35	87	1
38	120	45	75	12
39	118	42	76	1
40	116	68	48	28
41	114	71	43	5

g) Kymograph 7

Frame	Maximum	Minimum	Difference	Length
0	118	56	62	
1	118	56	62	1
2	117	54	63	1
3	119	47	72	9
4	119	47	72	1
5	119	44	75	3
6	119	44	75	1
7	119	41	78	3
8	119	39	80	2
9	119	36	83	3
10	120	40	80	3
11	120	46	74	6
12	120	46	74	1
13	119	35	84	10
14	119	30	89	5
15	119	30	89	1
16	120	30	90	1
17	120	37	83	7
18	119	36	83	1
19	119	37	82	1
20	119	35	84	2
21	120	33	87	3
22	120	33	87	1
23	121	46	75	12
24	121	33	88	13
25	120	37	83	5
26	121	28	93	10

27	122	35	87	6
28	122	35	87	1
29	123	33	90	3
30	123	39	84	6
31	123	36	87	3
32	122	30	92	5
33	123	31	92	1
34	122	27	95	3
35	123	21	102	7
36	123	34	89	13
37	124	34	90	1
38	122	46	76	14
39	120	40	80	4
40	120	71	49	31
41	119	70	49	1

h) Kymograph 8

Frame	Maximum	Minimum	Difference	Length
0	119	56	63	
1	119	56	63	1
2	119	54	65	2
3	120	47	73	8
4	120	47	73	1
5	121	45	76	3
6	120	44	76	1
7	120	41	79	3
8	120	40	80	1
9	121	36	85	5
10	121	39	82	3
11	121	46	75	7
12	121	41	80	5
13	121	35	86	6
14	119	31	88	2
15	121	30	91	3
16	121	31	90	1
17	121	40	81	9
18	121	37	84	3
19	121	37	84	1
20	121	35	86	2
21	121	34	87	1
22	121	33	88	1
23	123	44	79	9
24	122	31	91	12
25	121	39	82	9
26	123	30	93	11
27	125	34	91	2
28	125	31	94	3
29	125	31	94	1
30	125	36	89	5
31	125	35	90	1
32	125	30	95	5
33	125	33	92	3
34	124	25	99	7
35	124	21	103	4
36	124	37	87	16
37	126	36	90	3
38	122	47	75	15
39	122	49	73	2
40	121	72	49	24
41	121	70	51	2

B. Image Analysis Using ImageJ for Control

a) Kymograph 1

Frame	Position	Length
1	15	
2	14	1
3	14	1
4	13	1
5	12	1
6	12	1
7	11	1
8	12	1
9	12	1
10	12	1
11	12	1
12	12	1
13	11	1
14	11	1
15	13	2
16	13	1
17	14	1
18	13	1
19	14	1
20	14	1
21	14	1
22	14	1
23	14	1
24	14	1
25	14	1
26	14	1
27	14	1
28	13	1
29	12	1
30	12	1
31	11	1
32	10	1
33	10	1
34	11	1
35	10	1
36	10	1
37	10	1
38	10	1
39	10	1
40	9	1
41	11	2
42	10	1
43	11	1
44	11	1
45	10	1
46	11	1
47	10	1
48	10	1
49	10	1
50	10	1
51	11	1
52	12	1
53	10	2
54	11	1
55	10	1
56	11	1
57	10	1
58	11	1
59	12	1
60	11	1
61	11	1
62	12	1
63	13	1
64	13	1
65	11	2
66	11	1
67	12	1
68	11	1
69	12	1
70	12	1
71	12	1
72	11	1
73	11	1
74	10	1
75	10	1
76	9	1
77	9	1
78	9	1
79	9	1
80	9	1
81	9	1

b) Kymograph 2

Frame	Position	Length
1	14	
2	14	1
3	13	1
4	12	1
5	11	1
6	11	1
7	11	1
8	11	1
9	11	1
10	11	1
11	11	1
12	12	1
13	10	2
14	10	1
15	12	2
16	12	1
17	13	1
18	13	1
19	13	1
20	13	1
21	13	1
22	13	1
23	13	1
24	13	1
25	13	1
26	13	1
27	13	1
28	12	1
29	11	1
30	11	1
31	10	1
32	10	1
33	10	1
34	10	1
35	10	1
36	10	1
37	9	1
38	10	1
39	9	1
40	9	1
41	10	1
42	9	1
43	10	1
44	10	1
45	9	1
46	10	1
47	10	1
48	9	1
49	9	1
50	10	1
51	10	1
52	11	1
53	10	1
54	10	1
55	10	1
56	10	1
57	10	1
58	10	1
59	11	1
60	11	1
61	11	1
62	11	1
63	12	1
64	12	1
65	10	2
66	10	1
67	11	1
68	11	1
69	12	1
70	11	1
71	11	1

72	11	1
73	10	1
74	10	1
75	9	1
76	8	1
77	8	1
78	8	1
79	8	1
80	8	1
81	8	1

c) *Kymograph 3*

Frame	Position	Length
1	14	
2	13	1
3	13	1
4	12	1
5	10	2
6	11	1
7	10	1
8	10	1
9	10	1
10	11	1
11	10	1
12	11	1
13	10	1
14	10	1
15	11	1
16	11	1
17	12	1
18	12	1
19	12	1
20	13	1
21	13	1
22	12	1
23	12	1
24	12	1
25	12	1
26	13	1
27	12	1
28	11	1
29	10	1
30	10	1
31	9	1
32	9	1
33	9	1
34	9	1
35	9	1
36	9	1
37	9	1
38	9	1
39	9	1
40	8	1
41	9	1
42	9	1
43	10	1
44	10	1
45	8	2
46	9	1
47	9	1
48	9	1
49	8	1
50	9	1
51	9	1
52	10	1
53	9	1
54	9	1
55	9	1
56	9	1
57	9	1
58	10	1
59	11	1
60	10	1
61	10	1
62	11	1
63	12	1
64	11	1
65	10	1
66	10	1
67	10	1
68	10	1
69	11	1
70	10	1
71	11	1
72	10	1
73	10	1
74	10	1
75	9	1
76	8	1
77	7	1
78	7	1
79	8	1
80	8	1
81	8	1

d) *Kymograph 4*

Frame	Position	Length
1	12	
2	12	1
3	12	1
4	11	1
5	10	1
6	10	1
7	9	1
8	9	1
9	10	1
10	9	1
11	9	1
12	10	1
13	9	1
14	9	1
15	10	1
16	11	1
17	11	1
18	11	1
19	11	1
20	12	1
21	11	1
22	11	1
23	11	1
24	11	1
25	11	1
26	11	1
27	11	1
28	10	1
29	9	1
30	9	1
31	9	1
32	8	1
33	8	1
34	8	1
35	8	1
36	8	1
37	8	1
38	8	1
39	7	1
40	7	1
41	8	1
42	8	1
43	9	1
44	9	1
45	8	1
46	8	1
47	8	1
48	8	1
49	7	1
50	8	1
51	8	1
52	9	1
53	8	1
54	8	1
55	8	1
56	8	1
57	8	1
58	8	1
59	10	2
60	9	1
61	9	1
62	10	1
63	11	1
64	10	1
65	8	2

66	9	1
67	10	1
68	9	1
69	10	1
70	10	1
71	10	1

72	9	1
73	9	1
74	9	1
75	8	1
76	7	1
77	7	1

78	7	1
79	7	1
80	7	1
81	7	1

e) Kymograph 5

Frame	Position	Length
1	12	
2	12	1
3	11	1
4	11	1
5	10	1
6	10	1
7	10	1
8	10	1
9	10	1
10	10	1
11	10	1
12	10	1
13	9	1
14	9	1
15	10	1
16	10	1
17	11	1
18	11	1
19	11	1
20	11	1
21	12	1
22	11	1
23	11	1
24	11	1
25	10	1
26	11	1
27	11	1

28	10	1
29	9	1
30	9	1
31	8	1
32	8	1
33	8	1
34	7	1
35	7	1
36	8	1
37	7	1
38	7	1
39	7	1
40	7	1
41	8	1
42	7	1
43	8	1
44	9	1
45	7	2
46	8	1
47	8	1
48	7	1
49	7	1
50	8	1
51	8	1
52	9	1
53	8	1
54	8	1
55	8	1

56	8	1
57	8	1
58	9	1
59	9	1
60	9	1
61	9	1
62	10	1
63	10	1
64	10	1
65	9	1
66	9	1
67	10	1
68	9	1
69	10	1
70	10	1
71	10	1
72	9	1
73	9	1
74	9	1
75	8	1
76	7	1
77	7	1
78	7	1
79	7	1
80	7	1
81	7	1

f) Kymograph 6

Frame	Position	Length
1	12	
2	11	1
3	11	1
4	10	1
5	9	1
6	9	1
7	9	1
8	9	1
9	9	1
10	9	1
11	9	1
12	9	1
13	9	1
14	9	1
15	10	1
16	10	1
17	11	1
18	10	1
19	10	1

20	11	1
21	11	1
22	11	1
23	10	1
24	10	1
25	10	1
26	10	1
27	10	1
28	10	1
29	9	1
30	8	1
31	7	1
32	7	1
33	7	1
34	7	1
35	7	1
36	7	1
37	7	1
38	7	1
39	7	1

40	6	1
41	7	1
42	7	1
43	7	1
44	8	1
45	7	1
46	7	1
47	7	1
48	7	1
49	7	1
50	8	1
51	8	1
52	8	1
53	7	1
54	8	1
55	7	1
56	8	1
57	7	1
58	8	1
59	9	1

60	8	1
61	9	1
62	9	1
63	10	1
64	9	1
65	8	1
66	8	1
67	9	1

68	9	1
69	10	1
70	9	1
71	9	1
72	9	1
73	9	1
74	8	1
75	8	1

76	7	1
77	6	1
78	6	1
79	7	1
80	7	1
81	7	1

g) Kymograph 7

Frame	Position	Length
1	11	
2	11	1
3	10	1
4	10	1
5	9	1
6	9	1
7	8	1
8	9	1
9	9	1
10	9	1
11	8	1
12	9	1
13	8	1
14	9	1
15	9	1
16	9	1
17	10	1
18	10	1
19	10	1
20	10	1
21	10	1
22	10	1
23	10	1
24	10	1
25	9	1
26	10	1
27	10	1

28	9	1
29	8	1
30	8	1
31	7	1
32	7	1
33	7	1
34	7	1
35	7	1
36	7	1
37	6	1
38	6	1
39	6	1
40	6	1
41	7	1
42	7	1
43	7	1
44	7	1
45	7	1
46	7	1
47	7	1
48	6	1
49	6	1
50	7	1
51	7	1
52	8	1
53	7	1
54	7	1
55	7	1

56	7	1
57	7	1
58	8	1
59	9	1
60	8	1
61	8	1
62	8	1
63	9	1
64	9	1
65	8	1
66	8	1
67	9	1
68	8	1
69	9	1
70	9	1
71	9	1
72	8	1
73	8	1
74	8	1
75	7	1
76	6	1
77	6	1
78	6	1
79	7	1
80	7	1
81	7	1

h) Kymograph 8

Frame	Position	Length
1	11	
2	11	1
3	10	1
4	9	1
5	8	1
6	8	1
7	8	1
8	8	1
9	9	1
10	8	1
11	8	1
12	9	1
13	8	1
14	8	1
15	9	1
16	9	1
17	10	1

18	9	1
19	10	1
20	10	1
21	10	1
22	9	1
23	10	1
24	9	1
25	9	1
26	9	1
27	10	1
28	9	1
29	8	1
30	7	1
31	7	1
32	6	1
33	6	1
34	7	1
35	6	1

36	6	1
37	6	1
38	6	1
39	6	1
40	6	1
41	6	1
42	6	1
43	7	1
44	7	1
45	6	1
46	6	1
47	7	1
48	6	1
49	6	1
50	7	1
51	7	1
52	7	1
53	7	1

54	7	1
55	6	1
56	7	1
57	7	1
58	7	1
59	8	1
60	8	1
61	8	1
62	8	1
63	9	1

64	8	1
65	7	1
66	7	1
67	8	1
68	8	1
69	9	1
70	9	1
71	9	1
72	8	1
73	8	1

74	8	1
75	7	1
76	6	1
77	6	1
78	6	1
79	7	1
80	7	1
81	7	1

C. Validation – Using Camera Edge as Reference Point

a) Kymograph 1

Frame	Position	Length
1	31	1
2	31	1
3	30	2
4	31	1
5	31	1
6	31	1
7	31	1
8	31	1
9	31	1
10	32	0
11	32	0
12	31	1
13	32	0
14	32	0
15	31	1
16	31	1
17	31	1
18	31	1
19	31	1
20	31	1
21	31	1
22	32	0
23	31	1
24	31	1
25	32	0
26	31	1
27	32	0
28	32	0
29	32	0
30	32	0
31	32	0
32	33	1
33	33	1
34	33	1
35	32	0
36	32	0
37	33	1
38	33	1
39	33	1
40	33	1
41	33	1
42	33	1
43	33	1
44	33	1
45	33	1
46	33	1
47	33	1
48	34	2
49	33	1
50	32	0
51	33	1
52	32	0
53	33	1
54	32	0
55	33	1
56	32	0
57	33	1
58	33	1
59	32	0
60	33	1
61	33	1
62	33	1
63	32	0
64	33	1
65	33	1
66	32	0
67	31	1
68	32	0
69	30	2
70	30	2
71	29	3
72	29	3
73	29	3
74	30	2
75	30	2
76	30	2
77	28	4
78	28	4
79	28	4
80	28	4
81	28	4

b) Kymograph 2

Frame	Position	Length
1	30	1
2	30	1
3	30	1
4	30	1
5	31	0
6	31	0
7	30	1
8	30	1
9	31	0
10	31	0
11	31	0
12	30	1
13	31	0
14	31	0
15	31	0
16	31	0
17	31	0
18	31	0
19	31	0
20	31	0
21	31	0
22	31	0
23	31	0
24	31	0
25	30	1
26	31	0
27	31	0
28	31	0
29	32	1
30	32	1
31	32	1
32	32	1
33	33	2
34	32	1
35	32	1
36	33	2
37	33	2
38	33	2
39	33	2
40	33	2
41	33	2
42	33	2
43	33	2
44	33	2
45	33	2
46	33	2
47	33	2
48	33	2
49	33	2
50	32	1
51	32	1
52	32	1
53	32	1
54	32	1
55	32	1
56	32	1
57	33	2
58	33	2
59	32	1
60	32	1
61	32	1
62	33	2
63	32	1
64	33	2
65	33	2
66	32	1
67	31	0
68	31	0
69	30	1
70	30	1
71	29	2

72	29	2
73	29	2
74	29	2
75	29	2
76	29	2
77	28	3
78	28	3
79	28	3
80	28	3
81	27	4

c) *Kymograph 3*

Frame	Position	Length
1	30	1
2	30	1
3	30	1
4	30	1
5	30	1
6	30	1
7	30	1
8	30	1
9	31	0
10	31	0
11	31	0
12	30	1
13	30	1
14	30	1
15	31	0
16	31	0
17	31	0
18	31	0
19	30	1
20	30	1
21	30	1
22	31	0
23	31	0
24	30	1
25	30	1
26	31	0
27	31	0
28	31	0
29	32	1
30	32	1
31	32	1
32	32	1
33	32	1
34	32	1
35	32	1
36	32	1
37	33	2
38	32	1
39	32	1
40	33	2
41	33	2
42	33	2
43	32	1
44	32	1
45	33	2
46	33	2
47	32	1
48	32	1
49	32	1
50	32	1
51	32	1
52	32	1
53	32	1
54	31	0
55	32	1
56	32	1
57	32	1
58	32	1
59	31	0
60	32	1
61	32	1
62	33	2
63	32	1
64	33	2
65	32	1
66	32	1
67	31	0
68	31	0
69	29	2
70	29	2
71	28	3
72	29	2
73	28	3
74	28	3
75	29	2
76	28	3
77	28	3
78	28	3
79	27	4
80	27	4
81	27	4

d) *Kymograph 4*

Frame	Position	Length
1	29	1
2	30	0
3	29	1
4	29	1
5	30	0
6	29	1
7	29	1
8	29	1
9	30	0
10	31	1
11	30	0
12	29	1
13	30	0
14	30	0
15	30	0
16	30	0
17	30	0
18	30	0
19	30	0
20	30	0
21	30	0
22	31	1
23	30	0
24	30	0
25	30	0
26	31	1
27	31	1
28	31	1
29	31	1
30	31	1
31	32	2
32	32	2
33	32	2
34	32	2
35	32	2
36	31	1
37	33	3
38	32	2
39	32	2
40	33	3
41	32	2
42	33	3
43	32	2
44	32	2
45	32	2
46	32	2
47	32	2
48	32	2
49	32	2
50	31	1
51	31	1
52	31	1
53	31	1
54	31	1
55	31	1
56	31	1
57	32	2
58	32	2
59	31	1
60	31	1
61	31	1
62	32	2
63	31	1
64	32	2
65	32	2

66	31	1
67	31	1
68	30	0
69	29	1
70	29	1
71	28	2

72	28	2
73	28	2
74	28	2
75	29	1
76	28	2
77	27	3

78	28	2
79	27	3
80	27	3
81	27	3

e) Kymograph 5

Frame	Position	Length
1	29	1
2	29	1
3	29	1
4	29	1
5	29	1
6	29	1
7	29	1
8	29	1
9	29	1
10	30	0
11	30	0
12	29	1
13	30	0
14	29	1
15	29	1
16	30	0
17	29	1
18	30	0
19	30	0
20	30	0
21	30	0
22	30	0
23	30	0
24	29	1
25	30	0
26	30	0
27	30	0

28	30	0
29	31	1
30	31	1
31	31	1
32	31	1
33	32	2
34	31	1
35	31	1
36	31	1
37	32	2
38	32	2
39	32	2
40	32	2
41	31	1
42	32	2
43	31	1
44	31	1
45	31	1
46	32	2
47	31	1
48	31	1
49	31	1
50	31	1
51	30	0
52	31	1
53	31	1
54	31	1
55	31	1

56	31	1
57	32	2
58	31	1
59	31	1
60	31	1
61	31	1
62	31	1
63	30	0
64	32	2
65	31	1
66	31	1
67	30	0
68	30	0
69	28	2
70	28	2
71	27	3
72	28	2
73	27	3
74	28	2
75	28	2
76	27	3
77	27	3
78	27	3
79	26	4
80	26	4
81	26	4

f) Kymograph 6

Frame	Position	Length
1	28	1
2	28	1
3	28	1
4	28	1
5	29	0
6	29	0
7	28	1
8	28	1
9	29	0
10	30	1
11	29	0
12	29	0
13	29	0
14	29	0
15	29	0
16	29	0
17	29	0
18	29	0
19	29	0

20	29	0
21	29	0
22	29	0
23	29	0
24	29	0
25	29	0
26	30	1
27	30	1
28	30	1
29	30	1
30	30	1
31	30	1
32	30	1
33	30	1
34	31	2
35	31	2
36	30	1
37	31	2
38	31	2
39	31	2

40	31	2
41	31	2
42	32	3
43	30	1
44	31	2
45	31	2
46	31	2
47	31	2
48	30	1
49	31	2
50	30	1
51	30	1
52	30	1
53	30	1
54	30	1
55	31	2
56	30	1
57	31	2
58	30	1
59	30	1

60	30	1
61	30	1
62	31	2
63	30	1
64	31	2
65	31	2
66	30	1
67	29	0

68	29	0
69	27	2
70	28	1
71	27	2
72	27	2
73	26	3
74	27	2
75	27	2

76	27	2
77	26	3
78	26	3
79	26	3
80	26	3
81	26	3

g) Kymograph 7

Frame	Position	Length
1	28	1
2	28	1
3	28	1
4	27	2
5	28	1
6	28	1
7	27	2
8	28	1
9	28	1
10	29	0
11	28	1
12	28	1
13	29	0
14	28	1
15	28	1
16	28	1
17	28	1
18	28	1
19	28	1
20	28	1
21	28	1
22	28	1
23	28	1
24	28	1
25	28	1
26	29	0
27	29	0

28	29	0
29	29	0
30	30	1
31	30	1
32	30	1
33	30	1
34	30	1
35	30	1
36	30	1
37	31	2
38	30	1
39	30	1
40	31	2
41	30	1
42	31	2
43	30	1
44	30	1
45	30	1
46	30	1
47	31	2
48	30	1
49	30	1
50	29	0
51	29	0
52	30	1
53	30	1
54	29	0
55	30	1

56	29	0
57	30	1
58	30	1
59	29	0
60	29	0
61	30	1
62	30	1
63	29	0
64	30	1
65	30	1
66	30	1
67	29	0
68	28	1
69	27	2
70	27	2
71	26	3
72	27	2
73	26	3
74	27	2
75	26	3
76	26	3
77	25	4
78	25	4
79	25	4
80	24	5
81	25	4

h) Kymograph 8

Frame	Position	Length
1	27	1
2	28	0
3	27	1
4	27	1
5	28	0
6	27	1
7	27	1
8	27	1
9	28	0
10	28	0
11	28	0
12	28	0
13	28	0
14	28	0
15	28	0
16	28	0
17	28	0

18	28	0
19	28	0
20	28	0
21	28	0
22	28	0
23	28	0
24	28	0
25	28	0
26	29	1
27	28	0
28	29	1
29	29	1
30	30	2
31	30	2
32	30	2
33	30	2
34	30	2
35	30	2

36	30	2
37	30	2
38	30	2
39	30	2
40	31	3
41	30	2
42	31	3
43	30	2
44	30	2
45	30	2
46	30	2
47	30	2
48	30	2
49	30	2
50	29	1
51	29	1
52	30	2
53	29	1

54	29	1
55	30	2
56	29	1
57	30	2
58	30	2
59	29	1
60	30	2
61	30	2
62	30	2
63	29	1

64	30	2
65	30	2
66	29	1
67	28	0
68	28	0
69	27	1
70	27	1
71	26	2
72	26	2
73	26	2

74	26	2
75	26	2
76	26	2
77	25	3
78	25	3
79	24	4
80	24	4
81	24	4

D. Validation – Frame-by-Frame Analysis

a) Frame 5

Position	Position	Tangent
0	92	
1	97.567	5.567
2	88.4	-9.167
3	90.4	2
4	85.533	-4.867
5	81	-4.533
6	88.8	7.8
7	88.667	-0.133
8	90.067	1.4
9	88.9	-1.167
10	93.333	4.433
11	93.167	-0.166
12	94.6	1.433
13	92.7	-1.9
14	101.867	9.167
15	101.5	-0.367
16	107.067	5.567
17	111.133	4.066
18	113.8	2.667
19	117.467	3.667
20	118.667	1.2
21	121.9	3.233
22	132.267	10.367
23	136.167	3.9
24	132.6	-3.567
25	138.5	5.9
26	153.4	14.9
27	152	-1.4
28	155.533	3.533
29	155.2	-0.333
30	164	8.8
31	170.667	6.667
32	174.733	4.066
33	175.5	0.767
34	175.2	-0.3
35	181.333	6.133
36	191	9.667
37	196.7	5.7
38	207.4	10.7
39	201.8	-5.6
40	197	-4.8
41	190.267	-6.733
42	182.6	-7.667
43	164	-18.6
44	147.933	-16.067
45	109	-38.933
46	69.4	-39.6
47	43.867	-25.533
48	25	-18.867
49	19.733	-5.267
50	8.333	-11.4
51	7	-1.333
52	6	-1
53	4.767	-1.233
54	3	-1.767
55	3	0
56	2	-1
57	2	0
58	1	-1
59	1	0
60	2	1

b) Frame 10

Position	Position	Tangent
0	87	
1	86.8	-0.2
2	88.933	2.133
3	88.9	-0.033
4	92.6	3.7
5	89.167	-3.433
6	91.8	2.633
7	92.3	0.5
8	89.2	-3.1
9	91.7	2.5
10	90.667	-1.033
11	92.533	1.866
12	99	6.467
13	102.3	3.3
14	107.533	5.233
15	108.5	0.967
16	113.467	4.967
17	112.3	-1.167
18	122.8	10.5
19	127.633	4.833
20	130.333	2.7
21	134.1	3.767
22	140.8	6.7
23	140.1	-0.7
24	141.8	1.7
25	144.833	3.033
26	149.267	4.434
27	149.3	0.033
28	152.667	3.367
29	151.067	-1.6
30	154	2.933
31	157.867	3.867
32	157.8	-0.067
33	158.4	0.6
34	171.333	12.933
35	170.833	-0.5
36	164.8	-6.033
37	162.3	-2.5
38	165.133	2.833
39	163.5	-1.633
40	172	8.5
41	172.9	0.9
42	171.8	-1.1
43	166	-5.8
44	159.933	-6.067
45	159	-0.933
46	155.067	-3.933
47	142.867	-12.2
48	106.4	-36.467
49	74.433	-31.967
50	34.333	-40.1
51	22.3	-12.033
52	12.267	-10.033
53	11.233	-1.034
54	5	-6.233
55	5	0
56	4	-1
57	3	-1
58	1	-2
59	1	0
60	0	-1

c) Frame 15

Position	Position	Tangent
0	104	
1	103.9	-0.1
2	101.133	-2.767
3	101	-0.133
4	100.6	-0.4
5	100.167	-0.433
6	101.2	1.033
7	98.633	-2.567
8	106.2	7.567
9	107.6	1.4
10	103	-4.6
11	101.733	-1.267
12	107.2	5.467
13	106.967	-0.233
14	111.067	4.1
15	114.5	3.433
16	119.8	5.3
17	121.033	1.233
18	122.6	1.567
19	123.733	1.133

20	127.333	3.6
21	128.5	1.167
22	132	3.5
23	138	6
24	151.8	13.8
25	151.167	-0.633
26	174	22.833
27	175.1	1.1
28	173.867	-1.233
29	177.933	4.066
30	178	0.067
31	177.9	-0.1
32	174.933	-2.967
33	177.6	2.667

34	182.467	4.867
35	184.667	2.2
36	195	10.333
37	196	1
38	198.933	2.933
39	198.1	-0.833
40	210.333	12.233
41	210.9	0.567
42	207.2	-3.7
43	206	-1.2
44	193.067	-12.933
45	188	-5.067
46	160.133	-27.867
47	124.1	-36.033

48	82.2	-41.9
49	50.267	-31.933
50	32.333	-17.934
51	20	-12.333
52	12.267	-7.733
53	12	-0.267
54	6	-6
55	5	-1
56	4	-1
57	3	-1
58	1	-2
59	1	0
60	1	0

d) Frame 20

Position	Position	Tangent
0	92	
1	93.9	1.9
2	91.733	-2.167
3	90.7	-1.033
4	93.467	2.767
5	93.167	-0.3
6	93.8	0.633
7	95.3	1.5
8	86.333	-8.967
9	84.2	-2.133
10	84.333	0.133
11	83.933	-0.4
12	89.2	5.267
13	92.567	3.367
14	99.133	6.566
15	101.5	2.367
16	104.933	3.433
17	108.067	3.134
18	109.8	1.733
19	112.833	3.033

20	114.667	1.834
21	118.1	3.433
22	119.933	1.833
23	121.6	1.667
24	136.6	15
25	140.333	3.733
26	161.533	21.2
27	161.8	0.267
28	159.133	-2.667
29	161	1.867
30	157	-4
31	159.9	2.9
32	160.733	0.833
33	162.6	1.867
34	164.267	1.667
35	163.5	-0.767
36	164.6	1.1
37	165.767	1.167
38	178.867	13.1
39	181.8	2.933
40	178	-3.8

41	177.267	-0.733
42	170.4	-6.867
43	171	0.6
44	165	-6
45	163	-2
46	147.333	-15.667
47	122.267	-25.066
48	87.4	-34.867
49	56	-31.4
50	34.333	-21.667
51	22	-12.333
52	9	-13
53	8	-1
54	7	-1
55	6	-1
56	2	-4
57	1	-1
58	1	0
59	1	0
60	1	0

e) Frame 25

Position	Position	Tangent
0	96	
1	94	-2
2	102.267	8.267
3	102.6	0.333
4	93.533	-9.067
5	97.5	3.967
6	93.2	-4.3
7	92.633	-0.567
8	95.867	3.234
9	97	1.133
10	100.667	3.667
11	103.9	3.233
12	108.8	4.9
13	107.533	-1.267
14	115.333	7.8
15	117.5	2.167
16	116.8	-0.7
17	121.9	5.1

18	120.2	-1.7
19	125.233	5.033
20	140.667	15.434
21	144.6	3.933
22	159.067	14.467
23	160.8	1.733
24	168.4	7.6
25	171.333	2.933
26	169.667	-1.666
27	172.9	3.233
28	177.4	4.5
29	171.867	-5.533
30	177	5.133
31	171.2	-5.8
32	181.8	10.6
33	175.8	-6
34	179.2	3.4
35	180	0.8
36	177.6	-2.4

37	179.533	1.933
38	176	-3.533
39	176	0
40	179	3
41	179	0
42	176	-3
43	176	0
44	178.067	2.067
45	172.5	-5.567
46	154.8	-17.7
47	150.3	-4.5
48	147.8	-2.5
49	126.1	-21.7
50	77	-49.1
51	46	-31
52	23.067	-22.933
53	16	-7.067
54	8.2	-7.8
55	6	-2.2

56	3	-3
57	1	-2
58	0	-1
59	0	0
60	0	0

f) Frame 30

Position	Position	Tangent
0	114	
1	114.233	0.233
2	124	9.767
3	126.8	2.8
4	120.467	-6.333
5	126	5.533
6	129.8	3.8
7	131.767	1.967
8	127.067	-4.7
9	130.3	3.233
10	150.333	20.033
11	185.267	34.934
12	243	57.733
13	255	12
14	217.4	-37.6
15	215	-2.4
16	216.467	1.467
17	213.867	-2.6
18	217.4	3.533
19	218.8	1.4
20	218.667	-0.133
21	218.9	0.233
22	228.267	9.367
23	229.2	0.933
24	231	1.8
25	231.5	0.5
26	245.2	13.7
27	253.5	8.3
28	239.467	-14.033
29	252.8	13.333
30	246	-6.8
31	237.3	-8.7
32	247.267	9.967
33	238.9	-8.367
34	230	-8.9
35	223	-7
36	231	8
37	225	-6
38	227.067	2.067
39	219.1	-7.967
40	229.667	10.567
41	223.7	-5.967
42	227	3.3
43	220.833	-6.167
44	199	-21.833
45	201	2
46	188.533	-12.467
47	172.867	-15.666
48	117.6	-55.267
49	80	-37.6
50	40	-40
51	27	-13
52	13	-14
53	11.233	-1.767
54	8	-3.233
55	6	-2
56	6.733	0.733
57	5	-1.733
58	2	-3
59	2	0
60	1	-1

g) Frame 35

Position	Position	Tangent
0	129	
1	126.867	-2.133
2	130.8	3.933
3	139.1	8.3
4	128.267	-10.833
5	131.833	3.566
6	145.8	13.967
7	161.767	15.967
8	217.8	56.033
9	236.9	19.1
10	255	18.1
11	255	0
12	248.4	-6.6
13	248.2	-0.2
14	243.067	-5.133
15	242	-1.067
16	243.4	1.4
17	241.3	-2.1
18	239.6	-1.7
19	239.633	0.033
20	237.667	-1.966
21	232.7	-4.967
22	239.067	6.367
23	238.933	-0.134
24	243.6	4.667
25	242	-1.6
26	249.8	7.8
27	248.5	-1.3
28	239.333	-9.167
29	232.467	-6.866
30	240	7.533
31	232.867	-7.133
32	228.733	-4.134
33	226.2	-2.533
34	214	-12.2
35	212	-2
36	215	3
37	213	-2
38	216	3
39	210	-6
40	213.667	3.667
41	213	-0.667
42	214.8	1.8
43	214.133	-0.667
44	215.467	1.334
45	211	-4.467
46	194.6	-16.4
47	187.133	-7.467
48	156.4	-30.733
49	118	-38.4
50	68	-50
51	41	-27
52	21.733	-19.267
53	17.533	-4.2
54	12	-5.533
55	9	-3
56	6.267	-2.733
57	4.1	-2.167
58	2	-2.1
59	2	0
60	1	-1

h) Frame 40

Position	Position	Tangent
0	115	
1	113.833	-1.167
2	117.4	3.567
3	118.5	1.1
4	129.533	11.033
5	130.167	0.634
6	128.8	-1.367
7	133	4.2
8	143.267	10.267
9	156.9	13.633
10	184.333	27.433
11	191.033	6.7
12	210	18.967
13	212.267	2.267
14	209	-3.267
15	209	0
16	216.067	7.067
17	216.133	0.066
18	217.4	1.267
19	220	2.6
20	228	8
21	227.2	-0.8
22	239	11.8

23	244.6	5.6
24	254.2	9.6
25	254.333	0.133
26	254.733	0.4
27	254.4	-0.333
28	253.733	-0.667
29	254.3	0.567
30	249	-5.3
31	249.067	0.067
32	246.6	-2.467
33	249.2	2.6
34	254.467	5.267
35	247.667	-6.8
36	234.2	-13.467
37	235.3	1.1
38	236.2	0.9
39	230	-6.2
40	224.333	-5.667
41	225	0.667
42	222	-3
43	223.967	1.967
44	220.933	-3.034
45	217.5	-3.433
46	212	-5.5
47	212.9	0.9
48	183.4	-29.5
49	148.467	-34.933
50	77	-71.467
51	45.7	-31.3
52	23.533	-22.167
53	19.767	-3.766
54	11	-8.767
55	8	-3
56	7	-1
57	5	-2
58	1	-4
59	1	0
60	1	0

i) Frame 45

Position	Position	Tangent
0	121	
1	121.2	0.2
2	123.867	2.667
3	127.7	3.833
4	126.733	-0.967
5	131	4.267
6	157.8	26.8
7	190.767	32.967
8	217.267	26.5
9	215.6	-1.667
10	209.333	-6.267
11	216.433	7.1
12	218.2	1.767
13	214.267	-3.933
14	226.8	12.533
15	227.5	0.7
16	229.333	1.833
17	229.167	-0.166
18	229.4	0.233
19	227.467	-1.933
20	227	-0.467
21	226.8	-0.2
22	224.2	-2.6
23	223.333	-0.867
24	229.4	6.067
25	227.167	-2.233
26	237.933	10.766
27	237.7	-0.233
28	237.6	-0.1
29	237.367	-0.233
30	238	0.633
31	237.767	-0.233
32	238.667	0.9
33	238.1	-0.567
34	225.6	-12.5
35	223.5	-2.1
36	220.2	-3.3
37	217.9	-2.3
38	216.933	-0.967
39	216.2	-0.733
40	209.667	-6.533
41	208.967	-0.7
42	212.4	3.433
43	204.7	-7.7
44	213.867	9.167
45	206.5	-7.367
46	188	-18.5
47	182.4	-5.6
48	161	-21.4
49	141	-20
50	105.333	-35.667
51	63.9	-41.433
52	27.2	-36.7
53	21.233	-5.967
54	11	-10.233
55	10	-1
56	8	-2
57	5	-3
58	2	-3
59	2	0
60	1	-1

j) Frame 50

Position	Position	Tangent
0	103	
1	103	0
2	97.067	-5.933
3	97.3	0.233
4	98.4	1.1
5	101.5	3.1
6	108.2	6.7
7	116.4	8.2
8	125.8	9.4
9	135.6	9.8
10	138.667	3.067
11	144	5.333
12	167.6	23.6
13	183.033	15.433
14	190.467	7.434
15	188	-2.467
16	186.533	-1.467
17	187.067	0.534
18	189.4	2.333
19	190.633	1.233
20	190.667	0.034
21	190.7	0.033
22	190.733	0.033
23	189.233	-1.5
24	189.4	0.167
25	191	1.6
26	186.2	-4.8
27	188.2	2
28	187.4	-0.8
29	187.7	0.3
30	188	0.3
31	180.933	-7.067
32	181	0.067
33	180.8	-0.2
34	174	-6.8
35	172	-2
36	174.6	2.6
37	174.067	-0.533
38	165.067	-9
39	163.8	-1.267
40	178	14.2
41	183.1	5.1
42	182	-1.1
43	182	0
44	179	-3
45	176	-3
46	177.2	1.2
47	175.133	-2.067
48	158.6	-16.533
49	124.267	-34.333
50	80.333	-43.934
51	46.6	-33.733
52	19.533	-27.067
53	15.233	-4.3
54	8	-7.233
55	7.833	-0.167
56	5.867	-1.966
57	4.9	-0.967
58	2	-2.9

59	2	0

60	0	-2

k) Frame 55

Position	Position	Tangent
0	112	
1	114.767	2.767
2	120.067	5.3
3	125.6	5.533
4	121.667	-3.933
5	129.833	8.166
6	157.2	27.367
7	160.167	2.967
8	200.733	40.566
9	216	15.267
10	228	12
11	226.767	-1.233
12	228	1.233
13	227.667	-0.333
14	231.267	3.6
15	229	-2.267
16	235.733	6.733
17	235.2	-0.533
18	242.6	7.4
19	244.233	1.633
20	250	5.767
21	250.1	0.1
22	253.4	3.3
23	253.6	0.2
24	249	-4.6
25	249	0
26	247.533	-1.467
27	249.2	1.667
28	247.267	-1.933
29	249.067	1.8
30	251	1.933
31	253.067	2.067
32	246.867	-6.2
33	248.8	1.933
34	247	-1.8
35	247	0
36	240	-7
37	240	0
38	239.067	-0.933
39	236.6	-2.467
40	226	-10.6
41	223.433	-2.567
42	215.6	-7.833
43	208	-7.6
44	178.2	-29.8
45	154.5	-23.7
46	113.533	-40.967
47	73.7	-39.833
48	36.8	-36.9
49	26.9	-9.9
50	12	-14.9
51	9.7	-2.3
52	8.2	-1.5
53	6.467	-1.733
54	6	-0.467
55	5	-1
56	4	-1
57	3.1	-0.9
58	1	-2.1
59	1	0
60	0	-1

l) Frame 60

Position	Position	Tangent
0	115	
1	113.567	-1.433
2	106	-7.567
3	110	4
4	107.133	-2.867
5	113	5.867
6	119.2	6.2
7	125.533	6.333
8	137.733	12.2
9	146.1	8.367
10	159.667	13.567
11	176.567	16.9
12	192	15.433
13	204.133	12.133
14	206.133	2
15	207	0.867
16	214.533	7.533
17	215.433	0.9
18	225.2	9.767
19	221.767	-3.433
20	230	8.233
21	233.2	3.2
22	232.533	-0.667
23	232.467	-0.066
24	233.2	0.733
25	237.667	4.467
26	234.267	-3.4
27	235.7	1.433
28	240.067	4.367
29	239.933	-0.134
30	237	-2.933
31	239	2
32	239	0
33	239	0
34	237.4	-1.6
35	237.5	0.1
36	244	6.5
37	240.933	-3.067
38	245.2	4.267
39	241.8	-3.4
40	221.667	-20.133
41	219.533	-2.134
42	203.2	-16.333
43	183.267	-19.933
44	166.933	-16.334
45	129	-37.933
46	123.133	-5.867
47	80.7	-42.433
48	40	-40.7
49	26.267	-13.733
50	12.667	-13.6
51	11.3	-1.367
52	8	-3.3
53	6	-2
54	6	0
55	5	-1
56	4	-1
57	3	-1
58	1	-2
59	1	0
60	1	0

m) Frame 65

Position	Position	Tangent
0	100	
1	103.933	3.933
2	110.333	6.4
3	112	1.667
4	106.667	-5.333
5	108.333	1.666
6	118	9.667
7	132.7	14.7
8	154.933	22.233
9	163.8	8.867
10	148.333	-15.467
11	169.433	21.1
12	207	37.567
13	208.667	1.667
14	202.6	-6.067
15	208.5	5.9
16	206.133	-2.367
17	203.167	-2.966
18	237.8	34.633
19	230.733	-7.067
20	218	-12.733
21	215.5	-2.5
22	213.733	-1.767
23	212.267	-1.466
24	209.6	-2.667
25	213.667	4.067

26	216.467	2.8
27	214.6	-1.867
28	211.4	-3.2
29	206.867	-4.533
30	212	5.133
31	209	-3
32	205.467	-3.533
33	208.1	2.633
34	210.067	1.967
35	215	4.933
36	220	5
37	216.467	-3.533

38	208.133	-8.334
39	208.8	0.667
40	200.667	-8.133
41	200	-0.667
42	197.6	-2.4
43	185.833	-11.767
44	177.733	-8.1
45	142	-35.733
46	115.933	-26.067
47	77.867	-38.066
48	41.4	-36.467
49	27.467	-13.933

50	14	-13.467
51	12	-2
52	11	-1
53	6	-5
54	5	-1
55	5	0
56	3	-2
57	3	0
58	1	-2
59	1	0
60	1	0

n) Frame 70

Position	Position	Tangent
0	93	
1	92.933	-0.067
2	90.933	-2
3	90.9	-0.033
4	93.467	2.567
5	93.333	-0.134
6	97.8	4.467
7	101	3.2
8	98.2	-2.8
9	99.8	1.6
10	99	-0.8
11	106	7
12	112.2	6.2
13	120.567	8.367
14	124.867	4.3
15	130.5	5.633
16	131.2	0.7
17	136.967	5.767
18	157.4	20.433
19	162.267	4.867

20	162.333	0.066
21	164.1	1.767
22	172.733	8.633
23	176.7	3.967
24	177.4	0.7
25	180.333	2.933
26	186.6	6.267
27	186.7	0.1
28	189	2.3
29	190.8	1.8
30	187	-3.8
31	187	0
32	179.133	-7.867
33	179	-0.133
34	170.733	-8.267
35	173.5	2.767
36	176.6	3.1
37	177	0.4
38	179	2
39	183.8	4.8
40	180.667	-3.133

41	179.167	-1.5
42	177.4	-1.767
43	175.567	-1.833
44	165	-10.567
45	161	-4
46	130.867	-30.133
47	97.767	-33.1
48	78	-19.767
49	48.567	-29.433
50	17.667	-30.9
51	14.6	-3.067
52	8	-6.6
53	8	0
54	5.2	-2.8
55	5	-0.2
56	3	-2
57	1	-2
58	2	1
59	0	-2
60	0	0

o) Frame 75

Position	Position	Tangent
0	93	
1	92.867	-0.133
2	89.733	-3.134
3	88.7	-1.033
4	84.867	-3.833
5	84.833	-0.034
6	90.6	5.767
7	92.533	1.933
8	94.133	1.6
9	95.2	1.067
10	98.333	3.133
11	99.733	1.4
12	105.4	5.667
13	107.367	1.967
14	105.333	-2.034
15	109	3.667
16	115.333	6.333
17	120.333	5
18	126.6	6.267
19	129.467	2.867

20	133	3.533
21	136.5	3.5
22	137.667	1.167
23	142.867	5.2
24	144.4	1.533
25	147.833	3.433
26	161	13.167
27	156.4	-4.6
28	159.667	3.267
29	163.333	3.666
30	181	17.667
31	177.767	-3.233
32	178	0.233
33	180.3	2.3
34	181.467	1.167
35	177.5	-3.967
36	182	4.5
37	183	1
38	181.933	-1.067
39	185.8	3.867
40	178	-7.8

41	180.533	2.533
42	177.2	-3.333
43	178.4	1.2
44	163	-15.4
45	166.5	3.5
46	141.4	-25.1
47	134.333	-7.067
48	94.4	-39.933
49	62.267	-32.133
50	29	-33.267
51	21.7	-7.3
52	11	-10.7
53	9	-2
54	4	-5
55	4	0
56	5	1
57	4	-1
58	1	-3
59	1	0
60	0	-1

p) Frame 80

Position	Position	Tangent
0	92	
1	93.833	1.833
2	88.4	-5.433
3	89	0.6
4	85.667	-3.333
5	85.333	-0.334
6	86.8	1.467
7	88.3	1.5
8	89.733	1.433
9	91.4	1.667
10	96	4.6
11	93.8	-2.2
12	96.4	2.6
13	99.267	2.867
14	109.467	10.2
15	110.5	1.033
16	114.067	3.567
17	113.367	-0.7
18	120.6	7.233
19	121.733	1.133
20	127.333	5.6
21	128.8	1.467
22	128.8	0
23	137	8.2
24	130.4	-6.6
25	137.5	7.1
26	156.2	18.7
27	160.1	3.9
28	158.4	-1.7
29	162.133	3.733
30	172	9.867
31	175.867	3.867
32	173.6	-2.267
33	177.6	4
34	190.333	12.733
35	197.5	7.167
36	185	-12.5
37	196.833	11.833
38	210.933	14.1
39	207.9	-3.033
40	199	-8.9
41	195	-4
42	179	-16
43	169.967	-9.033
44	155.067	-14.9
45	120.5	-34.567
46	80.933	-39.567
47	51.133	-29.8
48	23.6	-27.533
49	18	-5.6
50	9	-9
51	8	-1
52	6.733	-1.267
53	6	-0.733
54	3	-3
55	3	0
56	1	-2
57	1	0
58	1	0
59	1	0
60	2	1

VIII. VITA

TanviShri Jatla

Education

University of Illinois at Chicago – Chicago, Illinois
Master of Science in Bioengineering, December 2015
Cumulative GPA: 4.0/4.0
Alpha Eta Mu Beta (Biomedical Engineering Honors Society); Tau Beta Pi (Engineering Honors Society)
Bachelor of Science in Bioengineering, May 2014
Cumulative GPA: 3.40/4.0; Major GPA: 3.64/4.0
Minor in Mathematics; Honors College; Tau Beta Pi; Dean's List (2010- 2013)

Posters & Presentations & Publications

Jatla T, Sun B, Zagariya A, Lerner L, Leiderman Y. "*A Shielded Needle to Prevent Bacterial Contamination During Intravitral Injection*." Presentation at the 2014 Annual Meeting of The Association for Research in Vision and Ophthalmology; Orlando, Florida; May 04-08, 2014.

Leiderman Y, Jatla T, Lerner L. "*An Intravitreal Injection Needle with Integrated Filter to Sterilize Injectable Pharmaceuticals*." Presentation at the 32nd Annual Meeting of The American Society of Retina Specialist; San Diego, California; August 09-13, 2014.

Jatla, TanviShri. "An Overview of Corneal Topography." *Undergraduate Bioengineering Student Journal* 6.1 (2015): 6-11.

Honors & Awards

Honors: Tau Beta Pi, Alpha Eta Mu Beta, Dean's List (2010-2013)
Scholarships: William Unger Scholarship, Steven J. Hampton Merit Scholarship, College of Engineering Scholarship
Certificates of Appreciation: Women in Science and Engineering, Bioengineering Organizational Alliance Outstanding Volunteer Award, Telugu Association of Greater Chicago

---

Society Membership

Society of Hispanic Professional Engineers (SHPE)
National Society of Black Engineers (NSBE)
Society of Women Engineers (SWE)
Engineering World Health (EWH)
Biomedical Engineering Society (BMES)
Association for Research in Vision and Ophthalmology (ARVO)